

Solving PDEs on Spheres with Physics-Informed Convolutional Neural Networks[†]

Guanhang Lei¹, Zhen Lei¹, Lei Shi¹, Chenyu Zeng¹, and Ding-Xuan Zhou²

¹School of Mathematical Sciences,
Shanghai Key Laboratory for Contemporary Applied Mathematics,
Fudan University, Shanghai, 200433, P. R. China
Email:ghlei21@m.fudan.edu.cn

{zlei, leishi, cyzeng19}@fudan.edu.cn
²School of Mathematics and Statistics,
University of Sydney,
Sydney NSW 2006, Australia
Email:dingxuan.zhou@sydney.edu.au

Abstract

Physics-informed neural networks (PINNs) have been demonstrated to be efficient in solving partial differential equations (PDEs) from a variety of experimental perspectives. Some recent studies have also proposed PINN algorithms for PDEs on surfaces, including spheres. However, theoretical understanding of the numerical performance of PINNs, especially PINNs on surfaces or manifolds, is still lacking. In this paper, we establish rigorous analysis of the physics-informed convolutional neural network (PICNN) for solving PDEs on the sphere. By using and improving the latest approximation results of deep convolutional neural networks and spherical harmonic analysis, we prove an upper bound for the approximation error with respect to the Sobolev norm. Subsequently, we integrate this with innovative localization complexity analysis to establish fast convergence rates for PICNN. Our theoretical results are also confirmed and supplemented by our experiments. In light of these findings, we explore potential strategies for circumventing the curse of dimensionality that arises when solving high-dimensional PDEs.

Keywords and phrases: Physics-Informed Neural Network; Convolutional Neural Network; Solving PDEs on spheres; Convergence analysis; Curse of dimensionality.

[†] The work described in this paper is supported partially by Shanghai Science and Technology Program (Project No. 21JC1400600) and NSFC/RGC Joint Research Scheme (Project No. 12061160462 and N_CityU102/20). The work of Zhen Lei is also supported by the New Cornerstone Science Foundation through the XPLOERER PRIZE and Sino-German Center Mobility Programme (Project No. M-0548). The work of Lei Shi is also supported by the National Natural Science Foundation of China (Grant No.12171039). The work of Ding-Xuan Zhou is partially supported by the Australian Research Council under project DP240101919. The corresponding author is Lei Shi.

1 Introduction

Solving partial differential equations (PDEs) is crucial in many science and engineering problems. Numerous methods, including finite differences, finite elements, and some meshless schemes, have been well-developed, particularly for low-dimensional PDEs. Nonetheless, these classical strategies often become impractical and time-consuming for high-dimensional PDEs attributed to their computational inefficiencies. The amalgamation of deep learning methodologies and data-driven architectures has recently exhibited superiority across various fields. There have been extensive studies on solving high-dimensional PDEs with deep neural networks, such as the Deep Ritz methods (DRMs) [11], Physics-Informed Neural Networks (PINNs) [47, 43], Neural Operators [32, 33, 28], and DeepONets [35]. DRMs and PINNs utilize the powerful approximation capabilities of neural networks to directly learn solutions of PDEs. In contrast, Neural Operators and DeepONets specialize in learning the operators that map initial or boundary conditions to solution functions. One can refer to [21] for an exhaustive review of deep learning techniques for resolving PDEs.

In this paper, we focus on the PINN approach. While previous research (e.g., [36, 18]) has performed convergence analysis on the generalization bound of PINNs, it primarily pertains to fully connected neural networks learning solutions to PDEs on a physical domain of a Euclidean space. However, there is still a gap in employing convolutional neural networks (CNNs) for this purpose. In addition, solving PDE systems on manifolds holds considerable relevance for practical applications, situating manifold learning as a vibrant domain within machine learning. The low intrinsic data dimensions have been validated as effective in shielding learning algorithms from the curse of dimensionality [56, 57, 37, 53, 15, 31]. Although there has been some exploration of the PINN framework for PDEs on manifolds [12, 50, 44, 5, 58], comprehensive convergence analysis is still absent. This study is the inaugural endeavor to address this gap. We propose the application of PINNs with CNN architectures, coined as PICNNs, to solve general PDEs of order s on a unit sphere, while concurrently establishing convergence analysis for such PDE solvers. We probe into the approximation potential of CNNs by employing the spherical harmonic analysis, assess the Rademacher complexity of our model, and derive elegant generalization bounds through various technical estimates. In this context, our research offers significant insights into the ability of deep learning to tackle high-dimensional PDEs and leverage the low-dimensional attributes of physical domains. We summarize the contributions of this paper as follows.

- We are the first to investigate PICNN PDE solvers on a unit sphere. Previous work (e.g., [12, 50]) employs fully connected neural networks as solvers on the sphere. Although we focus on PINNs working with CNNs, some discussions in this paper are also applicable to the general PINNs. Consequently, we may use the term PINN when referring to the non-convolutional architecture.
- We present comprehensive analysis of the relationship between PDEs and PINNs, facilitating rigorous assumptions on the well-posedness and regularity of PDEs. In contrast to previous studies (e.g., [36, 18]) that exclusively focus on second-order elliptic PDEs, our approach encompasses a broad class of PDEs.
- We demonstrate fast convergence of approximation using ReLU-ReLU^k CNNs operating on a unit sphere. Conversely, earlier studies [36, 18] solely explore the approximation

ability of ReLU³ fully connected networks, which frequently suffer from gradient explosion during training. Despite the success of the ReLU network in diverse machine learning tasks attributed to its gradient calculation simplicity, it proves inadequate for approximating high-order derivatives in PDE problems due to the saturation phenomena (e.g., see [6]). To tackle this issue, we propose a hybrid CNN architecture utilizing both ReLU and ReLU^k. Leveraging the advantages of each activation function, we achieve an effective approximation of the derivatives of PDE solutions while maintaining ease of network training. During the process of proof, we develop solid analysis employing ideas and techniques from spherical approximation theory and B-spline interpolation. These approximation analyses enable us to address a broad Sobolev smoothness condition, assuming the PDE solution u^* belongs to $W_p^r(\mathbb{S}^{d-1})$.

- We develop a novel approach involving localization Rademacher complexity analysis to establish an oracle inequality that bounds the statistical error. To the best of our knowledge, we are the first to compute the VC-dimensions of hypothesis spaces generated by the CNN architecture and high-order derivatives. Furthermore, unlike [36], our approach does not require a sup-norm restriction on network parameters, making it more aligned with practical algorithms. Additionally, our upper bound exhibits a significantly sharper estimation than that presented in [18] due to the absence of a localization technique in their work.
- We derive fast convergence upper bounds for the excess risk of PINNs in diverse scenarios, encompassing varying dimensions $d \geq 2$, PDE orders $s \geq 1$, smoothness orders $r \geq s + 1$, and suitably chosen activation degrees $k \geq s$ of ReLU^k. We establish a convergence rate in the form of $n^{-a}(\log n)^{2a}$, where

$$a = \begin{cases} \frac{r-s}{(r-s)+(d-1)}, & \text{if } r < \infty, d > 3, \\ 1 - \frac{d(k-s+2) + r + k}{d(k-s+2) + 2(r-s)(k-s+1) + r + k}, & \text{if } r < \infty, 2 \leq d \leq 3, \\ 1 - \frac{1}{2(k-s) + 3}, & \text{if } r = \infty, d \geq 2. \end{cases}$$

- We validate our theory through comprehensive numerical experiments, and by integrating our theoretical analysis with these experiments, we ascertain the conditions under which a PDE PINN solver can surmount the curse of dimensionality.

The rest of the paper is organized as follows. In Section 2, we first discuss the strong convexity of the PINN risk, subsequently formulating reasonable assumptions on the well-posedness and regularity of PDEs. We then introduce the structure of the CNN employed in our analysis. After elaborating on the assumptions, we present our main result in Theorem 1. In Section 3, we prove an upper bound for the approximation error, as evidenced in Theorem 2, leveraging techniques from the spherical harmonics analysis and B-spline interpolation. In Section 4, novel localization analysis related to the stochastic component of error evaluation is conducted, leading to the derivation of a pivotal oracle inequality as seen in Theorem 4. Section 5 amalgamates the derived approximation bound and the oracle inequality, culminating in the derivation of accelerated convergence rates for PICNN when applied to solving sphere PDEs, which gives a proof of Theorem 1. We present experimental results in Section 6 to validate our theoretical assertions and shed light on the conditions circumventing the algorithmic curse of dimensionality.

2 Preliminaries and Main Result

2.1 PINN for General PDEs

Consider solving the following PDE with a Dirichlet boundary condition:

$$\begin{cases} (\mathcal{L}u)(x) = f(x), & x \in \Omega \subset \mathbb{R}^d, \\ u(x) = g(x), & x \in \partial\Omega, \end{cases} \quad (2.1)$$

where \mathcal{L} is a general differential operator and Ω is a bounded domain. To construct an approximate solution, PINN converts (2.1) to a minimization problem with the objective function \mathcal{R} defined as

$$\mathcal{R}(u) = \frac{1}{\text{vol}(\Omega)} \int_{\Omega} |(\mathcal{L}u)(x) - f(x)|^2 dx + \frac{1}{\sigma(\partial\Omega)} \int_{\partial\Omega} |u(x) - g(x)|^2 d\sigma(x).$$

Here, vol is the Lebesgue measure and σ is the surface measure on $\partial\Omega$. This objective function is the mean squared error of the residual from (2.1) and the following empirical version is used for numerical optimization:

$$\mathcal{R}_{n,m}(u) = \frac{1}{n} \sum_{i=1}^n |(\mathcal{L}u)(X_i) - f(X_i)|^2 + \frac{1}{m} \sum_{i=1}^m |u(Y_i) - g(Y_i)|^2,$$

where $\{X_i\}_{i=1}^n \subset \Omega$, $\{Y_i\}_{i=1}^m \subset \partial\Omega$ are independent and identically distributed (i.i.d.) random samples from the uniform distribution. $\mathcal{R}(u)$ and $\mathcal{R}_{n,m}(u)$ are referred to as the population risk and empirical risk respectively. Given a function class \mathcal{F} , PINN solves the following empirical risk minimization (ERM) problem:

$$u_{n,m} = \arg \min_{u \in \mathcal{F}} \mathcal{R}_{n,m}(u). \quad (2.2)$$

If equation (2.1) has a unique classical solution, denoted by u^* , obviously $\mathcal{R}(u^*) = \mathcal{R}_{n,m}(u^*) = 0$. Under the framework of learning theory, this ideal solution u^* is termed the Bayes function since it minimizes the population risk $\mathcal{R}(u)$. The performance of the ERM estimator $u_{n,m}$ can be quantified by the excess risk $\mathcal{R}(u_{n,m}) - \mathcal{R}(u^*)$. In our PINN model, given our assumption that a true solution u^* exists, we have $\inf_u \mathcal{R}(u) = \mathcal{R}(u^*) = 0$. However, for the sake of conventional notation for excess risk, we will continue to express the excess risk as $\mathcal{R}(u_{n,m}) - \mathcal{R}(u^*)$ instead of $\mathcal{R}(u_{n,m})$. This study establishes rapidly decaying rates of $\mathcal{R}(u_{n,m}) - \mathcal{R}(u^*)$ as the size of the training data set increases. This decaying rate, often termed the convergence rate or learning rate, is an important measure of the algorithm's generalization performance. Contrastingly, the accuracy of an approximate PDE solution is traditionally measured by estimating the error $\|u_{n,m} - u^*\|$, where $\|\cdot\|$ represents the norm of a regularity space, such as the Sobolev space $W_p^r(\Omega)$. This raises a natural question: Can the excess risk $\mathcal{R}(u) - \mathcal{R}(u^*)$ bound $\|u - u^*\|$ in a manner that superior generalization performance corresponds to enhanced accuracy? This property is indispensable for constraining the statistical error through localization analysis. Equally significant is the converse question: Can $\|u - u^*\|$ control $\mathcal{R}(u) - \mathcal{R}(u^*)$? If so, an upper bound on $\|u - u^*\|$, derived from approximation analysis, could provide a bound for the approximation error $\mathcal{R}(u_{\mathcal{F}}) - \mathcal{R}(u^*)$ where $u_{\mathcal{F}} := \arg \min_{u \in \mathcal{F}} \mathcal{R}(u)$. Our primary objective is to establish an equivalence between

the excess risk $\mathcal{R}(u) - \mathcal{R}(u^*)$ and the error $\|u - u^*\|_{W_p^r(\Omega)}$. This relationship is known as the strong convexity of the PINN risk with respect to the $W_p^r(\Omega)$ norm, which is only determined by the underlying PDE.

For the sake of theoretical simplicity, we consider a linear PDE where the differential operator \mathcal{L} is linear. Hence we write

$$\begin{aligned}\mathcal{R}(u) - \mathcal{R}(u^*) &= \frac{1}{\text{vol}(\Omega)} \int_{\Omega} |(\mathcal{L}u)(x) - f(x)|^2 dx + \frac{1}{\sigma(\partial\Omega)} \int_{\partial\Omega} |u(x) - g(x)|^2 d\sigma(x) \\ &= \frac{1}{\text{vol}(\Omega)} \int_{\Omega} |\mathcal{L}(u - u^*)(x)|^2 dx + \frac{1}{\sigma(\partial\Omega)} \int_{\partial\Omega} |u(x) - u^*(x)|^2 d\sigma(x) \\ &= \frac{1}{\text{vol}(\Omega)} \|\mathcal{L}(u - u^*)\|_{L^2(\Omega)}^2 + \frac{1}{\sigma(\partial\Omega)} \|u - u^*\|_{L^2(\partial\Omega)}^2.\end{aligned}$$

Let us first consider controlling $\|u - u^*\|_{W_p^r(\Omega)}$ by $\mathcal{R}(u) - \mathcal{R}(u^*)$. This problem is intrinsically connected to the global W_p^r estimates for PDEs. For an elliptic operator \mathcal{L} of even order $2s$ where $s \in \mathbb{N}$, some prior estimates related to Gårding's inequality have already been well-established. See Lemma 1 and Lemma 2 below. Throughout the subsequent discourse, if A and B are two quantities (typically non-negative), the notation $A \lesssim B$ indicates that $A \leq CB$ for some positive constant C . It should be emphasized that C is independent of both A and B , or is universal for indexed A and B of a certain class. The constant C might depend on particular parameters, such as dimension, regularity, or exponent, as determined by the context. In this paper, we will not delve into the specifics of which parameters C relies on, nor will we discuss the optimal estimation of C . Moreover, we use the notation $A \asymp B$ when $A \lesssim B$ and $B \lesssim A$. Denote the Sobolev space $W_2^s(\cdot)$ by $H^s(\cdot)$ and its subspace consisting of functions vanishing on the boundary by $H_0^s(\Omega)$.

Lemma 1. (Theorem 12.8 in [1]) *Let $s \in \mathbb{N}$ and \mathcal{L} denote a uniformly elliptic operator of order $2s$ possessing bounded coefficients, with its leading coefficients being continuous. Furthermore, suppose \mathcal{L} is weakly positive semi-definite. For a sufficiently large positive λ , the inequality*

$$\|u\|_{H^{2s}(\Omega)} \lesssim \|(\mathcal{L} + \lambda)u\|_{L^2(\Omega)}$$

holds for every $u \in H^{2s}(\Omega) \cap H_0^s(\Omega)$.

Lemma 2. (Theorem 15.2 in [1] and remark therein) *Given $s \in \mathbb{N}$ and $1 < p < \infty$, consider an operator \mathcal{L} of even order $2s$ that is uniformly elliptic. Suppose the coefficients of \mathcal{L} belong to $C(\bar{\Omega})$ and the boundary $\partial\Omega$ is of class C^{2s} . If u is a solution to the equation (2.1) such that $\|u\|_{W_p^{2s}(\Omega)}$, $\|f\|_{L^p(\Omega)}$, and $\|g\|_{W_p^{2s-1/p}(\partial\Omega)}$ are all finite, then it follows that*

$$\|u\|_{W_p^{2s}(\Omega)} \lesssim \|f\|_{L^p(\Omega)} + \|g\|_{W_p^{2s-1/p}(\partial\Omega)} + \|u\|_{L^p(\Omega)}.$$

Additionally, given the uniqueness of the solution to (2.1) with derivatives of order up to $2s$ in L^p , the term $\|u\|_{L^p(\Omega)}$ can be excluded, resulting in

$$\|u\|_{W_p^{2s}(\Omega)} \lesssim \|f\|_{L^p(\Omega)} + \|g\|_{W_p^{2s-1/p}(\partial\Omega)}. \quad (2.3)$$

Remark 1. *Some similar conclusions can be generalized to elliptic PDEs on unbounded domains or Riemannian manifolds. Relevant discussions can be found in the referenced materials such as [1] (Chapter V) regarding unbounded domains, [51] (Chapter 5), [52], and [29] (Theorem 5.2. in Chapter III) that delve into Riemannian manifolds. Additionally, the W_p^r estimates for other types of PDEs are also extensively studied. These estimates are integral to understanding the existence, uniqueness, and regularity of the solution.*

Returning to the discussion on PINN, let us consider a $2s$ -order elliptic PDE that satisfies the conditions stated in inequality (2.3). By deriving the following inequality:

$$\|u - u^*\|_{H^{2s}(\Omega)} \lesssim \|\mathcal{L}(u - u^*)\|_{L^2(\Omega)} + \|u - u^*\|_{H^{2s-1/2}(\partial\Omega)},$$

we observe that the norm of the boundary term is inconsistent with $\mathcal{R}(u) - \mathcal{R}(u^*)$. This can be a touchy issue and one may have to impose a hard-constraint for the boundary condition to carry on the analysis, that is, assuming that any potential solution u from \mathcal{F} exactly satisfies the boundary condition:

$$u(x) = g(x), \quad x \in \partial\Omega, u \in \mathcal{F}. \quad (2.4)$$

Then

$$\|u - u^*\|_{H^{2s}(\Omega)} \lesssim \|\mathcal{L}(u - u^*)\|_{L^2(\Omega)}, \quad \text{for } u \in \mathcal{F} \cap H^{2s}(\Omega).$$

Generally, (2.4) is not a reasonable assumption for a neural network space. [36] directly assume (2.4) for a general neural network function space (see Theorem B.12 therein), which lacks theoretical rigor. Notably, PDEs formulated on the whole sphere can address this problem without necessitating a hard-constraint, as the sphere is a boundaryless manifold.

Now we consider controlling $\mathcal{R}(u) - \mathcal{R}(u^*)$ by $\|u - u^*\|_{H^s(\Omega)}$, which is much more direct, since

$$\begin{aligned} \mathcal{R}(u) - \mathcal{R}(u^*) &\lesssim \|\mathcal{L}(u - u^*)\|_{L^2(\Omega)}^2 + \|u - u^*\|_{L^2(\partial\Omega)}^2 \\ &\lesssim \|u - u^*\|_{H^s(\Omega)}^2 + \|u - u^*\|_{L^2(\partial\Omega)}^2, \end{aligned} \quad (2.5)$$

where we assume that \mathcal{L} is a linear differential operator of order s with essentially bounded coefficient functions.

We conclude that the strong convexity of the PINN risk is a non-trivial property, especially concerning the W_p^r error estimates of $u - u^*$. Another crucial consideration is the existence of a unique solution. If an exact solution does not exist or its existence remains unclear, one can still employ PINN to obtain an approximate solution through the minimization of residuals. Particularly, when the solution lacks uniqueness, PINN is still workable even though we might encounter challenges in ascertaining which solution PINN aims to approximate. Many references are available on the well-posedness of PDEs, and we will not go into further discussion here.

2.2 PINN for PDEs on Spheres

Prior to the discussion regarding PDEs on the sphere, one may refer to a brief introduction to the Laplace-Beltrami operator Δ_0 and Sobolev spaces $W_p^r(\mathbb{S}^{d-1}), H^r(\mathbb{S}^{d-1})$ on spheres in Appendix A. We now formulate the PINN algorithm on the sphere as follows. We focus on linear PDEs on \mathbb{S}^{d-1} with $d \geq 2$, thus eliminating the necessity of imposing a boundary condition:

$$(\mathcal{L}u)(x) = f(x), \quad x \in \mathbb{S}^{d-1}. \quad (2.6)$$

Let σ be the Lebesgue measure on \mathbb{S}^{d-1} and ω_d be the surface area of \mathbb{S}^{d-1} . The population PINN risk is then defined as

$$\mathcal{R}(u) = \frac{1}{\omega_d} \int_{\mathbb{S}^{d-1}} |(\mathcal{L}u)(x) - f(x)|^2 d\sigma(x).$$

After drawing n i.i.d. random variables $\{X_i\}_{i=1}^n$ from \mathbb{S}^{d-1} according to the uniform distribution, we define the empirical risk as

$$\mathcal{R}_n(u) = \frac{1}{n} \sum_{i=1}^n |(\mathcal{L}u)(X_i) - f(X_i)|^2.$$

Consequently, the ERM estimator u_n , which belongs to a predefined function space \mathcal{F} , is determined by the following optimization problem:

$$u_n = \arg \min_{u \in \mathcal{F}} \mathcal{R}_n(u). \quad (2.7)$$

To enhance the algorithm's stability for practical applications, it is advantageous to consider the use of uniform lattices when generating training sample points, as they can offer a minimal fill distance. An example of such a lattice is the Fibonacci lattice, which provides near-uniform coverage on the 2-D sphere (see [2]). However, generating almost uniform lattices on a general manifold can pose significant challenges. As an alternative, a uniform random sampling method may be employed. For the sake of simplicity in our analysis, we restrict our discussion to uniform random sampling on the sphere in this paper.

As previously discussed in Subsection 2.1, we can identify approximate solutions within a function space without the hard constraint (2.4), by the absence of a boundary on the sphere. It is also essential to assume that (2.6) possesses a unique solution u^* . Furthermore, the strong convexity of the PINN risk is a requirement for both approximation and statistical analysis. For the approximation of u^* using neural networks, it is imperative to make reasonable assumptions regarding the excess regularity of u^* . Take, for instance, \mathcal{L} , an elliptic operator of order s . By (2.5), our aim is to approximate u^* in $H^s(\mathbb{S}^{d-1})$ norm, necessitating a higher order of smoothness of u^* according to our approximation analysis. We should then presume $u^* \in H^r(\mathbb{S}^{d-1})$ for some $r \geq s + 1$. Based on the elliptic regularity theorem (Theorem 6.30 in [52]), we establish:

$$u^* \in H^{-\infty}(\mathbb{S}^{d-1}), f \in H^t(\mathbb{S}^{d-1}) \implies u^* \in H^{t+s}(\mathbb{S}^{d-1}),$$

where $H^{-\infty}(\mathbb{S}^{d-1})$ represents the dual space of $H^\infty(\mathbb{S}^{d-1})$. Consequently, it is sufficient to assume $f \in H^{r-s}(\mathbb{S}^{d-1})$ in this context.

To employ concentration inequalities such as Bernstein's and Talagrand's inequalities in the generalization analysis, the introduction of a boundedness assumption becomes necessary. This requirement must be satisfied by both u^* and the approximate function $u \in \mathcal{F}$ up to derivatives of order s . Our approximation analysis allows us to establish an upper bound for $\|u\|_{W_\infty^s(\mathbb{S}^{d-1})}$ only if $u^* \in W_\infty^r(\mathbb{S}^{d-1})$ where $r \geq s + 1$. As a result, it is essential to assume, at the very least, that $u^* \in W_\infty^r(\mathbb{S}^{d-1})$ for some $r \geq s + 1$. In conclusion, we state the following assumption.

Assumption 1. Consider the sphere PDE (2.6). Assume that \mathcal{L} is a linear differential operator of order $s \in \mathbb{N}$, taking the form:

$$\mathcal{L} = \sum_{|\alpha| \leq s} a_\alpha(x) D^\alpha, \quad (2.8)$$

where $\alpha = (\alpha_1, \alpha_2, \dots, \alpha_n)$ denotes a multi-index of non-negative integers, $|\alpha| = \alpha_1 + \alpha_2 + \dots + \alpha_n$, $a_\alpha \in L^\infty(\mathbb{S}^{d-1})$, and

$$D^\alpha = \frac{\partial^{|\alpha|}}{\partial x_1^{\alpha_1} \partial x_2^{\alpha_2} \dots \partial x_d^{\alpha_d}}.$$

Assume that (2.6) has a unique solution $u^* \in W_\infty^r(\mathbb{S}^{d-1})$ for some $r \geq s + 1$. Furthermore, assume that the following $H^s(\mathbb{S}^{d-1})$ estimate holds for all $u \in H^s(\mathbb{S}^{d-1})$:

$$\|u - u^*\|_{H^s(\mathbb{S}^{d-1})} \lesssim \|\mathcal{L}(u - u^*)\|_{L^2(\mathbb{S}^{d-1})}. \quad (2.9)$$

Remark 2. In Assumption 1, we suppose that the operator \mathcal{L} is linear. The linearity is assumed primarily to expound upon the strong convexity associated with the PINN risk. However, this property is barely used in the convergence analysis. As such, it is feasible to consider a nonlinear operator, denoted as \mathcal{T} , defined as:

$$\mathcal{T} = \sum_{|\alpha| \leq s} a_\alpha D^\alpha \text{ such that } \mathcal{T}u = f,$$

where coefficients a_α and the function f might be dependent on the unknown function u and its higher-order derivatives. Given that strong convexity is maintained with \mathcal{T} as:

$$\|\mathcal{T}u - \mathcal{T}u^*\|_{L^2(\mathbb{S}^{d-1})} \asymp \|u - u^*\|_{H^s(\mathbb{S}^{d-1})},$$

and that \mathcal{T} exhibits Lipschitz behavior for any $u_1, u_2 \in H^s(\mathbb{S}^{d-1})$ on a point-wise basis (refer to (E.2)):

$$|(\mathcal{T}u_1)(x) - (\mathcal{T}u_2)(x)| \lesssim \sum_{|\alpha| \leq s} |D^\alpha u_1(x) - D^\alpha u_2(x)|,$$

with coefficients a_α and f possessing bounded sup-norms, our analysis presented in this paper remains largely applicable. Nonetheless, it warrants mention that verifying such conditions is extremely nontrivial for nonlinear operators.

Consequently, the assumption immediately indicates that $f \in L^\infty(\mathbb{S}^{d-1})$ and (2.5) holds true. We admit that the assumption (2.9) is non-trivial and has been deliberated under certain conditions in Subsection 2.1, wherein (2.9) could be met. Subsequently, we provide two specific examples in Appendix B.

2.3 The CNN Architectures

In this study, we specifically concentrate on the computation of approximate solutions through the ERM algorithm (2.7) within a designated space \mathcal{F} , which is generated by 1-D Convolutional Neural Networks (CNNs) induced by 1-D convolutions. We present the following definition of the CNN architecture in the context of our analysis.

The CNN is specified by a series of convolution kernels, $\{w^{(l)}\}_{l=1}^L$, where each $w^{(l)} : \mathbb{Z} \rightarrow \mathbb{R}$ represents a vector indexed by \mathbb{Z} and supported on $\{0, \dots, S^{(l)} - 1\}$, given a kernel size $S^{(l)} \geq 3$. We can iteratively define a 1-D deep CNN with L hidden layers using the following expressions:

$$\begin{aligned} F^{(0)} : \mathbb{R}^d &\rightarrow \mathbb{R}^d, & F^{(0)}(x) &= x; \\ F^{(l)} : \mathbb{R}^d &\rightarrow \mathbb{R}^{d_l}, & F^{(l)}(x) &= \sigma^{(l)} \left(\left(\sum_{j=1}^{d_{l-1}} w_{i-j}^{(l)} (F^{(l-1)}(x))_j \right)_{i=1}^{d_l} - b^{(l)} \right), \\ & & l &= 1, \dots, L. \end{aligned} \quad (2.10)$$

In the above formulations, we denote the network widths as $d_0 = d, \{d_l = d_{l-1} + S^{(l)} - 1\}_{l=1}^L$ and define the bias as $b^{(l)} \in \mathbb{R}^{d_l}$. The element-wise activation function, $\sigma^{(l)} : \mathbb{R} \rightarrow \mathbb{R}$, utilizes the Rectified Linear Unit (ReLU) function, $\sigma(x) = \max\{x, 0\}$, which operates on each convolution layer. The convolution of a sequence $w^{(l)}$ on $F^{(l-1)}$ can be described through a convolutional matrix multiplication:

$$\left(\sum_{j=1}^{d_{l-1}} w_{i-j}^{(l)} (F^{(l-1)}(x))_j \right)_{i=1}^{d_l} = T^{(l)} F^{(l-1)}(x),$$

where $T^{(l)}$ represents a $d_l \times d_{l-1}$ matrix, defined as:

$$T^{(l)} = \begin{bmatrix} w_0^{(l)} & 0 & 0 & 0 & \cdots & 0 \\ w_1^{(l)} & w_0^{(l)} & 0 & 0 & \cdots & 0 \\ \vdots & \ddots & \ddots & \ddots & \ddots & \vdots \\ w_{S^{(l)}-1}^{(l)} & w_{S^{(l)}-2}^{(l)} & \cdots & w_0^{(l)} & 0 \cdots & 0 \\ 0 & w_{S^{(l)}-1}^{(l)} & \cdots & w_1^{(l)} & w_0^{(l)} \cdots & 0 \\ \vdots & \ddots & \ddots & \ddots & \ddots & \vdots \\ \cdots & \cdots & 0 & w_{S^{(l)}-1}^{(l)} & \cdots & w_0^{(l)} \\ \cdots & \cdots & 0 & 0 & w_{S^{(l)}-1}^{(l)} \cdots & w_1^{(l)} \\ \vdots & \ddots & \ddots & \ddots & \ddots & \vdots \\ 0 & \cdots & \cdots & 0 & w_{S^{(l)}-1}^{(l)} & w_{S^{(l)}-2}^{(l)} \\ 0 & \cdots & \cdots & 0 & 0 & w_{S^{(l)}-1}^{(l)} \end{bmatrix}.$$

Upon the completion of L convolution layers, a pooling operation is typically employed to decrease the output dimension. In this context, we consider a downsampling operator $\mathcal{D} : \mathbb{R}^{d_L} \rightarrow \mathbb{R}^{\lfloor d_L/d \rfloor}$ defined as $\mathcal{D}(x) = (x_{id})_{i=1}^{\lfloor d_L/d \rfloor}$. The convolution layers and pooling operator can be viewed as a feature extraction model. Finally, L_0 fully connected layers are implemented and an affine transformation computes the entire network's output $F^{(L+L_0+1)}(x) \in \mathbb{R}$ according to the following formulation:

$$\begin{aligned} F^{(L+1)} &: \mathbb{R}^d \rightarrow \mathbb{R}^{d_{L+1}}, \\ F^{(L+1)}(x) &= \sigma^{(L+1)} \left(W^{(L+1)} \mathcal{D}(F^{(L)}(x)) - b^{(L+1)} \right); \\ F^{(l)} &: \mathbb{R}^d \rightarrow \mathbb{R}^{d_l}, \\ F^{(l)}(x) &= \sigma^{(l)} \left(W^{(l)} F^{(l-1)}(x) - b^{(l)} \right), \quad l = L+2, \dots, L+L_0; \\ F^{(L+L_0+1)} &: \mathbb{R}^d \rightarrow \mathbb{R}, \\ F^{(L+L_0+1)}(x) &= W^{(L+L_0+1)} \cdot F^{(L+L_0)}(x) - b^{(L+L_0+1)}. \end{aligned} \tag{2.11}$$

Here, the terms $W^{(L+1)} \in \mathbb{R}^{d_{L+1} \times \lfloor d_L/d \rfloor}$, $W^{(l)} \in \mathbb{R}^{d_l \times d_{l-1}}$ for $l = L+2, \dots, L+L_0$, and $W^{(L+L_0+1)} \in \mathbb{R}^{d_{L+L_0+1} \times d_{L+L_0}}$ represent weight matrices. The elements $b^{(l)} \in \mathbb{R}^{d_l}$ for $l = L+1, \dots, L+L_0$, and $b^{(L+L_0+1)} \in \mathbb{R}$ are biases. As stated in Section 1, it is not appropriate to use the ReLU function as the single activation function in our PICNN model. The composite function of some ReLU and affine functions becomes a piecewise linear function, which results in the

network output's second derivative being strictly 0. This outcome prevents approximating the true solution with a smoothness order of at least $s + 1 \geq 2$, a phenomenon known as saturation in approximation theory. To address this issue, we utilize alternative activation functions with non-linear second derivatives in place of the ReLU function in at least one fully connected layer. Suitable alternatives encompass ReLU^k [54, 55] for $k \geq s$, the logistic function, and smooth approximations of ReLU such as Softplus and GeLU [17]:

$$\begin{aligned}\text{ReLU}^k(x) &= \max\{0, x\}^k; \\ \text{logistic}(x) &= \frac{1}{1 + e^{-x}}; \\ \text{Softplus}(x) &= \log(1 + e^x); \\ \text{GeLU}(x) &= x\Phi(x) \approx 0.5x(1 + \tanh[\sqrt{2/\pi}(x + 0.044715x^3)]).\end{aligned}$$

Here, Φ is the cumulative distribution function of the standard normal distribution. In comparison to the depth L of convolution layers, the depth L_0 of the Fully Connected Neural Network (FCNN) is typically much smaller. In this study, we focus on the ReLU^k case and set $L_0 = 2$. We emphasize here that we keep using ReLU in the convolution layers and only use ReLU^k in one fully connected layer. As we will show in the approximation error analysis (see Lemma 5 below), the convolution layers are used for calculating the inner products of input x and cubature samples $y_i \in \mathbb{S}^{d-1}$, which is a linear process and ReLU suffices. This aligns with the role of the convolutional layer in extracting features in practical applications. One fully connected layer of ReLU^k is sufficient to implement spline approximation (see Lemma 6 below) and address the phenomena of saturation. Additionally, minimizing the use of ReLU^k as the activation functions in network design helps prevent gradient explosion during training.

The function space \mathcal{F} is defined by the output $F^{(L+L_0+1)}$. More specifically, \mathcal{F} is characterized by network parameters $L, L_0, \{S^{(l)}\}_{l=1}^L, \{d_l\}_{l=L+1}^{L+L_0}$, activation functions $\{\sigma^{(l)}\}_{l=1}^{L+L_0}$, and supremum norm constraints B_i for $i = 1, \dots, 4$:

$$\begin{aligned}\max_{l=1, \dots, L} \|w^{(l)}\|_\infty &\leq B_1, \\ \max_{l=1, \dots, L} \|b^{(l)}\|_\infty &\leq B_2, \\ \max_{l=L+1, \dots, L+L_0+1} \|W^{(l)}\|_{\max} &\leq B_3, \\ \max_{l=L+1, \dots, L+L_0+1} \|b^{(l)}\|_\infty &\leq B_4.\end{aligned}\tag{2.12}$$

Additionally, the total number of free parameters \mathcal{S} also defines the function space. When counting the total number of free parameters, we consider sparsity and parameters sharing in the network, which can lead to a sharper bound on \mathcal{S} , a lower network complexity, and ultimately a faster convergence rate. Another perspective involves restricting the supremum norm of the network output and its derivatives up to the order of s , which is vital for ensuring a bounded condition in the contraction inequality. Therefore, we choose $M > 0$ to ensure

$$\max_{|\alpha| \leq s} \|D^\alpha F^{(L+L_0+1)}\|_\infty \leq M \text{ when restricting } F^{(L+L_0+1)} \text{ on } \mathbb{S}^{d-1}.\tag{2.13}$$

Precisely, we describe the function space \mathcal{F} generated by 1-D CNN, which is given by

$$\mathcal{F}(L, L_0, S, d_{L+1}, \dots, d_{L+L_0}, \text{ReLU}, \text{ReLU}^k, M, \mathcal{S}) = \left\{ F^{(L+L_0+1)} : \mathbb{S}^{d-1} \rightarrow \mathbb{R} \left| \begin{array}{l} F^{(L+L_0+1)} \text{ satisfies (2.13), which} \\ \text{is defined by (2.10) and (2.11) with} \\ S^{(l)} = S, \sigma^{(l)} = \text{ReLU for } l \neq L+1, \\ \sigma^{(l)} = \text{ReLU}^k \text{ for } l = L+1, k \geq s; \\ \text{the total number of free parameters} \\ \text{is less than or equal to } \mathcal{S}. \end{array} \right. \right\}. \quad (2.14)$$

When contextually appropriate, we will continue to use the abbreviated notation, \mathcal{F} , to denote the aforementioned function space. By leveraging an innovative localization technique developed by a series of works [27, 24, 4, 25, 26, 61], our function space associated with CNN does not mandate a sup-norm restriction (2.12) on the network's trainable parameters, setting us apart from the previous analysis in [36]. However, for the sake of comparison, we will provide sup-norm bounds during our discussion of CNN's approximation capabilities. In addition to Assumption 1, we propose a further assumption, as outlined below.

Assumption 2. *The function space, denoted by*

$$\mathcal{F} = \mathcal{F}(L, L_0, S, d_{L+1}, \dots, d_{L+L_0}, \text{ReLU}, \text{ReLU}^k, M, \mathcal{S}),$$

is defined as (2.14). Herein, M is chosen to be sufficiently large such that (2.13) is satisfied and

$$M \geq 3C_9 \|u^*\|_{W_\infty^r(\mathbb{S}^{d-1})}, \quad (2.15)$$

where $u^ \in W_\infty^r(\mathbb{S}^{d-1})$ with $r \geq s+1$ is the unique solution of equation (2.6) and the constant C_9 only depends on d, k and s (see Lemma 11 below).*

2.4 Main Result

In this subsection, our primary focus lies in presenting our main result, where we establish fast convergence rates for PICNN in solving PDEs on spheres. Recall that, the function space denoted by

$$\mathcal{F}(L, L_0, S, d_{L+1}, \dots, d_{L+L_0}, \text{ReLU}, \text{ReLU}^k, M, \mathcal{S})$$

produced by 1D CNNs is provided in (2.14). This space is parameterized by the number of convolutional layers (L), fully connected layers (L_0), the size of convolution kernels (S), the neuron count in fully connected layers ($\{d_l\}_{l=L+1}^{L+L_0}$), and the upper limits of output function and the overall count of free parameters (M and \mathcal{S} respectively). We highlight that the proposed CNN architecture (2.14) is supplemented with downsampling layers and utilizes both ReLU and ReLU^k activation functions. The former activation function is employed on the convolutional layers, while the latter operates on the fully connected layers. Our theoretical analysis and numerical experiments necessitate just $L_0 = 2$. This architecture has displayed impressive results in areas such as natural language processing, speech recognition, and biomedical data classification, as documented in [23] and the references therein. When contrasted with 2D CNNs that are only designed for 2D data like images and videos, 1D CNNs significantly curtail the computational load and are proven to be effective for handling data generated by low-cost applications, especially on portable devices. In this study, we apply

this CNN architecture to solve the spherical PDE represented by (2.6). We will demonstrate that under a regularity condition, i.e., when the spherical PDE (2.6) satisfies Assumption 1, both the excess risk and estimation error of PICNN estimators decay at polynomial rates. For two positive sequences, $\{A_n\}_{n \geq 1}$ and $\{B_n\}_{n \geq 1}$, recall that $A_n \lesssim B_n$ indicates there exists a positive constant C independent of n , such that $A_n \leq CB_n, \forall n \geq 1$. Moreover, we write $A_n \asymp B_n$ if and only if both $A_n \lesssim B_n$ and $B_n \lesssim A_n$ hold true. Recall that u^* denotes the solution of the equation (2.6).

Theorem 1. *Suppose that Assumption 1 is satisfied with some $d \geq 2, s \geq 1, r \geq s + 1$ and Assumption 2 holds. Let $d \geq 2$ and $\mathbf{x} = \{X_i\}_{i=1}^n$ be an i.i.d. sample following the uniform distribution on \mathbb{S}^{d-1} . Choose $3 \leq S \leq d + 1$ and k satisfying*

$$\begin{cases} k = s + \left\lceil \frac{r + s + 2}{d - 3} \right\rceil \geq s + 1, & \text{if } r < \infty, d > 3, \\ k \geq s, & \text{if } r < \infty, 2 \leq d \leq 3 \text{ or } r = \infty, d \geq 2. \end{cases}$$

Let u_n be the estimator of PICNN solving sphere PDE (2.6), which is defined by (2.7) in the function space of CNN

$$\mathcal{F} = \mathcal{F}(L, L_0 = 2, S, d_{L+1}, d_{L+2}, \text{ReLU}, \text{ReLU}^k, M, S)$$

with

$$\begin{aligned} L &\asymp n^{\frac{a(d-1)}{2(r-s)}} (\log n)^{-\frac{a(d-1)}{r-s}}, \\ d_{L+1} &\asymp n^{\frac{a(d+r+s-1)}{2(r-s)(k-s+1)} + \frac{a(d+1)}{2(r-s)}} (\log n)^{-\frac{a(d+r+s-1)}{(r-s)(k-s+1)} - \frac{a(d+1)}{r-s}}, \\ d_{L+2} &\asymp n^{\frac{a(d-1)}{2(r-s)}} (\log n)^{-\frac{a(d-1)}{r-s}}, \end{aligned}$$

and

$$S \asymp \begin{cases} n^{\frac{a(d-1)}{2(r-s)}} (\log n)^{-\frac{a(d-1)}{r-s}}, & \text{if } r < \infty, d > 3, \\ n^{\frac{a(d+r+s-1)}{2(r-s)(k-s+1)} + \frac{a}{r-s}} (\log n)^{-\frac{a(d+r+s-1)}{(r-s)(k-s+1)} - \frac{2a}{r-s}}, & \text{if } r < \infty, 2 \leq d \leq 3 \text{ or } r = \infty, d \geq 2. \end{cases}$$

Here, the constant a is given by

$$a = \begin{cases} \frac{r-s}{(r-s) + (d-1)}, & \text{for } r < \infty, d > 3, \\ 1 - \frac{d(k-s+2) + r+k}{d(k-s+2) + 2(r-s)(k-s+1) + r+k}, & \text{for } r < \infty, 2 \leq d \leq 3, \\ 1 - \frac{1}{2(k-s) + 3}, & \text{for } r = \infty, d \geq 2. \end{cases}$$

Then for all $n \geq 1$, with probability at least $1 - \exp(-n^{1-a}(\log n)^{2a})$, there hold

$$\mathcal{R}(u_n) - \mathcal{R}(u^*) \lesssim n^{-a}(\log n)^{2a}$$

and

$$\|u_n - u^*\|_{H^s(\mathbb{S}^{d-1})} \lesssim n^{-a/2}(\log n)^a.$$

To the best of our knowledge, Theorem 1 provides the first rigorous analysis of convergence for the PINN algorithm with a CNN architecture, thereby demonstrating its practical performance. Recent advancements in the theory of approximation and complexity for deep ReLU CNNs lay the foundation for our results. A significant contribution of our proof is the implementation of a scale-sensitive localization theory with scale-insensitive measures, such as VC-dimension. This approach is coupled with recent work on CNN approximation theory [60, 59, 13, 14], enabling us to derive these elegant bounds and fast rates. The idea of our localization is rooted in the work of [27, 24, 4, 61], which allows us to examine broader classes of neural networks. This contrasts with analyses that limit the networks to have bounded parameters for each unit, a constraint resulting from applying scale-sensitive measures like metric entropy. In our proof, we have broadened previous approximation results and established an estimation of VC-dimensions involving the function spaces generated by CNNs and their derivatives. These results hold significance in their own right and warrant special attention (refer to Section 3 and Section 4). To our knowledge, our work is the first to establish corresponding localization analysis for estimating the part of the stochastic error in the theoretical analysis framework of solving equations with neural networks. Our results can be generalized to theoretical analysis of other PDE solvers with CNNs. The sphere is commonly viewed as the quintessential low-dimension manifold; hence, our work has the potential to be extrapolated to PDE solvers operating on general manifolds. Exploring further possibilities by extending this approach to other neural network architectures and different types of PDEs can certainly be advantageous. We posit, with firm conviction, that for an s -order PDE PINN solver operating on an arbitrary m -dimensional manifold \mathcal{M} embedded in \mathbb{R}^d , and assuming the true solution $u^* \in C^r(\mathcal{M})$ (or within another regularity function space, such as Sobolev space), it is plausible to demonstrate a convergence rate of $n^{-\frac{r-s}{r-s+m}}$ (modulated by a logarithmic factor). This intriguing prospect presents promising avenues for future research.

2.5 Error Decomposition

This subsection primarily establishes the proof structure for Theorem 1, which is derived from an error decomposition of the excess risk that we introduce below. Error decomposition is a standard paradigm for deducing the generalization bounds of the ERM algorithm. Research on algorithmic generalization bounds is a fundamental concern in learning theory. Specifically, it involves providing a theoretical non-asymptotic bound for the excess risk $\mathcal{R}(u_n) - \inf_u \mathcal{R}(u)$ with respect to the number of training samples n . We now apply a standard error decomposition procedure to the excess risk of PINN. If we define $u_{\mathcal{F}} = \arg \min_{u \in \mathcal{F}} \mathcal{R}(u)$, we obtain the following decomposition:

$$\begin{aligned} \mathcal{R}(u_n) - \mathcal{R}(u^*) &\leq (\mathcal{R}(u_{\mathcal{F}}) - \mathcal{R}(u^*)) + (\mathcal{R}_n(u_{\mathcal{F}}) - \mathcal{R}_n(u^*) - \mathcal{R}(u_{\mathcal{F}}) + \mathcal{R}(u^*)) \\ &\quad + (\mathcal{R}(u_n) - \mathcal{R}(u^*) - \mathcal{R}_n(u_n) + \mathcal{R}_n(u^*)). \end{aligned}$$

The first term is often referred to as the approximation error, while the third term is known as the estimation error or statistical error. The second term can be bounded by Bernstein's inequality. See Appendix C. Therefore, it remains to derive upper bounds for the approximation error and the statistical error respectively. In Section 3, we will establish an estimation of the approximation error, and in Section 4, we will develop an estimation of the statistical error. By combining these two, we can derive a generalization bound for the excess risk $\mathcal{R}(u_n) - \mathcal{R}(u^*)$, and hence, provide the proof for Theorem 1. A comprehensive proof of Theorem 1 can be found in Section 5.

3 Approximation Error Analysis

This section focuses on the estimation of the approximation error. We provide a proof sketch here and see Appendix D for details. Recent progress in the approximation theory of deep ReLU CNN [60, 59, 13, 14] and spherical harmonic analysis [9] are important building blocks for our estimates. As referenced in Assumption 1, it is assumed that $u^* \in W_\infty^r(\mathbb{S}^{d-1})$ for some $r \geq s + 1$. To establish the generalization error analysis for spherical data classification, [14] has obtained an $L^p(\mathbb{S}^{d-1})$ norm approximation rate for functions in $W_p^r(\mathbb{S}^{d-1})$ using CNNs. In our PINN setup, the $L^p(\mathbb{S}^{d-1})$ approximation is insufficient as we require an approximation rate of the $H^s(\mathbb{S}^{d-1})$ norm, as outlined by (2.5). Moreover, their work only considers a ReLU network, which is suitable for an $L^p(\mathbb{S}^{d-1})$ norm approximation but not applicable here due to the phenomenon of saturation. Hence, we employ and extend their results to the Sobolev norm approximation and our ReLU-ReLU^k network architectures. The approximator [14] is known as the near-best approximation by polynomials. Let $u \in L^p(\mathbb{S}^{d-1})$ where $1 \leq p \leq \infty$. For $n_0 \in \mathbb{N}$, we define the error of the best approximation to u by polynomials of degree at most n_0 as

$$E_{n_0}(u)_p = \inf_{v \in \Pi_{n_0}(\mathbb{S}^{d-1})} \|u - v\|_p,$$

where $\Pi_{n_0}(\mathbb{S}^{d-1})$ denotes the space of polynomials of degree at most n_0 . Let $\lambda = \frac{d-2}{2}$, and let $C_i^\lambda(t)$ represent the Gegenbauer polynomial of degree i with parameter λ . Given a function $\eta \in C^\infty([0, \infty))$ where $\eta(t) = 1$ for $0 \leq t \leq 1$, $0 \leq \eta(t) \leq 1$ for $1 \leq t \leq 2$, and $\eta(t) = 0$ for $t \geq 2$, we define the kernel l_{n_0} by

$$l_{n_0}(t) = \sum_{i=0}^{2n_0} \eta\left(\frac{i}{n_0}\right) \frac{\lambda+i}{\lambda} C_i^\lambda(t), \quad t \in [-1, 1],$$

and the corresponding linear operator

$$L_{n_0}(u)(x) = \frac{1}{\omega_d} \int_{\mathbb{S}^{d-1}} u(y) l_{n_0}(\langle x, y \rangle) d\sigma(y), \quad x \in \mathbb{S}^{d-1}.$$

When $d = 2$, l_{n_0} and L_{n_0} are well-defined in the sense of limit, by using the relation

$$\lim_{\lambda \rightarrow 0} \frac{1}{\lambda} C_i^\lambda(\cos \theta) = \frac{2}{i} \cos i\theta.$$

This linear operator provides a near-best approximation in the L^p norm. Notice that the construction of the function η is not unique, but we can fix a specific η beforehand in the following statements, i.e., we can construct a uniform η applied to derive all the estimates.

However, $L_{n_0}(u)$ is not the approximator we ultimately use to estimate the error. We introduce a new kernel, \tilde{l}_{n_0} , and a linear operator, \tilde{L}_{n_0} , defined as follows:

$$\begin{aligned} \tilde{l}_{n_0}(t) &= \sum_{i=0}^{2n_0} \left[\eta\left(\frac{i}{n_0}\right) \right]^2 \frac{\lambda+i}{\lambda} C_i^\lambda(t), \quad t \in [-1, 1], \\ \tilde{L}_{n_0}(u)(x) &= \frac{1}{\omega_d} \int_{\mathbb{S}^{d-1}} u(y) \tilde{l}_{n_0}(\langle x, y \rangle) d\sigma(y), \quad x \in \mathbb{S}^{d-1}. \end{aligned} \tag{3.1}$$

Again, when $d = 2$, \tilde{l}_{n_0} and \tilde{L}_{n_0} are well-defined in the sense of limit $\lambda \rightarrow 0$. It should be noted that the function η^2 still meets all the conditions required above for the function η .

Additionally, $\tilde{L}_{n_0}(u)$ exhibits near-best approximation properties. We select $\tilde{L}_{n_0}(u)$ because the integral (3.1) can be discretized using a cubature formula, thereby expressing it as an additive ridge function. According to Lemma 3 in [14], we have the following lemma.

Lemma 3. *Let $u \in L^p(\mathbb{S}^{d-1})$ for $1 \leq p \leq \infty$. Then there exists a constant C_2 only depending on d such that, for all $m \geq C_2 n_0^{d-1}$, there exists a cubature rule $\{(\mu_i, y_i)\}_{i=1}^m$ of degree $4n_0$ with $\mu_i \in \mathbb{R}$, $y_i \in \mathbb{S}^{d-1}$ and we have*

$$\tilde{L}_{n_0}(u)(x) = \sum_{i=1}^m \mu_i L_{n_0}(u)(y_i) l_{n_0}(\langle x, y_i \rangle).$$

As a direct consequence, Lemma 3 in [14] asserts that for all $r \in \mathbb{N}$, $1 \leq p \leq \infty$ and $u \in W_p^r(\mathbb{S}^{d-1})$, one can obtain

$$\left\| u - \sum_{i=1}^m \mu_i L_{n_0}(u)(y_i) l_{n_0}(\langle x, y_i \rangle) \right\|_p \leq C_3 n_0^{-r} \|u\|_{W_p^r(\mathbb{S}^{d-1})}$$

with a constant C_3 only depends on η and d . This approximation bound can be extended to those with respect to the $W_p^s(\mathbb{S}^{d-1})$ norm with $s \leq r - 1$, as illustrated by Chapter 4 of [9].

Lemma 4. *If $u \in W_p^r(\mathbb{S}^{d-1})$ for $1 \leq p \leq \infty$ and $r \in \mathbb{N}$, then there exists a constant C_4 only depending on η and d , such that*

$$\begin{aligned} \left\| u - \sum_{i=1}^m \mu_i L_{n_0}(u)(y_i) l_{n_0}(\langle x, y_i \rangle) \right\|_{W_p^s(\mathbb{S}^{d-1})} &\leq C_4 n_0^{s-r} \|u\|_{W_p^r(\mathbb{S}^{d-1})}, \\ \left\| \sum_{i=1}^m \mu_i L_{n_0}(u)(y_i) l_{n_0}(\langle x, y_i \rangle) \right\|_{W_p^r(\mathbb{S}^{d-1})} &\leq C_4 \|u\|_{W_p^r(\mathbb{S}^{d-1})}. \end{aligned}$$

Remark 3. *According to Theorem 4.8.1 in [9], the approximation bound is also applicable to the Lipschitz space $W_p^{r,\alpha}(\mathbb{S}^{d-1})$ for $r \in \mathbb{N}$ and $\alpha \in [0, 1)$, as indicated by the following:*

$$E_{n_0}(u)_p \leq C_4 n_0^{-r-\alpha} \|u\|_{W_p^{r,\alpha}(\mathbb{S}^{d-1})}.$$

Thus, we can further extend the conclusion of Lemma 4 to encompass fractional-type Sobolev solutions $u \in W_p^r(\mathbb{S}^{d-1})$ where $r \geq 1$ is a real number.

Given the cubature rule $\{(\mu_i, y_i)\}_{i=1}^m$ as claimed in Lemma 3, convolution layers equipped with a downsampling operator can extract the inner product $\langle x, y_i \rangle$ for all $i = 1, \dots, m$ as representative features. The construction of the convolution layers and the total number of free parameters are given in the proof of Lemma 3 in [13]. We prove the sup-norm bounds on trainable parameters in Subsection D.2. Denote the constant 1 vector in \mathbb{R}^s as $\mathbf{1}_s$.

Lemma 5. *For $m \in \mathbb{N}$ and a set of cubature samples $y = \{y_1, \dots, y_m\} \subset \mathbb{S}^{d-1}$, there exists a sequence of convolution kernels $\{w^{(l)}\}_{l=1}^L$ supported on $\{0, \dots, S^{(l)} - 1\}$ of equal size $S^{(l)} = S$ and depth $L \leq \left\lceil \frac{md-1}{S-2} \right\rceil$. Additionally, bias vectors $b^{(l)}$ exist for $l = 1, \dots, L$ such that*

$$\mathcal{D}(F^{(L)}(x)) = \begin{bmatrix} \langle x, y_1 \rangle \\ \vdots \\ \langle x, y_m \rangle \\ 0 \\ \vdots \\ 0 \end{bmatrix} + B^{(L)} \mathbf{1}_{\lfloor \frac{d+L(S-1)}{d} \rfloor},$$

where $B^{(L)} = \prod_{l=1}^L \|w^{(l)}\|_1$. Further, we have the following sup-norm bounds:

$$\begin{aligned} \|w^{(l)}\|_\infty &\leq C_5, \quad l = 1, \dots, L, \\ \|b^{(l)}\|_\infty &\leq C_6^l, \quad l = 1, \dots, L, \end{aligned}$$

Here, the constants C_5 and C_6 only depend on S . The total number of free parameters contributed by $\{w^{(l)}\}_{l=1}^L$ and $\{b^{(l)}\}_{l=1}^L$ is $3LS - L$.

The additive ridge function $\sum_{i=1}^m \mu_i L_{n_0}(u)(y_i) l_{n_0}(\langle x, y_i \rangle)$ is employed to approximate the function $u \in W_p^r(\mathbb{S}^{d-1})$. This approximation requires an intermediary approximation of the univariate function $l_{n_0} : [-1, 1] \rightarrow \mathbb{R}$. For this purpose, the interpolant of B-spline functions is utilized for the ReLU^k FCNN.

Lemma 6. *Given the output $\mathcal{D}(F^{(L)}(x))$ in Lemma 5 from the convolution layers, for $N \in \mathbb{N}$, there exists a ReLU^k FCNN with two hidden layers of width $d_{L+1} = m(k^3 + 4k^2 + 4Nk + k + 8N)/2$ and $d_{L+2} = m$ such that the network output*

$$F^{(L+3)}(x) = \sum_{i=1}^m \mu_i L_{n_0}(u)(y_i) Q_N^{k+1}(l_{n_0})(\langle x, y_i \rangle), \quad (3.2)$$

where $Q_N^{k+1}(l_{n_0})$ is an interpolation spline satisfying

$$\|D^l(l_{n_0} - Q_N^{k+1}(l_{n_0}))\|_\infty \leq \frac{C_8 n_0^{d+2k+1}}{N^{k-l+1}}, \quad l = 0, \dots, k, \quad (3.3)$$

where D^l represents the l -th derivative, constant C_8 only depends on k and d . Moreover, this FCNN satisfies the following boundedness constraints:

$$\begin{aligned} \|W^{(L+1)}\|_{\max} &\lesssim N, & \|b^{(L+1)}\|_\infty &\lesssim NC_6^L, \\ \|W^{(L+2)}\|_{\max} &\leq 5 \cdot 3^{d-2} \cdot (2k+2)^{k+1} n_0^{d-1}, & \|b^{(L+2)}\|_\infty &\leq 5 \cdot 3^{d-2} \cdot (2k+2)^{k+1} n_0^{d-1}, \\ \|W^{(L+3)}\|_{\max} &\leq C_1 \|u\|_\infty, & |b^{(L+3)}| &\leq 5 \cdot 3^{d-2} \cdot (2k+2)^{k+1} n_0^{d-1} C_1 \|u\|_\infty, \end{aligned}$$

where C_1 only depends on η and d , and C_6 is from Lemma 5. The total number of free parameters of this FCNN is $\frac{3}{2} \cdot (k^3 + 4k^2 + 4Nk + k + 8N) + m + 2$.

At the end of this section, we can establish an upper bound for the approximation error $\mathcal{R}(u_{\mathcal{F}}) - \mathcal{R}(u^*)$ utilizing (2.5). Recall that u^* denotes the solution of the equation (2.6).

Theorem 2. *Assume that Assumption 1 is satisfied with some $d \geq 2, s \geq 1$ and $r \geq s + 1$. For any $0 < \varepsilon < \|u^*\|_{W_\infty^r(\mathbb{S}^{d-1})}^2$, let $\delta = \varepsilon / \|u^*\|_{W_\infty^r(\mathbb{S}^{d-1})}^2$ denote the relative error. If we take the function space of CNN*

$$\mathcal{F} = \mathcal{F}(L, L_0 = 2, S, d_{L+1}, d_{L+2}, \text{ReLU}, \text{ReLU}^k, M, \mathcal{S})$$

with

$$3 \leq S \leq d + 1, \quad k \geq s, \quad L \asymp \delta^{-\frac{d-1}{2(r-s)}},$$

$$\begin{aligned}
d_{L+1} &\asymp \delta^{-\frac{d+r+s-1}{2(r-s)(k-s+1)} - \frac{d+1}{2(r-s)}}, & d_{L+2} &\asymp \delta^{-\frac{d-1}{2(r-s)}}, \\
M &\geq 3C_9 \|u^*\|_{W_\infty^r(\mathbb{S}^{d-1})}, \\
\mathcal{S} &\asymp \max \left\{ \delta^{-\frac{d+r+s-1}{2(r-s)(k-s+1)} - \frac{1}{r-s}}, \delta^{-\frac{d-1}{2(r-s)}} \right\},
\end{aligned}$$

where constant C_9 is from Lemma 11 and only depends on d, k and s , then

$$\mathcal{R}(u_{\mathcal{F}}) - \mathcal{R}(u^*) \lesssim \varepsilon, \quad (3.4)$$

where $u_{\mathcal{F}} = \arg \min_{u \in \mathcal{F}} \mathcal{R}(u)$.

Remark 4. As previously emphasized in Remark 3, the bound above is also applicable for $r \in \mathbb{R}$ in the context of fractional Sobolev spaces.

4 Statistical Error Analysis

This section is dedicated to the estimation of statistical error by establishing an important oracle inequality. This can be done by a novel localization analysis, an estimation of the VC-dimension bounds of our CNN space and a peeling technique. We give key results here and refer the readers to Appendix E for details. The localization analysis is developed for the stochastic part of error analysis and presented in Subsection E.1. The VC-dimension bounds of our CNN space and its high-order derivative spaces will turn out to be an upper bound control on the Rademacher complexity of the network. The study by [16] substantiates near-precise VC-dimension bounds for piecewise linear neural networks, laying emphasis on feedforward neural networks with ReLU activation functions. Herein, we offer a novel evaluation on the VC-dimension bound for our specific CNN space, which incorporates derivatives and generalizes a bound for CNNs in [61]. The subsequent theorem, forming a cardinal contribution of this paper, warrants individual consideration owing to its central role in the analysis of stochastic error. Herein, we assume that Assumption 1 and Assumption 2 hold with some $s \geq 1, r \geq s + 1$ and $M > 0$. For ease of notation, we define the set $\{1, 2, \dots, m\}$, for $m \in \mathbb{N}$, as $[m]$. We also use the notation $D^\alpha \mathcal{F} := \{D^\alpha u : \mathbb{S}^{d-1} \rightarrow \mathbb{R} \mid u \in \mathcal{F}\}$.

Definition 1. Given a function class $\mathcal{G} : \mathcal{X} \rightarrow \mathbb{R}$ and a set $X = \{x_i\}_{i=1}^m$ of m points in the input space \mathcal{X} . Let $\text{sgn}(\mathcal{G}) = \{\text{sgn}(g) : g \in \mathcal{G}\}$ be the set of binary functions $\mathcal{X} \rightarrow \{0, 1\}$ induced by \mathcal{G} . If $\text{sgn}(\mathcal{G})$ can compute all dichotomies of X , that is, $\#\{\text{sgn}(g)|_X \in \{0, 1\}^m : g \in \mathcal{G}\} = 2^m$, we say that \mathcal{G} or $\text{sgn}(\mathcal{G})$ shatters X . The Vapnik-Chervonenkis dimension (or VC-dimension) of \mathcal{G} or $\text{sgn}(\mathcal{G})$ is the size of the largest shattered subset of \mathcal{X} , denoted by $\text{VCDim}(\text{sgn}(\mathcal{G}))$. Moreover, we say that X is pseudo-shattered by \mathcal{G} , if there are real numbers r_1, r_2, \dots, r_m , such that for each $v \in \{0, 1\}^m$, there exists a function $g_v \in \mathcal{G}$ with $\text{sgn}(g_v(x_i) - r_i) = v_i$ for $1 \leq i \leq m$. The pseudo-dimension of \mathcal{G} , denoted by $\text{PDim}(\mathcal{G})$, is the maximum cardinality of a subset X of \mathcal{X} that is pseudo-shattered by \mathcal{G} .

Theorem 3. Consider the CNN function space \mathcal{F} defined by (2.14) with hybrid activation functions, i.e., $\sigma^{(l)} = \text{ReLU}$ for $l \neq L+1$, $\sigma^{(L+1)} = \text{ReLU}^k$ with $k \geq s$, which is parameterized by $L, L_0, S^{(l)} \equiv S$ and the total number of free parameters \mathcal{S} . Then for all $|\alpha| \leq s$, it follows that

$$\text{VCDim}(\text{sgn}(D^\alpha \mathcal{F})) \lesssim \mathcal{S}(L + L_0) \log \left(k(L + L_0) \cdot \max\{d_l : l \in [L + L_0]\} \right).$$

Relying on the VC dimension estimates given in Theorem 3, we can utilize a peeling technique to demonstrate an important oracle inequality, which presents an upper bound for statistical error. Extensively studied within the realm of nonparametric statistics, oracle-type inequalities provide valuable insights (see [20] and references therein). In the field of nonparametric statistics, an oracle inequality outlines bounds of the risk associated with an estimator. This inequality offers an asymptotic guarantee for the performance of an estimator by contrasting it with an oracle procedure that possesses knowledge of some unobservable functions or parameters within the model. Theorem 4 establishes an oracle inequality for our PINN model.

Theorem 4. For all $t \geq 0$ and $n \geq \max_{|\alpha| \leq s} \text{PDim}(D^\alpha \mathcal{F}) \vee \frac{8e^2 M^2}{C_{11} + 3}$, with probability at least $1 - \exp(-t)$ we have

$$\mathcal{R}(u_n) - \mathcal{R}(u^*) \lesssim \mathcal{R}(u_{\mathcal{F}}) - \mathcal{R}(u^*) + \frac{\text{VC}_{\mathcal{F}}}{n} \log n + \frac{t}{n} + \frac{\exp(-t)}{\log(n/\log n)}.$$

Here, $C_{11} > 0$ is a constant satisfying the estimate (2.9):

$$\|u - u^*\|_{H^s(\mathbb{S}^{d-1})}^2 \leq C_{11} \|\mathcal{L}(u - u^*)\|_{L^2(\mathbb{S}^{d-1})}^2,$$

and the notation

$$\text{VC}_{\mathcal{F}} := \mathcal{S}(L + L_0) \log \left(k(L + L_0) \cdot \max\{d_l : l \in [L + L_0]\} \right). \quad (4.1)$$

is introduced for convenience, given the recurring usage of this VC-dimension bound.

5 Convergence Analysis: Proof of Theorem 1

In this section, we concentrate on proving Theorem 1 in order to finalize the convergence analysis of our PICNN model. The combination of the approximation bound (Theorem 2) and the oracle inequality (Theorem 4) allows us to infer fast convergence rates for PICNN applied to sphere PDEs.

Proof of Theorem 1. We assume $\varepsilon > 0, t > 0$, with their exact values to be specified later, and we denote the relative error as $\delta = \varepsilon / \|u\|_{W_\infty^r(\mathbb{S}^{d-1})}^2$. If we take the CNN hypothesis space as

$$\mathcal{F} = \mathcal{F}(L, L_0 = 2, S, d_{L+1}, d_{L+2}, \text{ReLU}, \text{ReLU}^k, M, \mathcal{S})$$

with

$$\begin{aligned} 3 \leq S \leq d + 1, \quad k \geq s, \quad L \asymp \delta^{-\frac{d-1}{2(r-s)}}, \\ d_{L+1} \asymp \delta^{-\frac{d+r+s-1}{2(r-s)(k-s+1)} - \frac{d+1}{2(r-s)}}, \quad d_{L+2} \asymp \delta^{-\frac{d-1}{2(r-s)}}, \\ M \geq 3C_9 \|u^*\|_{W_\infty^r(\mathbb{S}^{d-1})}, \\ \mathcal{S} \asymp \max \left\{ \delta^{-\frac{d+r+s-1}{2(r-s)(k-s+1)} - \frac{1}{r-s}}, \delta^{-\frac{d-1}{2(r-s)}} \right\}, \end{aligned}$$

where constant C_9 is from Lemma 11. Then by (3.4), we have

$$\mathcal{R}(u_{\mathcal{F}}) - \mathcal{R}(u^*) \lesssim \varepsilon.$$

By (4.1) one can calculate that

$$\begin{aligned} \text{VC}_{\mathcal{F}} &\lesssim \mathcal{S}(L + L_0) \log \left(k(L + L_0) \cdot \max\{d_l : l \in [L + L_0]\} \right) \\ &\asymp \mathcal{S}L \log(kLd_{L+1}) \\ &\asymp \max \left\{ \delta^{-\frac{d+r+s-1}{2(r-s)(k-s+1)} - \frac{d+1}{2(r-s)}}, \delta^{-\frac{d-1}{r-s}} \right\} \cdot \log(\delta^{-1}) \end{aligned}$$

If $r < \infty$ and $d > 3$, we can balance the terms in $\text{VC}_{\mathcal{F}}$ by choosing

$$k = s + \left\lceil \frac{r + s + 2}{d - 3} \right\rceil \geq s + 1,$$

then

$$\text{VC}_{\mathcal{F}} \lesssim \delta^{-\frac{d-1}{r-s}} \log \delta^{-1}.$$

By Theorem 4, with probability at least $1 - \exp(-t)$,

$$\begin{aligned} &\mathcal{R}(u_n) - \mathcal{R}(u^*) \\ &\lesssim \mathcal{R}(u_{\mathcal{F}}) - \mathcal{R}(u^*) + \frac{\text{VC}_{\mathcal{F}}}{n} \log n + \frac{t}{n} + \frac{\exp(-t)}{\log(n/\log n)} \\ &\lesssim \varepsilon + \frac{\log n}{n} \cdot \varepsilon^{-\frac{d-1}{r-s}} (-\log \varepsilon) + \frac{t}{n} + \frac{\exp(-t)}{\log(n/\log n)}. \end{aligned}$$

The trade-off between the first and second term implies that we can choose

$$\varepsilon = n^{-a}(\log n)^{2a}, \quad a = \frac{r-s}{(r-s) + (d-1)},$$

then with probability at least $1 - \exp(-t)$,

$$\mathcal{R}(u_n) - \mathcal{R}(u^*) \lesssim n^{-a}(\log n)^{2a} + \frac{t}{n} + \frac{\exp(-t)}{\log(n/\log n)}.$$

To specify t , the trade-off between the first and second term implies that we can choose $t = n^{1-a}(\log n)^{2a}$, then with probability at least $1 - \exp(-n^{1-a}(\log n)^{2a})$,

$$\mathcal{R}(u_n) - \mathcal{R}(u^*) \lesssim n^{-a}(\log n)^{2a}.$$

If $r < \infty$ and $2 \leq d \leq 3$, the first term in $\text{VC}_{\mathcal{F}}$ is always dominant. Then

$$\text{VC}_{\mathcal{F}} \lesssim \delta^{-\frac{d+r+s-1}{2(r-s)(k-s+1)} - \frac{d+1}{2(r-s)}} \log \delta^{-1}.$$

Let

$$b = 1 - \frac{d(k-s+2) + r + k}{d(k-s+2) + 2(r-s)(k-s+1) + r + k}.$$

By a similar argument, we can prove with probability at least $1 - \exp(-n^{1-b}(\log n)^{2b})$,

$$\mathcal{R}(u_n) - \mathcal{R}(u^*) \lesssim n^{-b}(\log n)^{2b}.$$

If $r = \infty$, then for all fixed $k \geq s$,

$$\text{VC}_{\mathcal{F}} \lesssim \delta^{-\frac{1}{2(k-s+1)}} \log \delta^{-1}.$$

Let

$$c = 1 - \frac{1}{2(k-s)+3}.$$

By a similar argument, we can prove with probability at least $1 - \exp(-n^{1-c}(\log n)^{2c})$,

$$\mathcal{R}(u_n) - \mathcal{R}(u^*) \lesssim n^{-c}(\log n)^{2c}.$$

By the $H^s(\mathbb{S}^{d-1})$ estimates (2.9), there holds

$$\|u_n - u^*\|_{H^s(\mathbb{S}^{d-1})}^2 \lesssim \mathcal{R}(u_n) - \mathcal{R}(u^*).$$

Then we have finished the proof. \square

Remark 5. *The polynomial convergence rates, established by Theorem 1, is of the form $n^{-a}(\log n)^{2a}$ where the index a is given by*

$$a = \begin{cases} \frac{r-s}{(r-s)+(d-1)}, & \text{if } r < \infty, d > 3, k = s + \left\lceil \frac{r+s+2}{d-3} \right\rceil, \\ 1 - \frac{d(k-s+2) + r + k}{d(k-s+2) + 2(r-s)(k-s+1) + r + k}, & \text{if } r < \infty, 2 \leq d \leq 3, k \geq s, \\ 1 - \frac{1}{2(k-s)+3}, & \text{if } r = \infty, d \geq 2, k \geq s. \end{cases} \quad (5.1)$$

Generally, a bigger k can lead to a faster convergence rate as it can reduce the term

$$\delta^{-\frac{d+r+s-1}{2(r-s)(k-s+1)} - \frac{d+1}{2(r-s)}},$$

which is a key factor in the VC-dimension estimation. Particularly, when $r < \infty, 2 \leq d \leq 3$ or $r = \infty, d \geq 2$, this term dominates the VC-dimension, as

$$\delta^{-\frac{d+r+s-1}{2(r-s)(k-s+1)} - \frac{d+1}{2(r-s)}} \geq \delta^{-\frac{d-1}{r-s}}.$$

Consequently, in such conditions, a larger k can potentially yield a faster convergence rate theoretically. However, the practical application of ReLU^k activation functions with a larger k may introduce complications in optimization due to the gradient explosion phenomenon, as observed in our experimental analysis.

6 Experiments

In this section, we conduct numerical experiments to verify our theoretical findings and shed light on the conditions that save the algorithm from the curse of dimensionality. As per Theorem 1, the convergence rate of the PICNN depends on the order s of the PDE, the smoothness r of the solution u^* , the dimension d , and the activation degrees k of ReLU^k . If the solution is smooth, the convergence rate becomes independent of d , indicating that the PICNN can circumvent the curse of dimensionality.

In this section, we consider Example 1 with $V(x) \equiv 1$ and different f :

$$-\Delta_0 u(x) + u(x) = f(x) \quad x \in \mathbb{S}^{d-1}. \quad (6.1)$$

After generating n training points $\{x^i\}_{i=1}^n \subset \mathbb{S}^{d-1}$ with random uniform sampling, we can compute the loss function as follows:

$$\mathcal{R}_n(u) = \frac{1}{n} \sum_{i=1}^n |\Delta_0 u(x^i) - u(x^i) + f(x^i)|^2,$$

where Δ_0 is substituted by the right hand of the equality (A.2). Note that all the derivatives can be computed by autograd in PyTorch.

Our analysis uses the ReLU-ReLU^k network, but in our preliminary trials, we find it difficult to train due to the singularity of the derivative of ReLU at $x = 0$. Hence, we opt to use GeLU-GeLU^k as a substitute. GeLU is a smooth substitute of ReLU and it was first introduced in [17] by combining the properties from dropout, zoneout and ReLU.

Theorem 1 suggests that as the training data increase, one should choose a more complex CNN architecture to accommodate the dataset and achieve a promised convergence rate. Additionally, different values for d, s, r and k result in various recommended architectures. However, it is challenging to optimize deep and wide CNNs, as they usually require numerous training epochs to reach loss convergence. In addition, for networks of varying scales, other hyper-parameters such as the step size of gradient descent, batch size and number of epochs are also difficult to select, as our theory only covers the generalization analysis but lacks a discussion on optimization. To ensure that all the tests can be easily implemented and obtain unified and comparable results, we fix the CNN and hyper-parameters setting as

- CNN architecture parameters: $S = 3, k = 3, L = 3, L_0 = 2, d_1 = 12, d_2 = 4$ and GeLU-GeLU³ as activation functions. We also use 56 channels in each convolution layer to increase the network expressivity power.
- Optimizer parameters: Adam [22] with sizes 10^{-3} or 10^{-4} , $1/128$ of the training size as batch size and 100 training epochs. Hence every training process takes 12800 parameter iterations.
- Data size: 5120 random points for test size and the train size varies from 128 and up to $2^{18} = 262144$. According to the definition of the minimizer (2.7), no validation set is used and we output the best model with the minimum training loss.

We train the network using the PICNN method on various sizes of sampled data points and we plot the relative test PINN loss against the training size on the log-log scale. All the experiments are conducted using PyTorch in Python. As mentioned in Theorem 1, the PINN loss decreases polynomially fast. Therefore, the scattered points are expected to align on a line, with the estimated slope approximately representing the convergence rate.

6.1 Smooth Solution on 2-D Sphere

We first consider a smooth solution on the 2-D sphere as a toy example. Let $u^*(x_1, x_2, x_3) = x_1 x_2 x_3$. By (A.2) and a straight calculation, $f = 13x_1 x_2 x_3$. The empirical PINN risk or we can say the train PINN loss, can be calculated as

$$\mathcal{R}_n(u) = \frac{1}{n} \sum_{i=1}^n |\Delta_0 u(x_1^i, x_2^i, x_3^i) - u(x_1^i, x_2^i, x_3^i) + 13x_1^i x_2^i x_3^i|^2.$$

Each $x^i \in \mathbb{S}^2$ represents a training point.

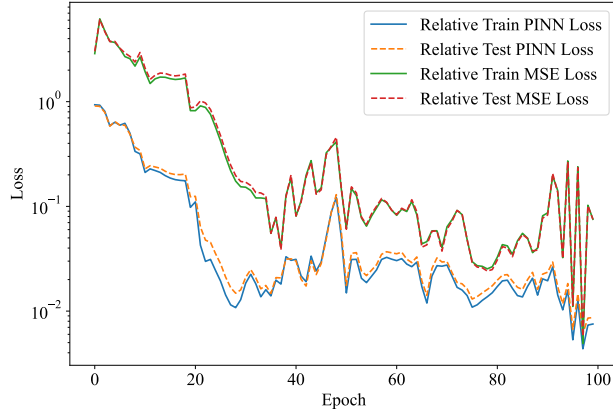


Figure 1: The relative loss history of PICNN model for $u^* = x_1x_2x_3$ on 2-D sphere. Each epoch contains 128 training iterations.

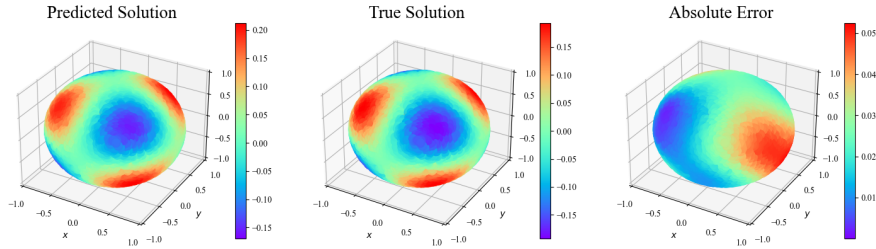


Figure 2: Scatter plots on the test points for $u^* = x_1x_2x_3$ on 2-D sphere. From left to right, we show the predicted solution given by the PICNN, the true solution u^* and the absolute error.

We first show that our PICNN model can learn the solution well. Figure 1 and Figure 2 illustrate the loss history and the absolute error of a trial with 5120 test points but only 256 train points. These four types of relative losses appeared in Figure 1 is defined as

$$\text{Relative Train PINN Loss} = \frac{\frac{1}{n} \sum_{i=1}^n |\Delta_0 u(x^i) - u(x^i) + f(x^i)|^2}{\frac{1}{n} \sum_{i=1}^n |f(x^i)|^2},$$

$$\text{Relative Test PINN Loss} = \frac{\frac{1}{m} \sum_{i=1}^m |\Delta_0 u(y^i) - u(y^i) + f(y^i)|^2}{\frac{1}{m} \sum_{i=1}^m |f(y^i)|^2},$$

$$\text{Relative Train MSE Loss} = \frac{\frac{1}{n} \sum_{i=1}^n |u(x^i) - u^*(x^i)|^2}{\frac{1}{n} \sum_{i=1}^n |u^*(x^i)|^2},$$

$$\text{Relative Test MSE Loss} = \frac{\frac{1}{m} \sum_{i=1}^m |u(y^i) - u^*(y^i)|^2}{\frac{1}{m} \sum_{i=1}^m |u^*(y^i)|^2},$$

where $\{x^i\}_{i=1}^n$ is the train set and $\{y^i\}_{i=1}^m$ is the test set. We observe that the test loss and train loss share a very similar value with a small gap, indicating a strong generalization ability of our model. Besides, the PINN loss and MSE loss follow a similar trend, which is a practical

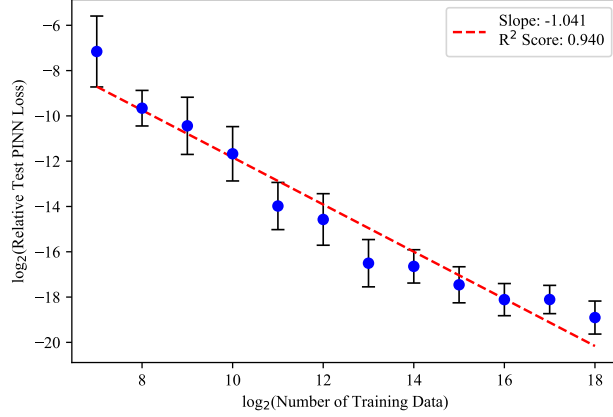


Figure 3: The log-log plot with an estimated convergence slope for $u^* = x_1x_2x_3$ on 2-D sphere. Each point shows the average over 10 replicates.

manifestation of the strong convexity of PINN risk. This emphasizes that the PINN model can learn the true solution accurately using the information from the physical equation.

To validate our theoretical prediction of the fast polynomial convergence rate, we use a log-log plot to visualize the decreasing trend of the PINN loss in Figure 3, with an estimated linear regression slope and the R^2 score. Each point represents the average log PINN loss from 10 independent training trials, with the standard deviation also shown. For a smooth solution, Theorem 1 suggests a decreases slope 0.8 for $k = 3$ and as k increases, the best slope we can expect is 1, which is discovered in our practical test.

6.2 Influence of Smoothness

We now consider other solutions with less smoothness order on the 2-D sphere. We construct

$$\begin{aligned}
 u^*(x_1, x_2, x_3) &= \sum_{i=1}^3 \text{ReLU}^r \left(\frac{1}{2} + \frac{x_i}{r} \right) + \sum_{i=1}^3 \text{ReLU}^r \left(\frac{1}{2} - \frac{x_i}{r} \right), \\
 f(x_1, x_2, x_3) &= \sum_{i=1}^3 \left\{ \text{ReLU}^r \left(\frac{1}{2} + \frac{x_i}{r} \right) + \text{ReLU}^r \left(\frac{1}{2} - \frac{x_i}{r} \right) \right. \\
 &\quad + 2x_i \left[\text{ReLU}^{r-1} \left(\frac{1}{2} + \frac{x_i}{r} \right) - \text{ReLU}^{r-1} \left(\frac{1}{2} - \frac{x_i}{r} \right) \right] \\
 &\quad \left. - \frac{r-1}{r} (1-x_i^2) \left[\text{ReLU}^{r-2} \left(\frac{1}{2} + \frac{x_i}{r} \right) + \text{ReLU}^{r-2} \left(\frac{1}{2} - \frac{x_i}{r} \right) \right] \right\}.
 \end{aligned}$$

Then, one may check that

$$\frac{\partial^r u^*}{\partial x_i^r} = \frac{r!}{r^r} \left(\text{sgn} \left(\frac{1}{2} + \frac{x_i}{r} \right) + (-1)^r \text{sgn} \left(\frac{1}{2} - \frac{x_i}{r} \right) \right)$$

and $u^* \in W_\infty^r(\mathbb{S}^2)$ but $u^* \notin W_\infty^{r+\varepsilon}(\mathbb{S}^2)$ for any $\varepsilon > 0$. We conduct the experiments for various smoothness ranging from $r = 3$ to $r = 8$ and an increasing convergence slope against r is expected by Theorem 1, which is also showed in Figure 4 and Figure 5.

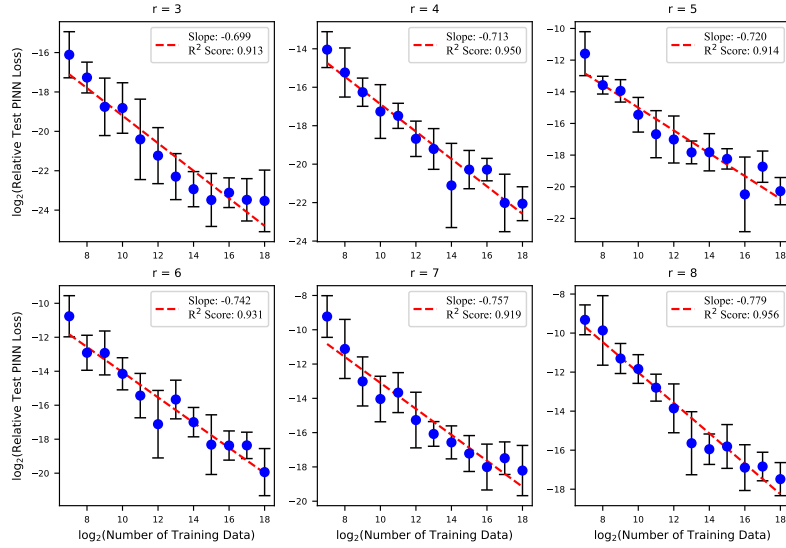


Figure 4: The log-log plot for solutions with different smoothness order on the 2-D sphere. Each point shows the average over 5 replicates.

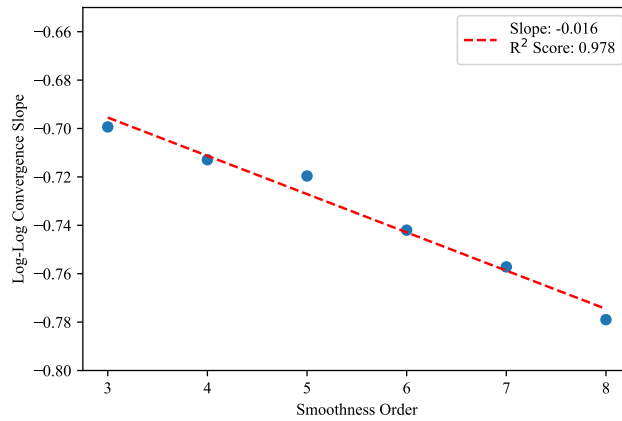


Figure 5: The log-log slope against smoothness order on the 2-D sphere.

6.3 Overcoming the Curse of Dimensionality

The convergence rate is heavily influenced by the dimension, which refers to the phenomenon called the curse of dimensionality. To address it in our framework, reasonable assumptions on the problem must be exploited. In this regard, we propose some promising perspectives.

The first perspective, as we have seen in Theorem 1 and Subsection 6.2, is to assume that the true solution u^* possesses a high degree of smoothness, i.e., $u^* \in W_\infty^r(\mathbb{S}^{d-1})$ with an r comparable to d . Notably, when u^* is smooth ($r = \infty$), Theorem 1 demonstrates that the convergence rate is independent of d . To show this in our experiment, we generalize the experiment from Subsection 6.1 and fix the ground truth solutions as simple polynomials:

$$u^*(x) = \sum_{i=1}^{d-2} x_i x_{i+1} x_{i+2} = x_1 x_2 x_3 + x_2 x_3 x_4 + \cdots + x_{d-2} x_{d-1} x_d, \quad f(x) = (3d+4)u^*(x).$$

Similarly, [36] also considers such polynomials in their experiment. We perform the experiments for various dimensions ranging from $d = 3$ to $d = 10$ and find no significant relationship between the convergence rate and dimension in this problem, as depicted in Figure 6 and Figure 7.

Smooth enough ground truth can lead to a fast convergence rate. However, the increasing d still places high demands on r . To achieve faster convergence, we turn to make use of some special structures of the ground truth function involving the variables. Some previous works have derived fast approximation rates with neural networks for functions of mixed smoothness [48, 10] or anisotropic smoothness [49], Korobov space [42, 39], additive ridge functions [13], radial functions [38] and generalized bandlimited functions [41]. Based on these results, we design ground truth functions $u^* \in W_\infty^3(\mathbb{S}^{d-1})$, similar to those in Subsection 6.2:

$$\begin{aligned} u^*(x_1, \dots, x_d) &= \sum_{i=1}^d \text{ReLU}^3\left(\frac{1}{2} + x_i\right) + \sum_{i=1}^d \text{ReLU}^3\left(\frac{1}{2} - x_i\right), \\ f(x_1, \dots, x_d) &= \sum_{i=1}^d \left\{ \text{ReLU}^3\left(\frac{1}{2} + x_i\right) + \text{ReLU}^3\left(\frac{1}{2} - x_i\right) \right. \\ &\quad \left. + 3(d-1)x_i \left[\text{ReLU}^2\left(\frac{1}{2} + x_i\right) - \text{ReLU}^2\left(\frac{1}{2} - x_i\right) \right] \right. \\ &\quad \left. - 6(1-x_i^2) \left[\text{ReLU}\left(\frac{1}{2} + x_i\right) + \text{ReLU}\left(\frac{1}{2} - x_i\right) \right] \right\}. \end{aligned}$$

Despite having a low general Sobolev smoothness order of $r = 3$, u^* can be expressed as a sum of univariate functions exhibiting isotropic smoothness on each variable. Due to this unique smoothness structure, one can anticipate a fast convergence independent of the increasing dimension for these functions. To verify this claim, we conduct the experiments for various dimensions ranging from $d = 3$ to $d = 10$ and we illustrate this independence in Figure 8 and Figure 9.

Our paper investigates functions and PDEs on sphere \mathbb{S}^{d-1} , which serves as a prime example of a low dimensional manifold embedded in the Euclidean space \mathbb{R}^d . Recall the approximation bound (Theorem 2), the convergence rate $\frac{r-s}{(r-s)+(d-1)}$ derived in our paper and compare to other related results discussing functions and PDEs on \mathbb{R}^d , one can observe

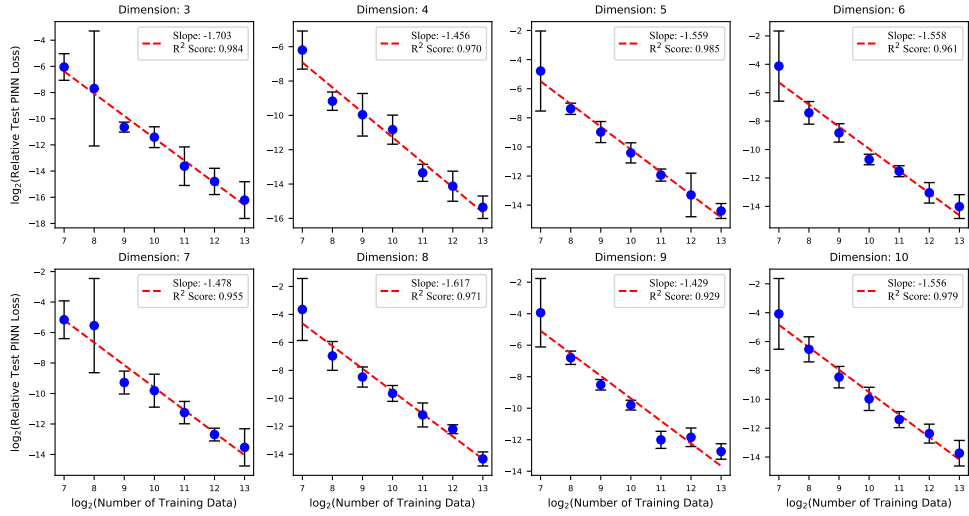


Figure 6: The log-log plot for smooth solutions on $d - 1$ dimension sphere. Each point shows the average over 5 replicates.

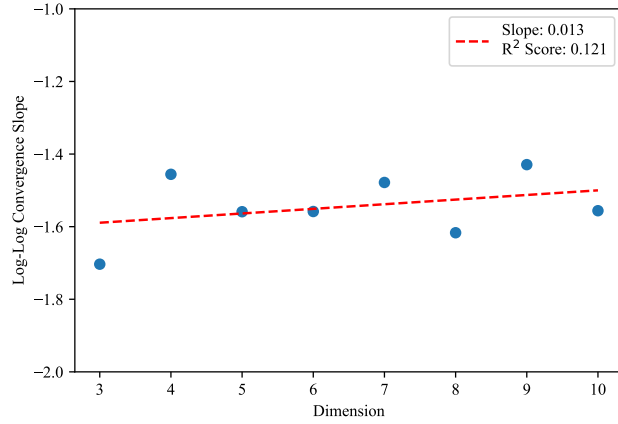


Figure 7: The log-log slope against dimension for smooth solutions on $d - 1$ dimension sphere.

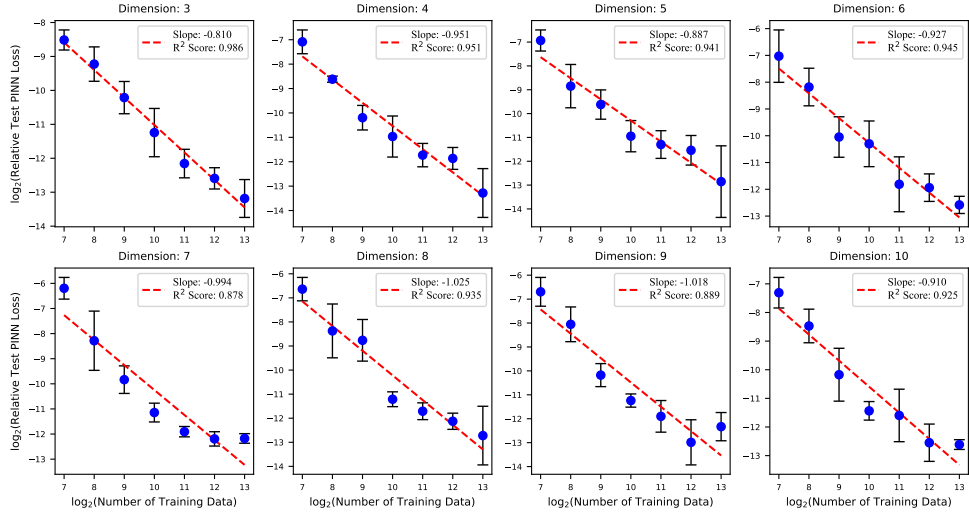


Figure 8: The log-log plot for solutions with special smoothness structure on $d - 1$ dimension sphere. Each point shows the average over 5 replicates.

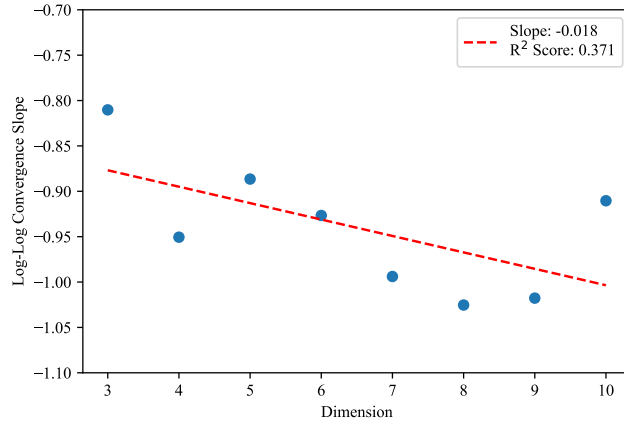


Figure 9: The log-log slope against dimension for solutions with special smoothness structure on $d - 1$ dimension sphere.

that the intrinsic dimension $d - 1$ replaces the ambient dimension d in our rate. This is also an important insight or question in learning theory: can a model accurately approximate functions on low-dimensional manifolds with a convergence rate that depends on the intrinsic dimension rather than the ambient dimension? Recent representative works [45, 7, 34, 8, 19] have studied the approximation, nonparametric regression and binary classification on low dimensional manifolds using deep ReLU network or convolutional residual networks. However, few studies have focused on learning solutions to PDEs on general manifolds by neural networks. While some relative works including [12, 50, 44, 5, 58] consider 2-D manifolds in \mathbb{R}^3 , convergence analysis has not yet been conducted to the best of our knowledge. Inspired by our result, we conjecture that when considering an s -order PDE PINN solver on a general m -dimensional manifold $\mathcal{M} \subset \mathbb{R}^d$ to approximate the true solution $u^* \in C^r(\mathcal{M})$ (or other regularity function spaces like Sobolev spaces), a fast theoretical convergence rate of $n^{-\frac{r-s}{r-s+m}}$ (up to a logarithmic factor) can be derived. To this end, one must extend existing neural network manifold approximation results to the approximation in high-order smoothness norm like Sobolev norm and bound the complexity of the high-order derivatives of neural networks. Additionally, intrinsic properties of PDEs, such as the strong convexity of PINN risk, must be carefully verified in a general manifold formulation.

We summarize that exploiting smoothness structures of the ground truth function, or the low dimensional manifolds setting, is crucial in overcoming the curse of dimensionality. Our experiments and theoretical analyses have demonstrated the former, while the latter is deserved further study in the future.

A The Laplace-Beltrami operator and Sobolev spaces on spheres

We give a brief introduction to the Laplace-Beltrami operator and Sobolev spaces on spheres. One may refer to [9] for more details. Consider a unit sphere $\mathbb{S}^{d-1} \subset \mathbb{R}^d$ for $d \geq 2$. Let Δ_0 symbolize the spherical aspect of the Laplace operator, also known as the Laplace-Beltrami operator, satisfying the equation

$$\Delta = \frac{\partial^2}{\partial \rho^2} + \frac{d-1}{\rho} \frac{\partial}{\partial \rho} + \frac{1}{\rho^2} \Delta_0 \quad (\text{A.1})$$

where $x = \rho\theta$ represents the spherical-polar coordinates, $\rho > 0$ indicates the radius, and $\theta \in \mathbb{S}^{d-1}$. Applying equation (A.1) and

$$\frac{\partial}{\partial \rho} = \frac{1}{\rho} \sum_{i=1}^d x_i \frac{\partial}{\partial x_i},$$

one can directly calculate that

$$\Delta_0 = \sum_{i=1}^d \frac{\partial^2}{\partial x_i^2} - \sum_{i=1}^d \sum_{j=1}^d x_i x_j \frac{\partial^2}{\partial x_i \partial x_j} - (d-1) \sum_{i=1}^d x_i \frac{\partial}{\partial x_i}. \quad (\text{A.2})$$

The operator Δ_0 is self-adjoint. Moreover, the spherical harmonics are eigenfunctions of Δ_0 , with corresponding eigenvalues $\lambda_n = -n(n+d-2)$, where $n = 0, 1, \dots$.

The Sobolev space on a sphere, designated as $W_p^r(\mathbb{S}^{d-1})$, is a particular subset of $L^p(\mathbb{S}^{d-1})$, given that $1 \leq p \leq \infty$ and $r \in \mathbb{N}$. This space is characterized by a finite Sobolev norm:

$$\|f\|_{W_p^r(\mathbb{S}^{d-1})} = \|f\|_p + \sum_{1 \leq i < j \leq d} \|D_{i,j}^r f\|_p,$$

where $\|\cdot\|_p$ denotes the $L^p(\mathbb{S}^{d-1})$ norm corresponding to the uniform measure on \mathbb{S}^{d-1} . Here, $D_{i,j}$ denotes the angular derivatives, defined as

$$D_{i,j} = x_i \frac{\partial}{\partial x_j} - x_j \frac{\partial}{\partial x_i}. \quad (\text{A.3})$$

Interestingly, the Laplace-Beltrami operator, Δ_0 , can be expressed in terms of these angular derivatives:

$$\Delta_0 = \sum_{1 \leq i < j \leq d} D_{i,j}^2.$$

For the case where $p = 2$, $W_2^r(\mathbb{S}^{d-1})$ is recognized as a Hilbert space, for which a specific notation, $H^r(\mathbb{S}^{d-1}) = W_2^r(\mathbb{S}^{d-1})$, is utilized. One could also consider a fractional-type Sobolev space, referred to as the Lipschitz space, denoted as $W_p^{r,\alpha}(\mathbb{S}^{d-1})$, with $\alpha \in [0, 1)$. As such, the Sobolev space $W_p^r(\mathbb{S}^{d-1})$ can be defined where $r \geq 0$. For an elaborate discussion of the Lipschitz space, the reader may refer to Chapter 4 of [9].

B Two PDE examples

We provide two PDE examples that satisfy the strong convexity of the PINN risk.

Example 1. Consider the static Schrödinger equation given by

$$-\Delta_0 u(x) + V(x)u(x) = f(x), \quad x \in \mathbb{S}^{d-1}. \quad (\text{B.1})$$

Notice that Δ_0 is self-adjoint with eigenvalues $\lambda \leq 0$. If V is a strictly positive constant function, then (B.1) has a unique solution u^* and exhibits a relation between the smoothness of f and u^* as described by the elliptic regularity theorem:

$$u^* \in H^r(\mathbb{S}^{d-1}) \iff f \in H^{r-2}(\mathbb{S}^{d-1}).$$

Furthermore, the strong convexity of the PINN risk is demonstrated in relation to the $H^2(\mathbb{S}^{d-1})$ norm: for all $u \in H^2(\mathbb{S}^{d-1})$, it can be computed that

$$\begin{aligned} \mathcal{R}(u) - \mathcal{R}(u^*) &= \frac{1}{\omega_d} \int_{\mathbb{S}^{d-1}} |\Delta_0 u(x) - Vu(x) + f(x)|^2 d\sigma(x) \\ &= \frac{1}{\omega_d} \int_{\mathbb{S}^{d-1}} |\Delta_0 u(x) - Vu(x) - \Delta_0 u^*(x) + Vu^*(x)|^2 d\sigma(x) \\ &= \frac{1}{\omega_d} \int_{\mathbb{S}^{d-1}} (\Delta_0 u - \Delta_0 u^*)^2 + (Vu - Vu^*)^2 - 2(\Delta_0 u - \Delta_0 u^*) \cdot (Vu - Vu^*) d\sigma \\ &= \frac{1}{\omega_d} \int_{\mathbb{S}^{d-1}} (\Delta_0 u - \Delta_0 u^*)^2 + V^2(u - u^*)^2 + 2V \|\nabla_0(u - u^*)\|^2 d\sigma. \end{aligned}$$

where ∇_0 is the projected gradient operator on \mathbb{S}^{d-1} (see Lemma 1.4.4. in [9]). Hence,

$$\frac{\min\{1, V^2, 2V\}}{\omega_d} \|u - u^*\|_{H^2(\mathbb{S}^{d-1})}^2 \leq \mathcal{R}(u) - \mathcal{R}(u^*) \leq \frac{\max\{1, V^2, 2V\}}{\omega_d} \|u - u^*\|_{H^2(\mathbb{S}^{d-1})}^2.$$

Having noticed that this equation enjoys many useful properties, we use it to implement our experiments in Section 6.

Example 2. Consider an elliptic equation of order $2s$ given by

$$(-\Delta_0 + \lambda I)^s u(x) = f(x), \quad x \in \mathbb{S}^{d-1}, \quad (\text{B.2})$$

where $\lambda > 0$. Similar to the discussion in Example 1, we can verify the strong convexity of PINN risk. An alternative definition of the Sobolev space $W_p^r(\mathbb{S}^{d-1})$ employs the operator $-\Delta_0 + I$:

$$\|u\|_{W_p^r(\mathbb{S}^{d-1})} = \|(-\Delta_0 + I)^{r/2} u\|_p.$$

In this context, $r \in \mathbb{R}$ and the fractional power is defined in the distributional sense via the spherical harmonic expansion. Therefore, this equation inherently obeys the regularity theorem, such that

$$u \in W_p^r(\mathbb{S}^{d-1}) \iff f \in W_p^{r-2s}(\mathbb{S}^{d-1}).$$

Accordingly, Assumption 1 is equivalent to assuming that $f \in W_\infty^{r-2s}(\mathbb{S}^{d-1})$ for some $r \geq 2s + 1$.

C Bernstein's bound

Lemma 7. If Assumption 1 and Assumption 2 hold, then for each $u \in \mathcal{F} \cup \{u^*\}$,

$$\mathbb{E}_P(L(X, u) - L(X, u^*))^2 \leq C_0 \mathbb{E}_P(L(X, u) - L(X, u^*)) = C_0(\mathcal{R}(u) - \mathcal{R}(u^*)), \quad (\text{C.1})$$

where P is the uniform distribution on \mathbb{S}^{d-1} , $C_0 = (M \cdot \sum_{|\alpha| \leq s} \|a_\alpha\|_\infty + \|f\|_\infty)^2$ and

$$L(x, u) = |(\mathcal{L}u)(x) - f(x)|^2.$$

Furthermore, for all $t > 0$, with probability at least $1 - \exp(-t)$,

$$\mathcal{R}_n(u_{\mathcal{F}}) - \mathcal{R}_n(u^*) - \mathcal{R}(u_{\mathcal{F}}) + \mathcal{R}(u^*) \leq \mathcal{R}(u_{\mathcal{F}}) - \mathcal{R}(u^*) + \frac{7C_0 t}{6n}.$$

Proof. Notice that u^* is the solution of the equation (2.6), $L(x, u^*) \equiv 0$ so (C.1) holds for $u = u^*$. For $u \in \mathcal{F}$ we have

$$\begin{aligned} & \mathbb{E}_P(L(X, u) - L(X, u^*))^2 \\ &= \frac{1}{\omega_d} \int_{\mathbb{S}^{d-1}} |(\mathcal{L}u)(x) - f(x)|^4 d\sigma(x) \\ &\leq \frac{C_0}{\omega_d} \int_{\mathbb{S}^{d-1}} |(\mathcal{L}u)(x) - f(x)|^2 d\sigma(x) \\ &= C_0 \mathbb{E}_P(L(X, u) - L(X, u^*)). \end{aligned}$$

By Bernstein's inequality and the above estimate, with probability at least $1 - \exp(-t)$,

$$\begin{aligned}
& \mathcal{R}_n(u_{\mathcal{F}}) - \mathcal{R}_n(u^*) - \mathcal{R}(u_{\mathcal{F}}) + \mathcal{R}(u^*) \\
& \leq \sqrt{\frac{2C_0\mathbb{E}_P(L(X, u_{\mathcal{F}}) - L(X, u^*))t}{n}} + \frac{2C_0t}{3n} \\
& \leq \mathbb{E}_P(L(X, u_{\mathcal{F}}) - L(X, u^*)) + \frac{7C_0t}{6n} \\
& = \mathcal{R}(u_{\mathcal{F}}) - \mathcal{R}(u^*) + \frac{7C_0t}{6n}.
\end{aligned}$$

Then we complete the proof. \square

D Supplement for approximation error analysis

Here, we aim to complete the proof in Section 3, through constructing the neural networks and estimating the approximation error. We first introduce an important lemma from [9, Theorem 2.6.3].

Lemma 8. *Let $u \in L^p(\mathbb{S}^{d-1})$ for $1 \leq p \leq \infty$. Then there exists a constant C_1 only depending on η and d , such that for all $n_0 > 0$,*

$$\begin{aligned}
& \|L_{n_0}(u)\|_p \leq C_1\|u\|_p, \\
& \|u - L_{n_0}(u)\|_p \leq (1 + C_1)E_{n_0}(u)_p.
\end{aligned}$$

D.1 Proof of Lemma 4

Recall that $D_{i,j}$ denotes the angular derivatives given by (A.3). We claim that

$$\|D_{i,j}^r(u - L_{n_0}(u))\|_p \leq C_4E_{n_0}(D_{i,j}^r u)_p, \quad 1 \leq i < j \leq d, \quad (\text{D.1})$$

$$\|D_{i,j}^r L_{n_0}(u)\|_p \leq C_4\|D_{i,j}^r u\|_p, \quad 1 \leq i < j \leq d, \quad (\text{D.2})$$

$$E_{n_0}(u)_p \leq C_4n_0^{-r}\|u\|_{W_p^r(\mathbb{S}^{d-1})}. \quad (\text{D.3})$$

Consequently, for any positive integer $s \leq r - 1$ we have

$$\|u - L_{n_0}(u)\|_{W_p^s(\mathbb{S}^{d-1})} \leq C_4n_0^{s-r}\|u\|_{W_p^r(\mathbb{S}^{d-1})}, \quad (\text{D.4})$$

$$\|L_{n_0}(u)\|_{W_p^r(\mathbb{S}^{d-1})} \leq C_4\|u\|_{W_p^r(\mathbb{S}^{d-1})}. \quad (\text{D.5})$$

All these inequalities are also valid for \tilde{L}_{n_0} . Hence, we have

$$\begin{aligned}
& \left\| u - \sum_{i=1}^m \mu_i L_{n_0}(u)(y_i) l_{n_0}(\langle x, y_i \rangle) \right\|_{W_p^s(\mathbb{S}^{d-1})} \leq C_4n_0^{s-r}\|u\|_{W_p^r(\mathbb{S}^{d-1})}, \\
& \left\| \sum_{i=1}^m \mu_i L_{n_0}(u)(y_i) l_{n_0}(\langle x, y_i \rangle) \right\|_{W_p^r(\mathbb{S}^{d-1})} \leq C_4\|u\|_{W_p^r(\mathbb{S}^{d-1})}.
\end{aligned}$$

For the validation of (D.1) and (D.3), one can refer to [9, Theorem 4.5.5 and Corollary 4.5.6]. Inequality (D.2) is a direct consequence of Lemma 8 and the equality $L_{n_0}D_{i,j}^r =$

$D_{i,j}^r L_{n_0}$. For any positive integer $s \leq r - 1$, we write

$$\|u - L_{n_0}(u)\|_{W_p^s(\mathbb{S}^{d-1})} = \|u - L_{n_0}(u)\|_p + \sum_{1 \leq i < j \leq d} \|D_{i,j}^s(u - L_{n_0}(u))\|_p. \quad (\text{D.6})$$

Observing that $D_{i,j}^s u \in W_p^{r-s}(\mathbb{S}^{d-1})$, the combination of (D.1) and (D.3) yields

$$\begin{aligned} \|u - L_{n_0}(u)\|_p &\leq C_4 E_{n_0}(u)_p \leq C_4 n_0^{-r} \|u\|_{W_p^r(\mathbb{S}^{d-1})}, \\ \|D_{i,j}^s(u - L_{n_0}(u))\|_p &\leq C_4 E_{n_0}(D_{i,j}^s u)_p \leq C_4 n_0^{s-r} \|u\|_{W_p^r(\mathbb{S}^{d-1})}. \end{aligned}$$

Combining these inequalities with (D.6) results in (D.4), and (D.5) is a direct inference from (D.2) (with a possible reselection of the constant C_4). Hence, the proof is completed.

D.2 Proof of the sup-norm bounds in Lemma 5

Define a sequence W supported in $\{0, \dots, md-1\}$ as $W_{(j-1)d+(d-i)} = (y_j)_i$, where $j = 1, \dots, m$ and $i = 1, \dots, d$. Following [60, Theorem 3], there exists a sequence of convolution kernels $\{w^{(l)}\}_{l=1}^L$ supported on $\{0, \dots, S-1\}$ with $L = \left\lceil \frac{md-1}{S-2} \right\rceil$ such that W admits the convolutional factorization:

$$W = w^{(L)} * w^{(L-1)} * \dots * w^{(1)}$$

with the corresponding convolution matrices satisfying

$$T = T^{(L)} T^{(L-1)} \dots T^{(1)}.$$

Given a convolution kernel w , one can define a polynomial on \mathbb{C} by $w(z) = \sum_{i=0}^{\infty} w_i z^i$. Also by the proof of [60, Theorem 3], we obtain the following polynomial factorization:

$$W(z) = w^{(L)}(z) w^{(L-1)}(z) \dots w^{(1)}(z),$$

according to the convolutional factorization above.

Considering a rotation of the cubature sample $y = \{y_1, \dots, y_m\}$, we can assume that $y_m = (1, 0, \dots, 0)$, which implies that $W_{md-1} = 1$. Consequently, the polynomial $W(z)$ can be entirely factorized as

$$W(z) = \prod_{i=1}^{s_1} (z^2 - 2x_i z + x_i^2 + y_i^2) \prod_{j=2s_1+1}^{md-1} (z - x_j),$$

comprising $2s_1$ complex roots $x_i \pm iy_i$ and $md - 2s_1 - 1$ real roots x_j , both appearing with multiplicity. We can construct $w^{(l)}$ by taking some quadratic factors and linear factors from the above factorization so that $w^{(l)}(z)$ is a polynomial of degree up to $S - 1$. Employing Cauchy's bound on the magnitudes of all complex roots, we establish that

$$|x_j| \vee |x_i \pm iy_i| \leq 1 + \max \left\{ \left| \frac{W_{md-2}}{W_{md-1}} \right|, \dots, \left| \frac{W_0}{W_{md-1}} \right| \right\} \leq 2.$$

Therefore, the coefficients of $w^{(l)}(z)$ are bounded by a constant C_5 , which depends only on S . This verifies that

$$\|w^{(l)}\|_{\infty} \leq C_5, \quad l = 1, \dots, L.$$

Adopting the proof of [13, Lemma 3], we set $b^{(1)} = -\|w^{(1)}\|_1 \mathbf{1}_{d_1}$ and

$$b^{(l)} = \left(\prod_{i=1}^{l-1} \|w^{(i)}\|_1 \right) T^{(l)} \mathbf{1}_{d_{l-1}} - \left(\prod_{i=1}^l \|w^{(i)}\|_1 \right) \mathbf{1}_{d_l}, \text{ for } l = 2, \dots, L,$$

where $\mathbf{1}_{d_l}$ is the constant 1 vector in \mathbb{R}^{d_l} . Consequently, we find that $\|b^{(1)}\|_\infty = \|w^{(1)}\|_1 \leq S \cdot C_5$ and

$$\|b^{(l)}\|_\infty \leq \left(\prod_{i=1}^{l-1} \|w^{(i)}\|_1 \right) \cdot \|w^{(l)}\|_1 + \prod_{i=1}^l \|w^{(i)}\|_1 \leq 2 \left(\prod_{i=1}^l \|w^{(i)}\|_1 \right) \leq 2S^l C_5^l.$$

Finally setting $C_6 = 2SC_5$ suffices to complete the proof of the sup-norm bounds.

D.3 Proof of Lemma 6

We begin with some preliminaries of B-spline interpolation. Consider u_1, \dots, u_k as functions defined on an interval $I \subset \mathbb{R}$, with $t_1 \leq t_2 \leq \dots \leq t_k$ as points in I . Suppose that

$$t_1, \dots, t_k = \tau_1, \dots, \tau_1, \dots, \tau_l, \dots, \tau_l,$$

where each τ_i is repeated k_i times and $\sum_{i=1}^l k_i = k$. The i -th derivative of u is denoted by $D^i u$, and we define a specific determinant based on these derivatives and the functions, as follows:

$$D \begin{pmatrix} t_1, \dots, t_k \\ u_1, \dots, u_k \end{pmatrix} = \det \begin{bmatrix} u_1(\tau_1) & u_2(\tau_1) & \dots & u_k(\tau_1) \\ Du_1(\tau_1) & Du_2(\tau_1) & \dots & Du_k(\tau_1) \\ \vdots & \vdots & & \vdots \\ D^{k_1-1}u_1(\tau_1) & D^{k_1-1}u_2(\tau_1) & \dots & D^{k_1-1}u_k(\tau_1) \\ \vdots & \vdots & & \vdots \\ u_1(\tau_l) & u_2(\tau_l) & \dots & u_k(\tau_l) \\ Du_1(\tau_l) & Du_2(\tau_l) & \dots & Du_k(\tau_l) \\ \vdots & \vdots & & \vdots \\ D^{k_l-1}u_1(\tau_l) & D^{k_l-1}u_2(\tau_l) & \dots & D^{k_l-1}u_k(\tau_l) \end{bmatrix}.$$

Given an integer $k > 0$, we define the $(k+1)$ -th order divided difference of function f on interval I over points t_1, \dots, t_{k+2} as

$$[t_1, \dots, t_{k+2}]f = \frac{D \begin{pmatrix} t_1, t_2, \dots, t_{k+1}, t_{k+2} \\ 1, x, \dots, x^k, f \end{pmatrix}}{D \begin{pmatrix} t_1, t_2, \dots, t_{k+1}, t_{k+2} \\ 1, x, \dots, x^k, x^{k+1} \end{pmatrix}}.$$

Consider a sequence of real numbers $\dots \leq t_{-1} \leq t_0 \leq t_1 \leq \dots$, and for integers i and $k \geq 0$, we define the normalized $(k+1)$ -th order B-spline associated with t_i, \dots, t_{i+k+1} as

$$N_i^{k+1}(x) = (-1)^{k+1} (t_{i+k+1} - t_i) [t_i, \dots, t_{i+k+1}] (x - t)_+^k.$$

Here we notice that $(x)_+^k$ is exactly the ReLU^k function.

For $N > 0$, we fix an extended uniform partition of $[-1, 1]$:

$$t_1 = \cdots = t_{k+1} = -1 < t_{k+2} < \cdots < t_{2N+k} < 1 = t_{2N+k+1} = \cdots = t_{2N+2k+1}$$

with $t_{k+i+1} = -1 + \frac{i}{N}$ for $i = 0, \dots, 2N$. For $f \in C[-1, 1]$, the corresponding interpolation spline is defined as

$$Q_N^{k+1}(f) = \sum_{i=1}^{2N+k} J_i(f) N_i^{k+1}(x), \quad (\text{D.7})$$

where J_i are certain fixed linear functionals. By [46, Theorem 6.22] we know that

$$\|Q_N^{k+1}(f)\|_\infty \vee |J_i(f)| \leq (2k+2)^{k+1} \|f\|_\infty. \quad (\text{D.8})$$

Moreover, we have the following lemma.

Lemma 9. [46, Corollary 6.21] *There exists a constant C_7 only depending on k such that, for all $f \in C^k[-1, 1]$ and $l = 0, \dots, k$, we have*

$$\|D^l(f - Q_N^{k+1}(f))\|_\infty \leq \frac{C_7}{N^{k-l}} \omega\left(D^k f, \frac{1}{N}\right).$$

Here, $\omega(D^k f, 1/N)$ is the modulus of continuity of the k -th derivative of f :

$$\omega\left(D^k f, \frac{1}{N}\right) = \sup_{\substack{t, t' \in [-1, 1], \\ |t-t'| \leq 1/N}} |D^k f(t) - D^k f(t')|.$$

Indeed, for a particular $l_{n_0} \in C^\infty[-1, 1]$, when $d \geq 3$, given that $\|C_i^\lambda\|_\infty = C_i^\lambda(1) = \binom{i+d-3}{i} \leq (i+1)^{d-3}$, we can establish the following inequality:

$$\|l_{n_0}\|_\infty \leq 5 \cdot 3^{d-2} n_0^{d-1}.$$

Obviously, this inequality also holds when $d = 2$. It is crucial to note that l_{n_0} represents a polynomial of degree at most $2n_0$. Applying the Markov inequality for polynomials, one can derive

$$\omega\left(D^k l_{n_0}, \frac{1}{N}\right) \leq \frac{1}{N} \|D^{k+1} l_{n_0}\|_\infty \leq \frac{1}{N} (2n_0)^{2k+2} \|l_{n_0}\|_\infty \leq \frac{5 \cdot 2^{2k+2} \cdot 3^{d-2} n_0^{d+2k+1}}{N}.$$

As a consequence, we obtain

$$\|D^l(l_{n_0} - Q_N^{k+1}(l_{n_0}))\|_\infty \leq \frac{C_8 n_0^{d+2k+1}}{N^{k-l+1}}$$

where the constant C_8 only depends on k and d , which is exactly (3.3).

To demonstrate that ReLU^k is capable of expressing the interpolation spline function, we rewrite $N_i^{k+1}(x)$ for all $x \in [-1, 1]$ explicitly, as stated by [46, Theorem 4.14 and Equation (4.49)]:

$$N_i^{k+1}(x) = \begin{cases} \sum_{j=1}^{k-i+2} \alpha_{ij} (x+1)_+^{k-j+1} + \sum_{j=1}^i \beta_{ij} (x+t_{k+j+1})_+^k, & 1 \leq i \leq k, \\ \frac{N^k}{k!} \sum_{j=0}^{k+1} (-1)^j \binom{k+1}{j} \left((x-t_i) - \frac{j}{N} \right)_+^k, & k+1 \leq i \leq 2N, \\ \sum_{j=1}^{2N+k-i+1} \gamma_{ij} (x-t_{i+j-1})_+^k, & 2N+1 \leq i \leq 2N+k, \end{cases} \quad (\text{D.9})$$

wherein $\alpha_{ij}, \beta_{ij}, \gamma_{ij}$ are constants depending on N with $\max(|\alpha_{ij}|, |\beta_{ij}|, |\gamma_{ij}|) \leq N^k$. To prove $(x+1)_+^{k-j+1}$ appearing in $N_i^{k+1}(x)$ for $i = 1, \dots, k$ and $j \geq 2$ can be represented using ReLU^k , we propose the following lemma.

Lemma 10. *Given integers $l, k \in \mathbb{N} \cup \{0\}$ with $l < k$, there exist constants ζ_{li} and $\xi_{li}, i = 0, \dots, k$, such that*

$$x^l = \sum_{i=0}^k \xi_{li}(x + \zeta_{li})^k, \quad x \geq 0.$$

Proof. Compare the coefficients on both sides results in a linear system of equations

$$\begin{bmatrix} \zeta_{l,0}^k & \zeta_{l,1}^k & \cdots & \zeta_{l,k}^k \\ \vdots & \vdots & \vdots & \vdots \\ \binom{k}{k-l} \zeta_{l,0}^{k-l} & \binom{k}{k-l} \zeta_{l,1}^{k-l} & \cdots & \binom{k}{k-l} \zeta_{l,k}^{k-l} \\ \vdots & \vdots & \vdots & \vdots \\ 1 & 1 & \dots & 1 \end{bmatrix} \begin{bmatrix} \xi_{l,0} \\ \xi_{l,1} \\ \vdots \\ \xi_{l,k} \end{bmatrix} = \begin{bmatrix} 0 \\ \vdots \\ 1 \\ \vdots \\ 0 \end{bmatrix}.$$

The solution requires finding $\zeta_{li}, i = 0, \dots, k$, such that the matrix is invertible. It is noteworthy that the determinant of the matrix is

$$\prod_{i=1}^k \binom{k}{i} \cdot \prod_{0 \leq i < j \leq k} (\zeta_{li} - \zeta_{lj}).$$

Thus, we only need to ensure that $\zeta_{li} \neq \zeta_{lj}$ for $i \neq j$. The proof is then finished. \square

For $x \in [-1, 1]$, $(x+1)_+ = x+1 \geq 0$, hence Lemma 10 can be applied to $(x+1)_+^{k-j+1}$. We can express $N_i^{k+1}(x)$ as a one hidden layer FCNN using ReLU^k . Now given the output of the convolution layer $\mathcal{D}(F^{(L)}(x))$ as presented in Lemma 5, we build the fully connected layer as follows.

We first consider a simpler FCNN that only accepts one input, denoted as $\langle x, y_1 \rangle + B^{(L)}$, which is also an output of the convolution layer $\mathcal{D}(F^{(L)}(x))$. For $j = 1, \dots, k+1$, Lemma 10 allows us to write

$$\begin{aligned} & \alpha_{ij} (\langle x, y_1 \rangle + 1)_+^{k-j+1} \\ = & \alpha_{ij} \sum_{s=0}^k \xi_{k-j+1,s} (\langle x, y_1 \rangle + \zeta_{k-j+1,s} + 1)_+^k \\ = & \sum_{s=0}^k \text{sgn}(\alpha_{ij} \xi_{k-j+1,s}) \left(\sqrt[k]{|\alpha_{ij} \xi_{k-j+1,s}|} \left(\langle x, y_1 \rangle + B^{(L)} \right) - \sqrt[k]{|\alpha_{ij} \xi_{k-j+1,s}|} \left(B^{(L)} - \zeta_{k-j+1,s} - 1 \right) \right)_+^k. \end{aligned}$$

Let $w = \sqrt[k]{|\alpha_{ij} \xi_{k-j+1,s}|}$ and $b = \sqrt[k]{|\alpha_{ij} \xi_{k-j+1,s}|} (B^{(L)} - \zeta_{k-j+1,s} - 1)$, we see that $|w| \lesssim N$, $|b| \lesssim NB^{(L)} \leq NC_6^L$ where C_6 is the constant from Lemma 5, and

$$\alpha_{ij} (\langle x, y_1 \rangle + 1)_+^{k-j+1} = \sum_{s=0}^k \text{sgn}(\alpha_{ij} \xi_{k-j+1,s}) (w(\mathcal{D}(F^{(L)}(x)))_1 - b)_+^k.$$

Here, $(w(\mathcal{D}(F^{(L)}(x)))_1 - b)_+^k$ can be represented by the output of one single hidden node using ReLU^k . Hence, $\alpha_{ij}(\langle x, y_1 \rangle + 1)_+^{k-j+1}$ is a linear combination of outputs from $k + 1$ hidden nodes. A similar argument also applies to

$$\begin{aligned} & \beta_{ij}(\langle x, y_1 \rangle + t_{k+j+1})_+^k, \\ & \frac{N^k}{k!} (-1)^j \binom{k+1}{j} \left((\langle x, y_1 \rangle - t_i) - \frac{j}{N} \right)_+^k \text{ and} \\ & \gamma_{ij}(\langle x, y_1 \rangle - t_{i+j-1})_+^k. \end{aligned}$$

Each of these terms can be represented as the multiplication of a sign and the output of a single hidden node. After calculating these terms, note by (D.9) that $N_i^{k+1}(\langle x, y_1 \rangle)$ is also a linear combination of them. The overall number of nodes needed to represent $N_i^{k+1}(\langle x, y_1 \rangle)$ is

$$\begin{cases} (k+1)(k-i+2) + i, & \text{for } 1 \leq i \leq k, \\ k+2, & \text{for } k+1 \leq i \leq 2N, \\ 2N+k-i+1, & \text{for } 2N+1 \leq i \leq 2N+k, \end{cases}$$

where the maximum number of nodes, $k^2 + 2k + 2$, is achieved when $i = 1$. By (D.7), $Q_N^{k+1}(l_{n_0})(\langle x, y_1 \rangle)$ can be expressed as a linear combination of $N_i^{k+1}(\langle x, y_1 \rangle)$. The total number of nodes needed to build $Q_N^{k+1}(l_{n_0})(\langle x, y_1 \rangle)$ is

$$\begin{aligned} & \sum_{i=1}^k \left((k+1)(k-i+2) + i \right) + (2N-k)(k+2) + \sum_{i=2N+1}^{2N+k} \left(2N+k-i+1 \right) \\ & = \frac{1}{2}(k^3 + 4k^2 + 4Nk + k + 8N). \end{aligned}$$

We regard $Q_N^{k+1}(l_{n_0})(\langle x, y_1 \rangle)$ as the output of this simpler FCNN which only accepts the input $\langle x, y_1 \rangle + B^{(L)}$ and uses $(k^3 + 4k^2 + 4Nk + k + 8N)/2$ hidden nodes.

Employing the same argument, we can construct m simpler FCNNs, each accepting only a single input, $\langle x, y_i \rangle + B^{(L)}$, and utilizing $(k^3 + 4k^2 + 4Nk + k + 8N)/2$ hidden nodes. These $m(k^3 + 4k^2 + 4Nk + k + 8N)/2$ hidden nodes are concatenated to form the first hidden layer $F^{(L+1)}$ of the FCNN, with the m output nodes forming the second hidden layer $F^{(L+2)}$. The first layer employs ReLU^k , while the second utilizes ReLU , i.e.,

$$\begin{aligned} F^{(L+1)}(x) &= \text{ReLU}^k \left(W^{(L+1)} \mathcal{D}(F^{(L)}(x)) - b^{(L+1)} \right) \in \mathbb{R}^{m(k^3+4k^2+4Nk+k+8N)/2}, \\ F^{(L+2)}(x) &= \text{ReLU} \left(W^{(L+2)} F^{(L+1)}(x) - b^{(L+2)} \right) \in \mathbb{R}^m. \end{aligned}$$

These FCNNs also employ identical parameters, thus resulting in shared weights and

biases. The parameters can be represented as follows:

$$\begin{aligned}
W^{(L+1)} &= \begin{bmatrix} \vec{w}_1 & \vec{0} & \dots & \vec{0} & \vec{0} & \dots & \vec{0} \\ \vec{0} & \vec{w}_1 & \dots & \vec{0} & \vec{0} & \dots & \vec{0} \\ \vdots & \vdots & \dots & \vdots & \vdots & \vdots & \vdots \\ \vec{0} & \vec{0} & \dots & \vec{w}_1 & \vec{0} & \dots & \vec{0} \\ \vec{0} & \vec{0} & \dots & \vec{0} & \vec{w}_1 & \dots & \vec{0} \end{bmatrix} \in \mathbb{R}^{m(k^3+4k^2+4Nk+k+8N)/2 \times [d_L/d]}, \\
b^{(L+1)} &= \begin{bmatrix} \vec{b}_1 \\ \vdots \\ \vec{b}_1 \end{bmatrix} \in \mathbb{R}^{m(k^3+4k^2+4Nk+k+8N)/2}, \\
W^{(L+2)} &= \begin{bmatrix} \vec{w}_2^T & \vec{0} & \dots & \vec{0} & \vec{0} \\ \vec{0} & \vec{w}_2^T & \dots & \vec{0} & \vec{0} \\ \vdots & \vdots & \dots & \vdots & \vdots \\ \vec{0} & \vec{0} & \dots & \vec{w}_2^T & \vec{0} \\ \vec{0} & \vec{0} & \dots & \vec{0} & \vec{w}_2^T \end{bmatrix} \in \mathbb{R}^{m \times m(k^3+4k^2+4Nk+k+8N)/2}, \\
b^{(L+2)} &= b_2 \mathbf{1}_m \in \mathbb{R}^m,
\end{aligned} \tag{D.10}$$

where $\vec{w}_1, \vec{b}_1, \vec{w}_2 \in \mathbb{R}^{(k^3+4k^2+4Nk+k+8N)/2}$, $\vec{0}$ is a 0 constant vector with a suitable size, and

$$b_2 = -\|Q_N^{k+1}(l_{n_0})\|_\infty.$$

From this construction, we see that for $1 \leq i \leq m$,

$$\begin{aligned}
(F^{(L+2)}(x))_i &= \text{ReLU}\left((W^{(L+2)}F^{(L+1)}(x) - b^{(L+2)})_i\right) \\
&= Q_N^{k+1}(l_{n_0})(\langle x, y_i \rangle) + \|Q_N^{k+1}(l_{n_0})\|_\infty.
\end{aligned}$$

Then we apply an additional affine transformation to yield the output for our entire network, e.g.,

$$\begin{aligned}
F^{(L+3)}(x) &= W^{(L+3)} \cdot F^{(L+2)}(x) - b^{(L+3)} \\
&= \sum_{i=1}^m \mu_i L_{n_0}(u)(y_i) (F^{(L+2)}(x))_i - \sum_{i=1}^m \mu_i L_{n_0}(u)(y_i) \|Q_N^{k+1}(l_{n_0})\|_\infty \\
&= \sum_{i=1}^m \mu_i L_{n_0}(u)(y_i) Q_N^{k+1}(l_{n_0})(\langle x, y_i \rangle).
\end{aligned}$$

In conclusion, we have constructed an FCNN with output (3.2) using two hidden layers of width $d_{L+1} = m(k^3 + 4k^2 + 4Nk + k + 8N)/2$ and $d_{L+2} = m$. This FCNN also satisfies the following boundedness constraints:

$$\begin{aligned}
\|W^{(L+1)}\|_{\max} &\lesssim N, \quad \|b^{(L+1)}\|_\infty \lesssim NC^L, \\
\|W^{(L+2)}\|_{\max} &= \max\{|J_i(l_{n_0})| : i = 1, \dots, 2N + k\} \leq 5 \cdot 3^{d-2} \cdot (2k + 2)^{k+1} n_0^{d-1}, \\
\|b^{(L+2)}\|_\infty &= \|Q_N^{k+1}(l_{n_0})\|_\infty \leq 5 \cdot 3^{d-2} \cdot (2k + 2)^{k+1} n_0^{d-1}, \\
\|W^{(L+3)}\|_{\max} &= \max\{|\mu_i L_{n_0}(u)(y_i)| : i = 1, \dots, m\} \leq C_1 \|u\|_\infty, \\
|b^{(L+3)}| &= \left| \sum_{i=1}^m \mu_i L_{n_0}(u)(y_i) \|Q_N^{k+1}(l_{n_0})\|_\infty \right| \leq 5 \cdot 3^{d-2} \cdot (2k + 2)^{k+1} n_0^{d-1} C_1 \|u\|_\infty,
\end{aligned}$$

where C_1 is from Lemma 8 and C_6 is from Lemma 5. The total number of free parameters contributed by the FCNN is

$$\|\vec{w}_1\|_0 + \|\vec{b}_1\|_0 + \|\vec{w}_2\|_0 + 1 + m + 1 = \frac{3}{2} \cdot (k^3 + 4k^2 + 4Nk + k + 8N) + m + 2.$$

The proof is then finished.

D.4 Sobolev approximation lemma

We now present Lemma 11, which asserts the approximation capability of our CNN architecture with respect to the Sobolev norm. The following lemma invokes a definition analogous to definition (2.14) to describe the CNN function space equipped with hybrid activation functions. This is denoted by $\mathcal{F}(L, L_0 = 2, S, d_{L+1}, d_{L+2}, \text{ReLU}, \text{ReLU}^k, M = \infty, \mathcal{S})$. Here, the network in this function space employs activation function $\sigma^{(l)} = \text{ReLU}$ for $l = 1, \dots, L, L+2$ and $\sigma^{(L+1)} = \text{ReLU}^k$. The condition $M = \infty$ signifies there are no constraints on the supremum norm of the output function or its derivatives.

Lemma 11. *Let $d \geq 2$, $3 \leq S \leq d+1$ and $1 \leq p \leq \infty$. Given non-negative integers s, k, r, n_0 satisfying $0 \leq s < \min\{r, k+1\}$ and $n_0 \geq 1$, then for all $u \in W_p^r(\mathbb{S}^{d-1})$, there exists a network*

$$F^{(L+3)} \in \mathcal{F}(L, L_0 = 2, S, d_{L+1}, d_{L+2}, \text{ReLU}, \text{ReLU}^k, M = \infty, \mathcal{S})$$

with

$$L = \left\lceil \frac{C_2 n_0^{d-1} d - 1}{S - 2} \right\rceil, \quad d_{L+1} \asymp n_0^{\frac{d+r+s-1}{k-s+1} + d+1}, \quad d_{L+2} \asymp n_0^{d-1},$$

$$\mathcal{S} \asymp \max \left\{ n_0^{2 + \frac{d+r+s-1}{k-s+1}}, n_0^{d-1} \right\},$$

and a constant C_9 only depending on d, p, k and s , such that

$$\|u - F^{(L+3)}\|_{W_p^s(\mathbb{S}^{d-1})} \leq C_9 n_0^{s-r} \|u\|_{W_p^r(\mathbb{S}^{d-1})}. \quad (\text{D.11})$$

Here, C_2 is the constant from Lemma 3. Furthermore, the network parameters satisfy the sup-norm constraints (2.12) with

$$B_1 = C_5, \quad B_2 = C_6^L, \quad B_3 \lesssim \max \left\{ n_0^{2 + \frac{d+r+s-1}{k-s+1}}, 3^d (k+1)^{k+1} n_0^{d-1} \right\},$$

$$B_4 \lesssim \max \left\{ C_6^L \cdot n_0^{2 + \frac{d+r+s-1}{k-s+1}}, 3^d (k+1)^{k+1} n_0^{d-1} \right\},$$

where the constants C_5 and C_6 are from Lemma 5.

Proof. We first prove (D.11). We leverage Lemma 5 which provides us with the equation

$$\mathcal{D}(F^{(L)}(x)) = (\langle x, y_1 \rangle, \dots, \langle x, y_m \rangle, 0, \dots, 0)^T + B^{(L)} \mathbf{1}_{\left\lfloor \frac{d+L(S-1)}{d} \right\rfloor},$$

where $m = \left\lceil C_2 n_0^{d-1} \right\rceil$ and the cubature rule $\{(\mu_i, y_i)\}_{i=1}^m$ is guaranteed by Lemma 3 for degree $4n_0$. As Lemma 6 stated, we can construct a fully connected neural network with two hidden

layers following the convolution layers. The activation functions of these hidden layers are $\sigma^{(L+1)} = \text{ReLU}^k$ and $\sigma^{(L+2)} = \text{ReLU}$, respectively. This network outputs

$$F^{(L+3)}(x) = \sum_{i=1}^m \mu_i L_{n_0}(u)(y_i) Q_N^{k+1}(l_{n_0})(\langle x, y_i \rangle).$$

Define $B_N^{k+1} = l_{n_0} - Q_N^{k+1}(l_{n_0})$. For $1 \leq i < j \leq d, 1 \leq p < \infty$ and $q = p/(p-1)$, by Hölder's inequality, we have

$$\begin{aligned} & \left\| D_{i,j}^s \left(F^{(L+3)} - \sum_{t=1}^m \mu_t L_{n_0}(u)(y_t) l_{n_0}(\langle \cdot, y_t \rangle) \right) \right\|_p^p \\ &= \frac{1}{\omega_d} \int_{\mathbb{S}^{d-1}} \left| \sum_{t=1}^m \mu_t L_{n_0}(u)(y_t) D_{i,j}^s B_N^{k+1}(\langle x, y_t \rangle) \right|^p d\sigma(x) \\ &\leq \frac{1}{\omega_d} \sum_{t=1}^m \mu_t |L_{n_0}(u)(y_t)|^p \\ &\quad \cdot \int_{\mathbb{S}^{d-1}} \left(\sum_{t=1}^m \mu_t \left| \left(x_i \frac{\partial}{\partial x_j} - x_j \frac{\partial}{\partial x_i} \right)^s B_N^{k+1}(\langle x, y_t \rangle) \right|^q \right)^{\frac{p}{q}} d\sigma(x). \end{aligned} \tag{D.12}$$

It is shown by [14, Theorem 1] that, there exists a constant C'_1 that only depends on d, p and η , such that

$$\sum_{t=1}^m \mu_t |L_{n_0}(u)(y_t)|^p \leq C'_1{}^p \|u\|_{W_p^r(\mathbb{S}^{d-1})}^p.$$

Further, using the chain rule, we can validate the existence of a constant C'_2 depending only on s which ensures that

$$\left| \left(x_i \frac{\partial}{\partial x_j} - x_j \frac{\partial}{\partial x_i} \right)^s B_N^{k+1}(\langle x, y_t \rangle) \right| \leq C'_2 \sum_{i=1}^s \|D^i B_N^{k+1}\|_\infty.$$

By (3.3), there exists a constant C'_3 dependent only on k, s and d such that

$$\sum_{i=1}^s \|D^i B_N^{k+1}\|_\infty \leq \frac{C'_3 n_0^{d+2k+1}}{N^{k-s+1}}.$$

Therefore, we have

$$\begin{aligned} & \frac{1}{\omega_d} \int_{\mathbb{S}^{d-1}} \left(\sum_{t=1}^m \mu_t \left| \left(x_i \frac{\partial}{\partial x_j} - x_j \frac{\partial}{\partial x_i} \right)^s B_N^{k+1}(\langle x, y_t \rangle) \right|^q \right)^{\frac{p}{q}} d\sigma(x) \\ &\leq \left(\frac{C'_2 C'_3 n_0^{d+2k+1}}{N^{k-s+1}} \right)^p \left(\sum_{t=1}^m \mu_t \right)^{\frac{p}{q}} = \left(\frac{C'_2 C'_3 n_0^{d+2k+1}}{N^{k-s+1}} \right)^p. \end{aligned}$$

Combining the aforementioned inequalities, we obtain

$$\left\| D_{i,j}^s \left(F^{(L+3)} - \sum_{t=1}^m \mu_t L_{n_0}(u)(y_t) l_{n_0}(\langle \cdot, y_t \rangle) \right) \right\|_p \leq \frac{C'_1 C'_2 C'_3 n_0^{d+2k+1} \|u\|_{W_p^r(\mathbb{S}^{d-1})}}{N^{k-s+1}}.$$

An analogous process substantiates that (with a reselection of the constants C'_1, C'_2 , and C'_3)

$$\left\| F^{(L+3)} - \sum_{t=1}^m \mu_t L_{n_0}(u)(y_t) l_{n_0}(\langle \cdot, y_t \rangle) \right\|_p \leq \frac{C'_1 C'_2 C'_3 n_0^{d+2k+1} \|u\|_{W_p^r(\mathbb{S}^{d-1})}}{N^{k+1}},$$

and the above analysis pertains equally when $p = \infty$. Therefore, there exists a constant C'_4 only depends on d, p, k, s and η such that

$$\left\| F^{(L+3)} - \sum_{t=1}^m \mu_t L_{n_0}(u)(y_t) l_{n_0}(\langle \cdot, y_t \rangle) \right\|_{W_p^s(\mathbb{S}^{d-1})} \leq \frac{C'_4 n_0^{d+2k+1} \|u\|_{W_p^r(\mathbb{S}^{d-1})}}{N^{k-s+1}}. \quad (\text{D.13})$$

Combining the above estimates with Lemma 4 leads to

$$\begin{aligned} \|u - F^{(L+3)}\|_{W_p^s(\mathbb{S}^{d-1})} &\leq \left\| u - \sum_{i=1}^m \mu_i L_{n_0}(u)(y_i) l_{n_0}(\langle \cdot, y_i \rangle) \right\|_{W_p^s(\mathbb{S}^{d-1})} + \\ &\quad \left\| F^{(L+3)} - \sum_{i=1}^m \mu_i L_{n_0}(u)(y_i) l_{n_0}(\langle \cdot, y_i \rangle) \right\|_{W_p^s(\mathbb{S}^{d-1})} \\ &\leq C_4 n_0^{s-r} \|u\|_{W_p^r(\mathbb{S}^{d-1})} + \frac{C'_4 n_0^{d+2k+1} \|u\|_{W_p^r(\mathbb{S}^{d-1})}}{N^{k-s+1}}. \end{aligned}$$

Next, we select $N = \left\lceil n_0^{\frac{d+r+2k-s+1}{k-s+1}} \right\rceil = \left\lceil n_0^{2+\frac{d+r+s-1}{k-s+1}} \right\rceil$, and noting that η is fixed beforehand, which yields

$$\|u - F^{(L+3)}\|_{W_p^s(\mathbb{S}^{d-1})} \leq C_9 n_0^{s-r} \|u\|_{W_p^r(\mathbb{S}^{d-1})}$$

with a constant C_9 only depends on d, p, k and s . By applying the preceding analysis with $m = \left\lceil C_2 n_0^{d-1} \right\rceil$ and $N = \left\lceil n_0^{2+\frac{d+r+s-1}{k-s+1}} \right\rceil$, we derive the parameters of \mathcal{F} and their corresponding sup-norm constraints. Thus we complete the proof. \square

D.5 Proof of Theorem 2

Now we can complete the proof of Theorem 2, deriving an upper bound of the approximation error. Let

$$n_0 = \left\lceil \delta^{-\frac{1}{2(r-s)}} \right\rceil.$$

Then by Lemma 11, we can take a CNN hypothesis space

$$\mathcal{F} = \mathcal{F}(L, L_0 = 2, S, d_{L+1}, d_{L+2}, \text{ReLU}, \text{ReLU}^k, M = \infty, \mathcal{S})$$

where $L, S, k, d_{L+1}, d_{L+2}, \mathcal{S}$ are specified in Lemma 11. Consequently, there exists a $u \in \mathcal{F}$ satisfying

$$\|u - u^*\|_{W_\infty^s(\mathbb{S}^{d-1})}^2 \leq C_9^2 n_0^{2(s-r)} \|u^*\|_{W_\infty^r(\mathbb{S}^{d-1})}^2 \leq 2C_9^2 \varepsilon, \quad (\text{D.14})$$

where C_9 is from Lemma 11. By the triangle inequality, we can deduce that

$$\|u\|_{W_\infty^s(\mathbb{S}^{d-1})} \leq C_9 \sqrt{2\varepsilon} + \|u^*\|_{W_\infty^r(\mathbb{S}^{d-1})} \leq 3C_9 \|u^*\|_{W_\infty^r(\mathbb{S}^{d-1})}.$$

We then further constrain the function space with the extra sup-norm constraint (2.13) stipulating that

$$M \geq 3C_9 \|u^*\|_{W_\infty^s(\mathbb{S}^{d-1})}.$$

Then we ensure that $u \in \mathcal{F}$ remains valid and that u meets the approximation bound defined in (D.14). Combining (D.14) with (2.5), we conclude that

$$\mathcal{R}(u_{\mathcal{F}}) - \mathcal{R}(u^*) \leq \mathcal{R}(u) - \mathcal{R}(u^*) \lesssim \|u - u^*\|_{W_\infty^s(\mathbb{S}^{d-1})}^2 \leq 2C_9^2 \varepsilon.$$

The proof is then finished.

E Supplement for statistical error analysis

Recall that we have defined $L : \mathbb{S}^{d-1} \times \mathcal{F} \rightarrow \mathbb{R}$ by

$$L(x, u) = |(\mathcal{L}u)(x) - f(x)|^2, \tag{E.1}$$

which measures the residual of equation (2.6). Then the PINN risk is the expectation of L over a uniform distribution P on \mathbb{S}^{d-1} , given by

$$\mathcal{R}(u) = \mathbb{E}_P[L(X, u)].$$

Whereas the empirical PINN risk

$$\mathcal{R}_n(u) = \frac{1}{n} \sum_{i=1}^n L(X_i, u)$$

is the empirical mean of i.i.d. sample $\{X_i\}_{i=1}^n$ from P .

Define the composition of L and \mathcal{F} as

$$L \circ \mathcal{F} = \{g : \mathbb{S}^{d-1} \rightarrow \mathbb{R} | g(x) = L(x, u), u \in \mathcal{F}\}.$$

The Rademacher complexity of $L \circ \mathcal{F}$ plays a pivotal role in bounding the statistical error. For an i.i.d. sequence $\{\varepsilon_i\}_{i=1}^n$ with $\varepsilon_i = \pm 1$ having equal probability independent of X and sample data $\mathbf{x} = \{X_i\}_{i=1}^n$, define the empirical Rademacher complexity of \mathcal{F} as

$$\text{Rad}(\mathcal{F}, \mathbf{x}) = \mathbb{E}_\varepsilon \sup_{u \in \mathcal{F}} \left| \frac{1}{n} \sum_{i=1}^n \varepsilon_i u(X_i) \right|.$$

The Rademacher complexity is calculated by taking a secondary expectation over the sample data:

$$\text{Rad}(\mathcal{F}) := \mathbb{E}_P \mathbb{E}_\varepsilon \sup_{u \in \mathcal{F}} \left| \frac{1}{n} \sum_{i=1}^n \varepsilon_i u(X_i) \right|.$$

Accordingly, the empirical Rademacher complexity and Rademacher complexity of $L \circ \mathcal{F}$ are defined as

$$\begin{aligned} \text{Rad}(L \circ \mathcal{F}, \mathbf{x}) &:= \mathbb{E}_\varepsilon \sup_{u \in \mathcal{F}} \left| \frac{1}{n} \sum_{i=1}^n \varepsilon_i L(X_i, u) \right|, \\ \text{Rad}(L \circ \mathcal{F}) &:= \mathbb{E}_P \mathbb{E}_\varepsilon \sup_{u \in \mathcal{F}} \left| \frac{1}{n} \sum_{i=1}^n \varepsilon_i L(X_i, u) \right|. \end{aligned}$$

Additionally, we will employ the following notations:

$$\begin{aligned}\tilde{\mathcal{F}} &:= \mathcal{F} - u^* = \{u - u^* : u \in \mathcal{F}\}, \\ D^\alpha \tilde{\mathcal{F}} &:= \{D^\alpha(u - u^*) : u \in \mathcal{F}\}, \quad |\alpha| \leq s.\end{aligned}$$

as well as their respective Rademacher complexities in our subsequent analysis.

A frequently applied constraint on L requires it to be Lipschitz with respect to u . This constraint allows us to bound $\text{Rad}(L \circ \mathcal{F}, \mathbf{x})$ by $\text{Rad}(\mathcal{F}, \mathbf{x})$ employing a contraction lemma. Within our PINN framework, note that we impose sup-norm constraints as defined in Assumption 1 and Assumption 2. Consequently, for all $u_1, u_2 \in \mathcal{F} \cup \{u^*\}$, the following is true:

$$\begin{aligned}& |L(x, u_1) - L(x, u_2)| \\ &= |(\mathcal{L}u_1)(x) + (\mathcal{L}u_2)(x) - 2f(x)| \cdot |(\mathcal{L}u_1)(x) - (\mathcal{L}u_2)(x)| \\ &\leq 2 \left(M \cdot \sum_{|\alpha| \leq s} \|a_\alpha\|_\infty + \|f\|_\infty \right) \cdot \left(\sum_{|\alpha| \leq s} \|a_\alpha\|_\infty \cdot |D^\alpha u_1(x) - D^\alpha u_2(x)| \right).\end{aligned}\tag{E.2}$$

Hence, by a contraction technique, we derive the subsequent lemma.

Lemma 12. *Assume that $L(x, u)$ defined by (E.1) is Lipschitz with respect to u . Then*

$$\text{Rad}(L \circ \mathcal{F}, \mathbf{x}) \leq C_{10} \sum_{|\alpha| \leq s} \text{Rad}(D^\alpha \tilde{\mathcal{F}}, \mathbf{x}),$$

where $C_{10} := 4(M \cdot \sum_{|\alpha| \leq s} \|a_\alpha\|_\infty + \|f\|_\infty) \cdot \max_{|\alpha| \leq s} \|a_\alpha\|_\infty$.

Proof. By (E.2), for all $x \in \mathbb{S}^{d-1}$ and $u_1, u_2 \in \mathcal{F} \cup \{u^*\}$ we have

$$\begin{aligned}& |L(x, u_1) - L(x, u_2)| \\ &\leq \frac{C_{10}}{2} \cdot \sum_{|\alpha| \leq s} |D^\alpha u_1(x) - D^\alpha u_2(x)| \\ &= \frac{C_{10}}{2} \cdot \sum_{|\alpha| \leq s} |D^\alpha(u_1 - u^*)(x) - D^\alpha(u_2 - u^*)(x)|.\end{aligned}$$

Using the contraction lemma [30, Theorem 4.12], the Lipschitz property of L yields a bound of the empirical Rademacher complexity:

$$\text{Rad}(L \circ \mathcal{F}, \mathbf{x}) \leq C_{10} \text{Rad}\left(\sum_{|\alpha| \leq s} D^\alpha \tilde{\mathcal{F}}, \mathbf{x}\right) \leq C_{10} \sum_{|\alpha| \leq s} \text{Rad}(D^\alpha \tilde{\mathcal{F}}, \mathbf{x}).$$

The proof is then finished. \square

Next, we aim to establish a novel localized complexity analysis to bound the statistical error by the Rademacher complexity.

E.1 Localized complexity analysis

To estimate the term

$$\mathcal{R}(u_n) - \mathcal{R}(u^*) - \mathcal{R}_n(u_n) + \mathcal{R}_n(u^*),$$

we propose a novel localization approach that makes use of standard tools from empirical process analysis, including peeling, symmetrization, and Dudley's chaining. Firstly, we bound the estimated error by considering the supremum norm of an empirical process:

$$\mathcal{R}(u_n) - \mathcal{R}(u^*) - \mathcal{R}_n(u_n) + \mathcal{R}_n(u^*) \leq \sup_{u \in \mathcal{F}} \mathcal{R}(u) - \mathcal{R}(u^*) - \mathcal{R}_n(u) + \mathcal{R}_n(u^*). \quad (\text{E.3})$$

For all $u \in \mathcal{F}$ and $\gamma > 0$, we define an auxiliary function $g_u : \mathbb{S}^{d-1} \rightarrow \mathbb{R}$ as

$$g_u(x) := L(x, u) - L(x, u^*).$$

Furthermore, for all $\gamma > \inf_{u \in \mathcal{F}} \mathbb{E}_P(g_u(X))$, we introduce the following localized function classes:

$$\begin{aligned} \mathcal{F}_\gamma &:= \{u : \mathbb{S}^{d-1} \rightarrow \mathbb{R} \mid u \in \mathcal{F}, \mathbb{E}_P(g_u(X)) = \mathcal{R}(u) - \mathcal{R}(u^*) \leq \gamma\}, \\ \widetilde{\mathcal{F}}_\gamma &:= \{u - u^* : \mathbb{S}^{d-1} \rightarrow \mathbb{R} \mid u \in \mathcal{F}_\gamma\}, \\ \mathcal{G}_\gamma &:= \{g_u : \mathbb{S}^{d-1} \rightarrow \mathbb{R} \mid u \in \mathcal{F}_\gamma\}, \\ D^\alpha \mathcal{F}_\gamma &:= \{D^\alpha u : \mathbb{S}^{d-1} \rightarrow \mathbb{R} \mid u \in \mathcal{F}_\gamma\}, \\ D^\alpha \widetilde{\mathcal{F}}_\gamma &:= \{D^\alpha u - D^\alpha u^* : \mathbb{S}^{d-1} \rightarrow \mathbb{R} \mid u \in \mathcal{F}_\gamma\}. \end{aligned}$$

Given a sequence of i.i.d. samples $\mathbf{x} = \{X_i\}_{i=1}^n$ and some function class \mathcal{G} of measurable functions on \mathbb{S}^{d-1} , we can define the empirical L^2 -norm $\|\cdot\|_{L^2(\mathbf{x})}$ of $g \in \mathcal{G}$ as

$$\|g\|_{L^2(\mathbf{x})}^2 := \frac{1}{n} \sum_{i=1}^n g(X_i)^2,$$

and the sample expectation as

$$\mathbb{E}_{\mathbf{x}} g := \frac{1}{n} \sum_{i=1}^n g(X_i).$$

Next, we introduce the symmetrization and Dudley's chaining lemmas, which can be found in [4] and [40].

Lemma 13. *Consider an i.i.d. sample sequence $\mathbf{x} = \{X_i\}_{i=1}^n$. For any function $g \in \mathcal{G}$, if $\|g\|_\infty \leq G$ and $\text{Var}(g) \leq V$, then the following inequalities hold: for all $t > 0$, with probability at least $1 - \exp(-t)$,*

$$\sup_{g \in \mathcal{G}} \mathbb{E}_{\mathbf{x}} g - \mathbb{E}_P g \leq 3\text{Rad}(\mathcal{G}) + \sqrt{\frac{2Vt}{n}} + \frac{4Gt}{3n};$$

and with probability at least $1 - 2\exp(-t)$,

$$\sup_{g \in \mathcal{G}} \mathbb{E}_{\mathbf{x}} g - \mathbb{E}_P g \leq 6\text{Rad}(\mathcal{G}, \mathbf{x}) + \sqrt{\frac{2Vt}{n}} + \frac{23Gt}{3n}.$$

The above inequalities are also valid for $\sup_{g \in \mathcal{G}} \mathbb{E}_P g - \mathbb{E}_{\mathbf{x}} g$.

Lemma 14. Let $\mathcal{N}(\delta, \mathcal{G}, \|\cdot\|_{L^2(\mathbf{x})})$ denote the covering number of \mathcal{G} , taking radius δ and metric $\|\cdot\|_{L^2(\mathbf{x})}$. There holds

$$\text{Rad}(\{g : g \in \mathcal{G}, \|g\|_{L^2(\mathbf{x})} \leq \gamma\}, \mathbf{x}) \leq \inf_{0 < \beta < \gamma} \left\{ 4\beta + \frac{12}{\sqrt{n}} \int_{\beta}^{\gamma} \sqrt{\log \mathcal{N}(\delta, \mathcal{G}, \|\cdot\|_{L^2(\mathbf{x})})} d\delta \right\}.$$

The quantity $\log \mathcal{N}(\delta, \mathcal{G}, \|\cdot\|_{L^2(\mathbf{x})})$ is recognized as the metric entropy of \mathcal{G} . Its upper bound can be defined by the pseudo-dimension, hence by the VC-dimension of \mathcal{G} , as outlined in [3, Theorem 12.2 and Theorem 14.1].

Lemma 15. Suppose that for every function $g \in \mathcal{G}$, $\|g\|_{\infty} \leq M$. For a set of points $\{x_i\}_{i=1}^n$, define $\mathcal{G}|_{x_1, \dots, x_n} := \{g|_{x_1, \dots, x_n} : \{x_i\}_{i=1}^n \rightarrow \mathbb{R} | g \in \mathcal{G}\}$. Then for all $n \geq \text{PDim}(\mathcal{F})$ and $\delta > 0$,

$$\mathcal{N}(\delta, \mathcal{G}|_{x_1, \dots, x_n}, \|\cdot\|_{\infty}) \leq \left(\frac{2enM}{\delta \text{PDim}(\mathcal{G})} \right)^{\text{PDim}(\mathcal{G})}.$$

Lemma 16. For a class of neural networks \mathcal{G} with a fixed architecture and fixed activation functions. Then,

$$\text{PDim}(\mathcal{G}) \leq \text{VCDim}(\text{sgn}(\mathcal{G}_0)),$$

where \mathcal{G}_0 is a set extended from \mathcal{G} by adding one extra input neuron and one extra computational neuron. The additional computational neuron is a linear threshold neuron that takes inputs from the output unit of \mathcal{G} and the new input neuron.

When Lemma 14 is later employed, it is essential to control the empirical norm $\|\cdot\|_{L^2(\mathbf{x})}$ by limiting the excess risk $\mathbb{E}_P(g_u(X))$ to no more than γ . We formalize this idea in the following lemma. We define $\kappa = \#\{\alpha : |\alpha| \leq s, a_{\alpha}(\cdot) \neq 0\}$ to represent the number of non-zero terms in \mathcal{L} satisfying Assumption 1.

Lemma 17. For $t > 0$, if

$$\gamma \geq \max_{|\alpha| \leq s} \left\{ 12M \text{Rad}(D^{\alpha} \widetilde{\mathcal{F}}_{\gamma}), \frac{8C_{11}M^2t}{n}, \frac{16M^2t}{3n} \right\},$$

then with probability at least $1 - \kappa \exp(-t)$, there holds

$$\max_{|\alpha| \leq s} \sup_{u \in \mathcal{F}_{\gamma}} \|D^{\alpha}u - D^{\alpha}u^*\|_{L^2(\mathbf{x})} \leq \sqrt{(C_{11} + 3)\gamma},$$

where $C_{11} > 0$ is the constant satisfying the estimate (2.9):

$$\|u - u^*\|_{H^s(\mathbb{S}^{d-1})}^2 \leq C_{11} \|\mathcal{L}(u - u^*)\|_{L^2(\mathbb{S}^{d-1})}^2. \quad (\text{E.4})$$

Proof. Consider the class

$$D^{\alpha} \widetilde{\mathcal{F}}_{\gamma}^2 := \{g^2 : g \in D^{\alpha} \widetilde{\mathcal{F}}_{\gamma}\} = \{(D^{\alpha}u - D^{\alpha}u^*)^2 : u \in \mathcal{F}_{\gamma}\}.$$

Note that for all $u \in \mathcal{F}_{\gamma}$ and $|\alpha| \leq s$, we have $\|(D^{\alpha}u - D^{\alpha}u^*)^2\|_{\infty} \leq 4M^2$ and by (E.4),

$$\text{Var}((D^{\alpha}u - D^{\alpha}u^*)^2) \leq \mathbb{E}_P[(D^{\alpha}u - D^{\alpha}u^*)^4] \leq 4M^2 C_{11} (\mathcal{R}(u) - \mathcal{R}(u^*)) \leq 4C_{11} M^2 \gamma.$$

Apply Lemma 13 to $D^\alpha \widetilde{\mathcal{F}}_\gamma^2$. With probability at least $1 - \exp(-t)$, we have

$$\begin{aligned} & \sup_{u \in \mathcal{F}_\gamma} \|D^\alpha u - D^\alpha u^*\|_{L^2(\mathbf{x})}^2 - \mathbb{E}_P[(D^\alpha u - D^\alpha u^*)^2] \\ & \leq 3\text{Rad}(D^\alpha \widetilde{\mathcal{F}}_\gamma^2) + \sqrt{\frac{8C_{11}M^2\gamma t}{n}} + \frac{16M^2t}{3n}. \end{aligned}$$

Note that $\|D^\alpha u - D^\alpha u^*\|_\infty \leq 2M$ and the square function is locally $4M$ Lipschitz on $[-2M, 2M]$. By the contraction lemma [30, Theorem 4.12], we have

$$\text{Rad}(D^\alpha \widetilde{\mathcal{F}}_\gamma^2) \leq 4M\text{Rad}(D^\alpha \widetilde{\mathcal{F}}_\gamma).$$

Hence, if we choose

$$\gamma \geq \max_{|\alpha| \leq s} \left\{ 12M\text{Rad}(D^\alpha \widetilde{\mathcal{F}}_\gamma), \frac{8C_{11}M^2t}{n}, \frac{16M^2t}{3n} \right\},$$

then with probability at least $1 - \exp(-t)$,

$$\sup_{u \in \mathcal{F}_\gamma} \|D^\alpha u - D^\alpha u^*\|_{L^2(\mathbf{x})}^2 \leq \sup_{u \in \mathcal{F}_\gamma} \mathbb{E}_P[(D^\alpha u - D^\alpha u^*)^2] + \gamma + \gamma + \gamma \leq (C_{11} + 3)\gamma,$$

This probability inequality holds for all $|\alpha| \leq s$. By the union bound, we have finished the proof. \square

E.2 Proof of Theorem 3

This subsection provides a proof on the VC-dimension bound for our specific CNN space. For such an endeavor, the ensuing lemma is essential.

Lemma 18. [3, Theorem 8.3] *Suppose p_1, \dots, p_m represent polynomials of degree not exceeding q in $t \leq m$ variables. Let the sign function be defined as $\text{sgn}(x) := \mathbf{1}_{x>0}$ and consider*

$$K := |\{(\text{sgn}(p_1(x)), \dots, \text{sgn}(p_m(x))) : x \in \mathbb{R}^t\}|,$$

where K denotes the total quantity of all sign vectors furnished by p_1, \dots, p_m . Then, we have $K \leq 2(2emq/t)^t$.

Recall that in our CNN space, for $l \in [L]$, the convolution kernel $w^{(l)}$ and bias $b^{(l)}$ are the parameters of convolutional layer l . For $l \geq L + 1$, the weight matrices $W^{(l)}$ and bias $b^{(l)}$ are the parameters of fully connected layer l . Let \mathcal{S}_l denote the total number of free parameters up to layer l and $\theta^{(l)} \in \mathbb{R}^{\mathcal{S}_l}$ denote the concatenated free parameters vector up to layer l . We see that $\mathcal{S}_1 \leq \mathcal{S}_2 \leq \dots \leq \mathcal{S}_{L+L_0+1} = \mathcal{S}$.

We first consider the function space \mathcal{F} itself. For simplicity, let $f(x; \theta)$ denote the output of network with input $x \in \mathbb{R}^d$ and parameters vector $\theta \in \mathbb{R}^{\mathcal{S}}$. Thus, every $\theta \in \mathbb{R}^{\mathcal{S}}$ corresponds to a unique $f(\cdot; \theta) \in \mathcal{F}$. Assume that the VC-dimension of the network is m so we can let $\{x^1, \dots, x^m\} \subset \mathbb{R}^d$ be a shattered set, that is,

$$K := |\{(\text{sgn}(f(x^1; \theta)), \dots, \text{sgn}(f(x^m; \theta))) : \theta \in \mathbb{R}^{\mathcal{S}}\}| = 2^m.$$

If $m \leq \mathcal{S}$, the conclusion is immediate so we assume that $m > \mathcal{S}$. We will give a bound for K , which will imply a bound for m .

To this end, we find a partition \mathcal{P} of the parameter space $\mathbb{R}^{\mathcal{S}}$ such that for all $P \in \mathcal{P}$, the functions $f(x^1; \cdot), \dots, f(x^m; \cdot)$ are polynomials on P . Then,

$$K \leq \sum_{P \in \mathcal{P}} |\{(\text{sgn}(f(x^1; \theta)), \dots, \text{sgn}(f(x^m; \theta))) : \theta \in P\}|, \quad (\text{E.5})$$

and we can bound the summand by Lemma 18. To construct such \mathcal{P} , we follow an inductive step to construct a sequence of partitions $\mathcal{P}_1, \mathcal{P}_2, \dots, \mathcal{P}_{L+L_0} = \mathcal{P}$, where \mathcal{P}_i is a refinement of \mathcal{P}_{i-1} . For $l \in [L], i \in [d_l]$ and $j \in [m]$, let

$$h_{l,i}(x^j; \theta) := \sum_{s=1}^{d_{l-1}} w_{i-s}^{(l)} (F^{(l-1)}(x^j; \theta))_s - b_i^{(l)}, \quad (\text{E.6})$$

i.e., $h_{l,i}(x^j; \theta)$ is the input into the i -th neuron in the l -th layer which is inactive. Hence

$$(F^{(l)}(x^j; \theta))_i = \sigma^{(l)}(h_{l,i}(x^j; \theta)) = \text{ReLU}(h_{l,i}(x^j; \theta)), \quad (\text{E.7})$$

where we note that we abbreviate the dependency of θ when defining $F^{(l)}(x^j; \theta)$ in Subsection 2.3 but we emphasize it in this proof.

We start with $l = 1$. Consider the concatenated vector $(\text{sgn}(h_{1,i}(x^j; \cdot)))_{i \in [d_1], j \in [m]}$. Since each $h_{1,i}(x^j; \cdot)$ is a polynomial of degree 1 in $\mathcal{S}_1 \leq \mathcal{S} < md_1$ variables, by Lemma 18, we can choose a partition \mathcal{P}_1 of $\mathbb{R}^{\mathcal{S}}$ such that $|\mathcal{P}_1| \leq 2(2emd_1/\mathcal{S}_1)^{\mathcal{S}_1}$ and the concatenated vector $(\text{sgn}(h_{1,i}(x^j; \cdot)))_{i \in [d_1], j \in [m]}$ is constant in each $P \in \mathcal{P}_1$. By (E.7), clearly, in each $P \in \mathcal{P}_1$, each $(F^{(1)}(x^j; \cdot))_i$ is either a polynomial of degree 1 or a zero function in \mathcal{S}_1 variables.

In the induction step, suppose that we have constructed $\mathcal{P}_1, \dots, \mathcal{P}_{l-1}$ for an $l \in [L]$, and for $i \in [d_{l-1}], j \in [m]$, $(F^{(l-1)}(x^j; \cdot))_i$ is a polynomial of degree at most $l-1$ in \mathcal{S}_{l-1} variables in any $P \in \mathcal{P}_{l-1}$. By (E.6) we see that for $i \in [d_l], j \in [m]$, $h_{l,i}(x^j; \cdot)$ is a polynomial of degree at most l in $\mathcal{S}_l < md_l$ variables in any $P \in \mathcal{P}_{l-1}$. By Lemma 18, we can take a partition $\mathcal{P}_{P,l}$ of P such that $|\mathcal{P}_{P,l}| \leq 2(2elmd_l/\mathcal{S}_l)^{\mathcal{S}_l}$ and in each $P' \in \mathcal{P}_{P,l}$, the concatenated vector $(\text{sgn}(h_{l,i}(x^j; \cdot)))_{i \in [d_l], j \in [m]}$ is a fixed value vector. Define

$$\mathcal{P}_l := \bigcup_{P \in \mathcal{P}_{l-1}} \mathcal{P}_{P,l}.$$

Then by (E.7), in each $P \in \mathcal{P}_l$, each $(F^{(l)}(x^j; \cdot))_i$ is either a polynomial of degree at most l or a zero function. Moreover, we have

$$|\mathcal{P}_l| \leq 2(2elmd_l/\mathcal{S}_l)^{\mathcal{S}_l} |\mathcal{P}_{l-1}|.$$

The case for $l = L+1$ needs an additional discussion. For $i \in [d_{L+1}]$ and $j \in [m]$, let

$$h_{L+1,i}(x^j; \theta) := \sum_{s=1}^{\lfloor d_L/d \rfloor} (W^{(L+1)})_{i,s} (\mathcal{D}(F^{(L)}(x^j; \theta)))_s - b_i^{(L+1)}.$$

Clearly, by induction, $h_{L+1,i}(x^j; \cdot)$ is a polynomial of degree at most $L+1$ in $\mathcal{S}_{L+1} < md_{L+1}$ variables in each $P \in \mathcal{P}_L$. Similarly, we can take a \mathcal{P}_{L+1} such that

$$|\mathcal{P}_{L+1}| \leq 2(2e(L+1)md_{L+1}/\mathcal{S}_{L+1})^{\mathcal{S}_{L+1}} |\mathcal{P}_L|.$$

In each $P \in \mathcal{P}_{L+1}$, each $(F^{(L+1)}(x^j; \cdot))_i = \text{ReLU}^k(h_{L+1,i}(x^j; \cdot))$ is either a polynomial of degree at most $k(L+1)$ or a zero function. Hence we can carry on our induction to $l \geq L+1$. We conclude that, a partition $\mathcal{P} = \mathcal{P}_{L+L_0}$ of $\mathbb{R}^{\mathcal{S}}$ can be constructed. In each $P \in \mathcal{P}$, $(F^{(L+L_0)}(x^j; \cdot))_i$ is a polynomial of degree at most $k(L+1) + L_0 - 1$ or zero function in \mathcal{S}_{L+L_0} variables. Now, the $(L+L_0+1)$ -th layer has a single output neuron and

$$f(x^j; \cdot) = \sum_{s=1}^{d_{L+L_0}} (W^{(L+L_0+1)})_s (F^{(L+L_0)}(x^j; \cdot))_s - b^{(L+L_0+1)}$$

is a polynomial of degree at most $k(L+1) + L_0$ in $\mathcal{S}_{L+L_0+1} = \mathcal{S} < m$ variables in any $P \in \mathcal{P}$. By Lemma 18 and (E.5), we conclude that

$$\begin{aligned} 2^m &= K \leq 2 \left(\frac{2e(k(L+1) + L_0)m}{\mathcal{S}} \right)^{\mathcal{S}} |\mathcal{P}| \\ &\leq 2^{L+L_0+1} \left(\frac{2e(k(L+1) + L_0)m}{\mathcal{S}} \right)^{\mathcal{S}} \\ &\quad \cdot \prod_{l=1}^{L+1} \left(\frac{2elmd_l}{\mathcal{S}_l} \right)^{\mathcal{S}_l} \prod_{l=L+2}^{L+L_0} \left(\frac{2e(k(L+1) + l - L - 1)md_l}{\mathcal{S}_l} \right)^{\mathcal{S}_l} \\ &\leq 2^{2(L+L_0)} \left(4emk(L+L_0) \cdot \max\{d_l : l \in [L+L_0]\} \right)^{2\mathcal{S}(L+L_0)} \end{aligned}$$

where we use crude bounds $L+L_0+1 \leq 2(L+L_0)$, $\mathcal{S}_l \leq \mathcal{S}$, $k(L+1) + L_0 \leq 2k(L+L_0)$ and $d_l \leq \max\{d_l : l \in [L+L_0]\}$. Taking logarithms we yield that

$$\begin{aligned} m &\leq 2(L+L_0) + 2\mathcal{S}(L+L_0) \log_2 \left(4emk(L+L_0) \cdot \max\{d_l : l \in [L+L_0]\} \right) \\ &\leq 4\mathcal{S}(L+L_0) \log_2 \left(4emk(L+L_0) \cdot \max\{d_l : l \in [L+L_0]\} \right), \end{aligned}$$

which implies

$$m \lesssim \mathcal{S}(L+L_0) \log \left(k(L+L_0) \cdot \max\{d_l : l \in [L+L_0]\} \right).$$

Now we turn to bound the VC-dimension of the derivatives of functions in our CNN function space. To this end, we first bound the VC-dimension of the derivative $\text{sgn}(\partial\mathcal{F}/\partial x_1)$ following a similar step. For simplicity, let $f'(x; \theta) := \partial f(x; \theta)/\partial x_1$. In a slight abuse of notation, assume that the VC-dimension of $\text{sgn}(\mathcal{F}')$ is $m > \mathcal{S}$ and let $\{x^1, \dots, x^m\} \subset \mathbb{R}^d$ be a shattered set. Define

$$K := |\{(\text{sgn}(f'(x^1; \theta)), \dots, \text{sgn}(f'(x^m; \theta))) : \theta \in \mathbb{R}^{\mathcal{S}}\}| = 2^m.$$

For $l=1$ and $i \in [d_1]$, we have

$$h'_{1,i}(x^j; \theta) = w_{i-1}^{(1)}. \quad (\text{E.8})$$

For $l=2, \dots, L$ and $i \in [d_l]$, we have

$$h'_{l,i}(x; \theta) = \sum_{s=1}^{d_{l-1}} w_{i-s}^{(l)} (F^{(l-1)'})_s(x; \theta) = \sum_{s=1}^{d_{l-1}} w_{i-s}^{(l)} h'_{l-1,s}(x; \theta) \text{sgn}(h_{l-1,s}(x; \theta)). \quad (\text{E.9})$$

For $l = L + 1$ and $i \in [d_{L+1}]$, we have

$$\begin{aligned} h'_{L+1,i}(x; \theta) &= \sum_{s=1}^{\lfloor d_L/d \rfloor} (W^{(L+1)})_{i,s} (\mathcal{D}(F^{(L)'}(x^j; \theta)))_s \\ &= \sum_{s=1}^{\lfloor d_L/d \rfloor} (W^{(L+1)})_{i,s} h'_{L,sd}(x; \theta) \text{sgn}(h_{L,sd}(x; \theta)). \end{aligned} \quad (\text{E.10})$$

For $l = L + 2$ and $i \in [d_{L+2}]$, we have

$$\begin{aligned} h'_{L+2,i}(x; \theta) &= \sum_{s=1}^{d_{L+1}} (W^{(L+2)})_{i,s} (F^{(L+1)'}(x^j; \theta))_s \\ &= k \sum_{s=1}^{d_{L+1}} (W^{(L+1)})_{i,s} h'_{L+1,s}(x; \theta) h_{L+1,s}^{k-1}(x; \theta) \text{sgn}(h_{L+1,s}(x; \theta)). \end{aligned}$$

For $l \geq L + 3$ and $i \in [d_l]$, we have

$$h'_{l,i}(x; \theta) = \sum_{s=1}^{d_{l-1}} (W^{(l)})_{i,s} h'_{l-1,s}(x; \theta) \text{sgn}(h_{l-1,s}(x; \theta)).$$

Define $[\lfloor d_L/d \rfloor]d := \{d, 2d, \dots, \lfloor d_L/d \rfloor d\} \subset \mathbb{Z}$. By induction, for the derivative of the network output, we can write

$$f'(x; \theta) = k \sum_s \left[\left(\prod_{l=1}^{L+L_0+1} \theta_{l,s} \right) \cdot \left(\prod_{l=1}^{L+L_0} \text{sgn}(h_{l,s_l}(x; \theta)) \right) \cdot h_{L+1,s_{L+1}}^{k-1}(x; \theta) \right], \quad (\text{E.11})$$

where s running all over $\prod_{l=1}^{L-1} [d_l] \times [\lfloor d_L/d \rfloor]d \times \prod_{l=L+1}^{L+L_0} [d_l] \subset \mathbb{Z}^{L+L_0}$ and $\theta_{l,s}$ is a specific parameter appears in the l -th layer.

Similarly, we can construct an identical partition \mathcal{P} of the parameter space $\mathbb{R}^{\mathcal{S}}$ such that, in each $P \in \mathcal{P}$, $\text{sgn}(h_{l,s_l}(x^j; \cdot))$ are constants for all $s \in \prod_{l=1}^{L-1} [d_l] \times [\lfloor d_L/d \rfloor]d \times \prod_{l=L+1}^{L+L_0} [d_l]$, $l \in [L]$ and $j \in [m]$. Moreover, $h_{L+1,s_{L+1}}(x^j; \cdot)$ is a polynomial of degree at most $L+1$. Hence, in each $P \in \mathcal{P}$, $f'(x^j; \cdot)$ is a polynomial of degree at most $(L+L_0+1) + (k-1)(L+1) = k(L+1) + L_0$ in $\mathcal{S} < m$ variables. By Lemma 18 and (E.5), we can derive

$$m \lesssim \mathcal{S}(L+L_0) \log \left(k(L+L_0) \cdot \max\{d_l : l \in [L+L_0]\} \right)$$

once more.

Notice that this bound also holds for other derivatives $\partial f(x; \theta) / \partial x_i$ of order 1, and they share a similar expression (E.11) with different $\theta_{l,s}$. With this observation, we can now

consider higher order derivatives D^α , $|\alpha| \geq 2$. We claim that for all $|\alpha| \geq 1$, we have

$$\begin{aligned}
& D^\alpha f(x; \theta) \\
&= \left(\prod_{l=0}^{|\alpha|-1} (k-l) \right) \sum_{s^1} \sum_{s^2} \cdots \sum_{s^{|\alpha|}} \left[\left(\prod_{l=1}^{L+L_0+1} \theta_{l,s^1} \right) \left(\prod_{l=1}^{L+1} \theta_{l,s^2,s^1_{L+1}} \right) \right. \\
&\quad \cdots \left(\prod_{l=1}^{L+1} \theta_{l,s^{|\alpha|},s^1_{L+1}} \right) \left(\prod_{l=1}^{L+L_0} \text{sgn}(h_{l,s^1_l}(x; \theta)) \right) \left(\prod_{l=1}^L \text{sgn}(h_{l,s^2_l}(x; \theta)) \right) \\
&\quad \left. \cdots \left(\prod_{l=1}^L \text{sgn}(h_{l,s^l_{|\alpha|}}(x; \theta)) \right) h_{L+1,s^1_{L+1}}^{k-|\alpha|}(x; \theta) \right], \tag{E.12}
\end{aligned}$$

where

$$\begin{aligned}
s^1 \text{ is ranging all over } & \prod_{l=1}^{L-1} [d_l] \times [[d_L/d]]d \times \prod_{l=L+1}^{L+L_0} [d_l] \subset \mathbb{Z}^{L+L_0}, \\
s^2, \dots, s^{|\alpha|} \text{ is ranging all over } & \prod_{l=1}^{L-1} [d_l] \times [[d_L/d]]d \subset \mathbb{Z}^L,
\end{aligned}$$

and $\theta_{l,s^1}, \theta_{l,s^2,s^1_{L+1}}, \dots, \theta_{l,s^{|\alpha|},s^1_{L+1}}$ are some parameters appearing in the l -th layer and the specific locations are determined by their subscripts.

We prove this claim by induction on $|\alpha|$. For $|\alpha| = 1$, (E.12) is exactly (E.11). Now assume that the claim holds for all $|\beta| \leq |\alpha|$. Without loss of generality, assume that $\alpha_1 \geq 1$ and $\alpha = \beta + (1, 0, 0, \dots, 0)$. By induction, we calculate that

$$\begin{aligned}
& D^\alpha f(x; \theta) = \left(D^\beta f(x; \theta) \right)' \\
&= \left(\prod_{l=0}^{|\beta|-1} (k-l) \right) \sum_{s^1} \sum_{s^2} \cdots \sum_{s^{|\beta|}} \left[\left(\prod_{l=1}^{L+L_0+1} \theta_{l,s^1} \right) \left(\prod_{l=1}^{L+1} \theta_{l,s^2,s^1_{L+1}} \right) \right. \\
&\quad \cdots \left(\prod_{l=1}^{L+1} \theta_{l,s^{|\beta|},s^1_{L+1}} \right) \left(\prod_{l=1}^{L+L_0} \text{sgn}(h_{l,s^1_l}(x; \theta)) \right) \left(\prod_{l=1}^L \text{sgn}(h_{l,s^2_l}(x; \theta)) \right) \\
&\quad \left. \cdots \left(\prod_{l=1}^L \text{sgn}(h_{l,s^l_{|\beta|}}(x; \theta)) \right) \left(h_{L+1,s^1_{L+1}}^{k-|\beta|}(x; \theta) \right)' \right],
\end{aligned}$$

where

$$\left(h_{L+1,s^1_{L+1}}^{k-|\beta|}(x; \theta) \right)' = (k - |\beta|) h_{L+1,s^1_{L+1}}^{k-|\beta|-1}(x; \theta) h'_{L+1,s^1_{L+1}}(x; \theta).$$

Plugging in (E.10)(E.9)(E.8) yield the conclusion immediately.

Now with the expression (E.12), we are ready to bound the VC-dimension of $\text{sgn}(D^\alpha \mathcal{F})$. Again, in a slight abuse of notation, assume that the VC-dimension of $\text{sgn}(D^\alpha \mathcal{F})$ is $m > \mathcal{S}$ and let $\{x^1, \dots, x^m\} \subset \mathbb{R}^d$ be a shattered set. Define

$$K := |\{(\text{sgn}(D^\alpha f(x^1; \theta)), \dots, \text{sgn}(D^\alpha f(x^m; \theta))) : \theta \in \mathbb{R}^{\mathcal{S}}\}| = 2^m.$$

By (E.12), clearly, in each $P \in \mathcal{P}$, for all $j \in [m]$, $D^\alpha f(x^j; \cdot)$ is a polynomial of degree at most

$$(L + L_0 + 1) + (|\alpha| - 1)(L + 1) + (k - |\alpha|)(L + 1) = L(k + 1) + L_0$$

in $\mathcal{S} < m$ variables. Hence, we yield

$$m \lesssim \mathcal{S}(L + L_0) \log \left(k(L + L_0) \cdot \max\{d_l : l \in [L + L_0]\} \right)$$

again. The proof is then finished.

E.3 Proof of the oracle inequality

In this subsection, we will give an estimate of the statistical error by proving the oracle inequality (4). To this end, we first prove a series of lemmas. Recall that $\text{VC}_{\mathcal{F}}$ is given by (4.1), the function classes \mathcal{F}_γ and $\widetilde{\mathcal{F}}_\gamma$ are defined at the beginning of Subsection E.1.

Lemma 19. *Given a dataset $\mathbf{x} = \{X_i\}_{i=1}^n$, if there exists $C_{12} > 0$ and $\gamma > 0$ satisfying*

$$\begin{aligned} \max_{|\alpha| \leq s} \sup_{u \in \mathcal{F}_\gamma} \|D^\alpha u - D^\alpha u^*\|_{L^2(\mathbf{x})} &\leq C_{12} \sqrt{\gamma}, \\ (1/n)^2 &\leq \gamma, \\ \max_{|\alpha| \leq s} \text{PDim}(D^\alpha \mathcal{F}) \vee (4eM/C_{12})^2 &\leq n, \end{aligned} \tag{E.13}$$

then we have

$$\max_{|\alpha| \leq s} \text{Rad}(D^\alpha \widetilde{\mathcal{F}}_\gamma, \mathbf{x}) \lesssim \sqrt{\frac{\text{VC}_{\mathcal{F}}}{n} \gamma \log n},$$

Moreover, for any $t > 0$, with a probability exceeding $1 - 2 \exp(-t)$, there holds

$$\sup_{u \in \mathcal{F}_\gamma} \mathbb{E}_P g_u - \mathbb{E}_{\mathbf{x}} g_u \lesssim 6C_{10} \kappa \sqrt{\frac{\text{VC}_{\mathcal{F}}}{n} \gamma \log n} + \sqrt{\frac{2C_{10} M \gamma t}{n}} + \frac{23C_{10} M t}{3n}.$$

Here, $M > 0$ is the constant required in Assumption 2 and $C_{10} > 0$ is from Lemma 12.

Proof. Consider the class

$$\mathcal{G}_\gamma = \{g_u : \mathbb{S}^{d-1} \rightarrow \mathbb{R} \mid u \in \mathcal{F}_\gamma\}.$$

For all $g_u \in \mathcal{G}_\gamma$, $\|g_u\|_\infty \leq C_{10} M$, $\text{Var}(g_u) \leq \mathbb{E}_P(g_u^2) \leq C_{10} M \gamma$. We can apply Lemma 13 to yield that, with probability at least $1 - 2 \exp(-t)$,

$$\sup_{u \in \mathcal{F}_\gamma} \mathbb{E}_P g_u - \mathbb{E}_{\mathbf{x}} g_u \leq 6 \text{Rad}(\mathcal{G}_\gamma, \mathbf{x}) + \sqrt{\frac{2C_{10} M \gamma t}{n}} + \frac{23C_{10} M t}{3n}.$$

To bound the empirical Rademacher complexity term, we apply Lemma 12, the condition (E.13) and Lemma 14 to yield

$$\begin{aligned} &\text{Rad}(\mathcal{G}_\gamma, \mathbf{x}) \\ &\leq C_{10} \sum_{|\alpha| \leq s} \text{Rad}(D^\alpha \widetilde{\mathcal{F}}_\gamma, \mathbf{x}) \\ &\leq C_{10} \sum_{|\alpha| \leq s} \text{Rad}(\{D^\alpha u - D^\alpha u^* : u \in \mathcal{F}, \|D^\alpha u - D^\alpha u^*\|_{L^2(\mathbf{x})} \leq C_{12} \sqrt{\gamma}\}, \mathbf{x}) \\ &\leq C_{10} \sum_{|\alpha| \leq s} \inf_{0 < \beta < C_{12} \sqrt{\gamma}} \left\{ 4\beta + \frac{12}{\sqrt{n}} \int_\beta^{C_{12} \sqrt{\gamma}} \sqrt{\log \mathcal{N}(\delta, D^\alpha \mathcal{F}, \|\cdot\|_{L^2(\mathbf{x})})} d\delta \right\} \\ &\leq C_{10} \sum_{|\alpha| \leq s} \inf_{0 < \beta < C_{12} \sqrt{\gamma}} \left\{ 4\beta + \frac{12}{\sqrt{n}} \int_\beta^{C_{12} \sqrt{\gamma}} \sqrt{\log \mathcal{N}(\delta, D^\alpha \mathcal{F}|_{x_1, \dots, x_n}, \|\cdot\|_\infty)} d\delta \right\}. \end{aligned}$$

When $n \geq \max_{|\alpha| \leq s} \text{PDim}(D^\alpha \mathcal{F})$, by Lemma 15, with

$$\beta = C_{12} \sqrt{\text{PDim}(D^\alpha \mathcal{F}) \gamma / n} \leq C_{12} \sqrt{\gamma}$$

we have

$$\begin{aligned} & \inf_{0 < \beta < C_{12} \sqrt{\gamma}} \left\{ 4\beta + \frac{12}{\sqrt{n}} \int_{\beta}^{C_{12} \sqrt{\gamma}} \sqrt{\log \mathcal{N}(\delta, D^\alpha \mathcal{F}|_{x_1, \dots, x_n}, \|\cdot\|_\infty)} d\delta \right\} \\ & \leq \inf_{0 < \beta < C_{12} \sqrt{\gamma}} \left\{ 4\beta + \frac{12}{\sqrt{n}} \int_{\beta}^{C_{12} \sqrt{\gamma}} \sqrt{\text{PDim}(D^\alpha \mathcal{F}) \log \left(\frac{2enM}{\delta \text{PDim}(D^\alpha \mathcal{F})} \right)} d\delta \right\} \\ & \leq 16 \sqrt{\frac{\text{PDim}(D^\alpha \mathcal{F}) \gamma}{n} \left(\log \frac{4eM}{C_{12} \sqrt{\gamma}} + \frac{3}{2} \log n \right)}. \end{aligned}$$

If we choose $\gamma \geq (1/n)^2$ and $n \geq (4eM/C_{12})^2$, then

$$16 \sqrt{\frac{\text{PDim}(D^\alpha \mathcal{F}) \gamma}{n} \left(\log \frac{4eM}{C_{12} \sqrt{\gamma}} + \frac{3}{2} \log n \right)} \leq 32 \sqrt{\frac{\text{PDim}(D^\alpha \mathcal{F}) \gamma}{n} \log n}.$$

By Lemma 16 and Theorem 3, note that

$$\text{VCDim}(\text{sgn}((D^\alpha \mathcal{F})_0)) \asymp \text{VCDim}(\text{sgn}(D^\alpha \mathcal{F}))$$

we have

$$32 \sqrt{\frac{\text{PDim}(D^\alpha \mathcal{F}) \gamma}{n} \log n} \leq 32 \sqrt{\frac{\text{VCDim}(\text{sgn}((D^\alpha \mathcal{F})_0))}{n} \gamma \log n} \lesssim \sqrt{\frac{\text{VC}_{\mathcal{F}}}{n} \gamma \log n}.$$

We conclude that, if $\gamma \geq (1/n)^2$ and $n \geq \max_{|\alpha| \leq s} \text{PDim}(D^\alpha \mathcal{F}) \vee (4eM/C_{12})^2$, then

$$\max_{|\alpha| \leq s} \text{Rad}(D^\alpha \widetilde{\mathcal{F}}_\gamma, \mathbf{x}) \lesssim \sqrt{\frac{\text{VC}_{\mathcal{F}}}{n} \gamma \log n}, \quad \text{Rad}(\mathcal{G}_\gamma, \mathbf{x}) \lesssim C_{10} \kappa \sqrt{\frac{\text{VC}_{\mathcal{F}}}{n} \gamma \log n}$$

and with probability at least $1 - 2 \exp(-t)$,

$$\sup_{u \in \mathcal{F}_\gamma} \mathbb{E}_P g_u - \mathbb{E}_{\mathbf{x}} g_u \lesssim 6C_{10} \kappa \sqrt{\frac{\text{VC}_{\mathcal{F}}}{n} \gamma \log n} + \sqrt{\frac{2C_{10} M \gamma t}{n}} + \frac{23C_{10} M t}{3n}.$$

The proof is then finished. \square

The critical radius, denoted as γ_* , is defined as the smallest non-zero fixed point that satisfies the inequality

$$\gamma \geq \max_{|\alpha| \leq s} \left\{ 12M \text{Rad}(D^\alpha \widetilde{\mathcal{F}}_\gamma), \frac{8C_{11} M^2 t}{n}, \frac{16M^2 t}{3n} \right\},$$

where $C_{11} > 0$ is the constant from (E.4). Therefore, γ_* can be expressed as

$$\gamma_* := \inf \left\{ \gamma > 0 : \gamma' \geq \max_{|\alpha| \leq s} \left\{ 12M \text{Rad}(D^\alpha \widetilde{\mathcal{F}}_{\gamma'}), \frac{8C_{11} M^2 t}{n}, \frac{16M^2 t}{3n} \right\}, \forall \gamma' \geq \gamma \right\}. \quad (\text{E.14})$$

This γ_* is a positive value that relies on $t > 0$. An upper bound for the critical radius can be determined, shedding light on the inherent complexity of the problem to some extent.

Lemma 20. Assume that $t \geq 1$ and

$$n \geq \max_{|\alpha| \leq s} \text{PDim}(D^\alpha \mathcal{F}) \vee \frac{8e^2 M^2}{C_{11} + 3}.$$

Here, $C_{11} > 0$ is the constant from (E.4). Then

$$\gamma_* \lesssim 144M^2 \frac{\text{VC}_{\mathcal{F}}}{n} \log n + 48\kappa M^2 \exp(-t) + \frac{16C_{11}M^2 t}{n} + \frac{32M^2 t}{3n}.$$

Proof. By definition of γ_* , for all $\varepsilon > 0$, there exists a $\gamma \in [\gamma_* - \varepsilon, \gamma_*]$, such that

$$\begin{aligned} \gamma &< \max_{|\alpha| \leq s} \left\{ 12M \text{Rad}(D^\alpha \widetilde{\mathcal{F}}_\gamma), \frac{8C_{11}M^2 t}{n}, \frac{16M^2 t}{3n} \right\} \\ &\leq \max_{|\alpha| \leq s} \left\{ 12M \text{Rad}(D^\alpha \widetilde{\mathcal{F}}_{\gamma_*}), \frac{8C_{11}M^2 t}{n}, \frac{16M^2 t}{3n} \right\}. \end{aligned}$$

Letting $\varepsilon \rightarrow 0$ yields that

$$\gamma_* \leq \max_{|\alpha| \leq s} \left\{ 12M \text{Rad}(D^\alpha \widetilde{\mathcal{F}}_{\gamma_*}), \frac{8C_{11}M^2 t}{n}, \frac{16M^2 t}{3n} \right\}.$$

Then we define an event

$$E = \left\{ \max_{|\alpha| \leq s} \sup_{u \in \mathcal{F}_{2\gamma_*}} \|D^\alpha u - D^\alpha u^*\|_{L^2(\mathbf{x})} \leq \sqrt{2(C_{11} + 3)\gamma_*} \right\}.$$

By Lemma 17, $P(E) \geq 1 - \kappa \exp(-t)$ for all $t \geq 1$. Notice that $\gamma_* \geq 16M^2 t / (3n) \geq (1/n)^2$, by Lemma 19,

$$\begin{aligned} \gamma_* &\leq \max_{|\alpha| \leq s} \left\{ 12M \text{Rad}(D^\alpha \widetilde{\mathcal{F}}_{\gamma_*}), \frac{8C_{11}M^2 t}{n}, \frac{16M^2 t}{3n} \right\} \\ &\lesssim 12M \max_{|\alpha| \leq s} \mathbb{E}_P(\mathbf{1}_E \cdot \text{Rad}(D^\alpha \widetilde{\mathcal{F}}_{\gamma_*}, \mathbf{x})) + 24M^2(1 - P(E)) + \frac{8C_{11}M^2 t}{n} + \frac{16M^2 t}{3n} \\ &\lesssim 12M \sqrt{\frac{\text{VC}_{\mathcal{F}}}{n} \gamma_* \log n} + 24\kappa M^2 \exp(-t) + \frac{8C_{11}M^2 t}{n} + \frac{16M^2 t}{3n}. \end{aligned}$$

We solve this quadratic inequality for γ_* and yield that

$$\gamma_* \lesssim 144M^2 \frac{\text{VC}_{\mathcal{F}}}{n} \log n + 48\kappa M^2 \exp(-t) + \frac{16C_{11}M^2 t}{n} + \frac{32M^2 t}{3n}.$$

We then complete the proof of this lemma. \square

In the final part of this subsection, we utilize a peeling technique to demonstrate the oracle inequality Theorem 4.

Proof of Theorem 4. Define the critical radius γ_* as (E.14) with some $t' \geq 1$ to be specified. Considering $\gamma > \gamma_* \vee (\log n/n)$, its precise value will also be specified subsequently.

Recall that we have defined the localized class

$$\mathcal{F}_\gamma := \{u \in \mathcal{F} : \mathbb{E}_P(g_u(X)) = \mathcal{R}(u) - \mathcal{R}(u^*) \leq \gamma\}.$$

We can partition \mathcal{F} into shells without intersection

$$\mathcal{F} = \mathcal{F}_\gamma \cup (\mathcal{F}_{2\gamma} \setminus \mathcal{F}_\gamma) \cup \cdots \cup (\mathcal{F}_{2^l \gamma} \setminus \mathcal{F}_{2^{l-1} \gamma}),$$

where $l \leq \log_2(C_{10}M/\gamma) \leq \log_2(C_{10}Mn/\log n)$ and C_{10} is from Lemma 12.

Assume that for some $j \leq l, u_n \in \mathcal{F}_{2^j \gamma}$. Notice that $2^j \gamma > \gamma_*$ satisfies the condition of Lemma 17, with probability at least $1 - \kappa \exp(-t')$, there holds

$$\max_{|\alpha| \leq s} \|D^\alpha u_n - D^\alpha u^*\|_{L^2(\mathbf{x})} \leq \max_{|\alpha| \leq s} \sup_{u \in \mathcal{F}_{2^j \gamma}} \|D^\alpha u - D^\alpha u^*\|_{L^2(\mathbf{x})} \leq \sqrt{2^j(C_{11} + 3)\gamma},$$

where $\kappa := \#\{\alpha : |\alpha| \leq s, a_\alpha(\cdot) \neq 0\}$ to represent the number of non-zero terms in \mathcal{L} satisfying Assumption 1.

From Lemma 19, with probability at least $1 - (\kappa + 2) \exp(-t')$ we obtain

$$\mathbb{E}_P g_{u_n} - \mathbb{E}_{\mathbf{x}} g_{u_n} \lesssim 6C_{10}\kappa \sqrt{\frac{\text{VC}_{\mathcal{F}}}{n} 2^j \gamma \log n} + \sqrt{\frac{2C_{10}M2^j \gamma t'}{n}} + \frac{23C_{10}Mt'}{3n}.$$

Using Lemma 7, with probability at least $1 - (\kappa + 3) \exp(-t')$, there holds

$$\begin{aligned} & \mathbb{E}_P g_{u_n} \\ & \lesssim \mathbb{E}_{\mathbf{x}} g_{u_n} + 6C_{10}\kappa \sqrt{\frac{\text{VC}_{\mathcal{F}}}{n} 2^j \gamma \log n} + \sqrt{\frac{2C_{10}M2^j \gamma t'}{n}} + \frac{23C_{10}Mt'}{3n} \\ & \leq \mathbb{E}_{\mathbf{x}} g_{u_{\mathcal{F}}} - \mathbb{E}_P g_{u_{\mathcal{F}}} + \mathbb{E}_P g_{u_{\mathcal{F}}} + 6C_{10}\kappa \sqrt{\frac{\text{VC}_{\mathcal{F}}}{n} 2^j \gamma \log n} + \sqrt{\frac{2C_{10}M2^j \gamma t'}{n}} + \frac{23C_{10}Mt'}{3n} \\ & \leq 2\mathbb{E}_P g_{u_{\mathcal{F}}} + 6C_{10}\kappa \sqrt{\frac{\text{VC}_{\mathcal{F}}}{n} 2^j \gamma \log n} + \sqrt{\frac{2C_{10}M2^j \gamma t'}{n}} + \frac{23C_{10}Mt'}{3n} + \frac{7C_0 t'}{6n}, \end{aligned}$$

where C_0 is the constant from Lemma 7.

Assume that we have chosen a suitable γ such that

$$2\mathbb{E}_P g_{u_{\mathcal{F}}} + 6C_{10}\kappa \sqrt{\frac{\text{VC}_{\mathcal{F}}}{n} 2^j \gamma \log n} + \sqrt{\frac{2C_{10}M2^j \gamma t'}{n}} + \frac{23C_{10}Mt'}{3n} + \frac{7C_0 t'}{6n} \leq 2^{j-1} \gamma. \quad (\text{E.15})$$

Then with probability at least $1 - (\kappa + 3) \exp(-t')$, we have $u_n \in \mathcal{F}_{2^{j-1} \gamma}$. We continue this process with a shell-by-shell argument and conclude that, with probability at least $1 - l(\kappa + 3) \exp(-t')$, there holds $u_n \in \mathcal{F}_\gamma$. Now we choose a suitable γ . The selected γ must satisfy (E.15) for all $1 \leq j \leq l$ and

$$\gamma_* \vee \frac{\log n}{n} \leq \gamma.$$

(E.15) can be ensured for all $1 \leq j \leq l$ if

$$2\mathbb{E}_P g_{u_{\mathcal{F}}} + \frac{23C_{10}Mt'}{3n} + \frac{7C_0 t'}{6n} \leq 2^{j-2} \gamma, \quad \forall 1 \leq j \leq l,$$

and

$$6C_{10}\kappa\sqrt{\frac{\text{VC}_{\mathcal{F}}}{n}2^j\gamma\log n} + \sqrt{\frac{2C_{10}M2^j\gamma t'}{n}} \leq 2^{j-2}\gamma, \quad \forall 1 \leq j \leq l.$$

Hence, it is sufficient to choose

$$\gamma = 1152C_{10}^2\kappa^2\frac{\text{VC}_{\mathcal{F}}}{n}\log n + \frac{64C_{10}Mt'}{n} + 4\mathbb{E}_{Pg_{u_{\mathcal{F}}}} + \frac{46C_{10}Mt'}{3n} + \frac{7C_0t'}{3n} + \frac{\log n}{n} + \gamma_*.$$

Now we choose $t' = t + \log((\kappa + 3)\log_2(C_{10}Mn/\log n)) \geq 1$, with probability at least $1 - l(\kappa + 3)\exp(-t') \geq 1 - \exp(-t)$, we have $u_n \in \mathcal{F}_{\gamma}$ and by Lemma 20,

$$\begin{aligned} & \mathcal{R}(u_n) - \mathcal{R}(u^*) \\ & \leq 1152C_{10}^2\kappa^2\frac{\text{VC}_{\mathcal{F}}}{n}\log n + \frac{64C_{10}Mt'}{n} + 4\mathbb{E}_{Pg_{u_{\mathcal{F}}}} + \frac{46C_{10}Mt'}{3n} + \frac{7C_0t'}{3n} + \frac{\log n}{n} + \gamma_* \\ & \lesssim 1152C_{10}^2\kappa^2\frac{\text{VC}_{\mathcal{F}}}{n}\log n + 144M^2C^2\frac{\text{VC}_{\mathcal{F}}}{n}\log n + 48\kappa M^2\exp(-t') + 4\mathbb{E}_{Pg_{u_{\mathcal{F}}}} \\ & \quad + \frac{7C_0t' + 238C_{10}Mt' + 48C_{11}M^2t' + 32M^2t'}{3n} + \frac{\log n}{n} \\ & \lesssim \mathbb{E}_{Pg_{u_{\mathcal{F}}}} + \frac{\text{VC}_{\mathcal{F}}}{n}\log n + \frac{t}{n} + \frac{\exp(-t)}{\log(n/\log n)}. \end{aligned}$$

Thus we complete the proof. \square

References

- [1] S. Agmon, A. Douglis, and L. Nirenberg. Estimates near the boundary for solutions of elliptic partial differential equations satisfying general boundary conditions. I. *Comm. Pure Appl. Math.*, 12(4):623–727, 1959.
- [2] C. Aistleitner, J. S. Brauchart, and J. Dick. Point sets on the sphere \mathbb{S}^2 with small spherical cap discrepancy. *Discrete Comput. Geom.*, 48(4):990–1024, 2012.
- [3] Martin Anthony and Peter Bartlett. *Neural Network Learning: Theoretical Foundations*. Cambridge University Press, Cambridge, 1999.
- [4] Peter L. Bartlett, Olivier Bousquet, and Shahar Mendelson. Local Rademacher complexities. *Ann. Statist.*, 33(4):1497–1537, 2005.
- [5] Jan-Hendrik Bastek and Dennis M. Kochmann. Physics-informed neural networks for shell structures. *Eur. J. Mech. A Solids*, 97:1–16, 2023.
- [6] Jingrun Chen, Rui Du, and Keke Wu. A comparison study of deep Galerkin method and deep Ritz method for elliptic problems with different boundary conditions. *Commun. Math. Res.*, 36(3):354–376, 2020.
- [7] Minshuo Chen, Haoming Jiang, Wenjing Liao, and Tuo Zhao. Efficient approximation of deep ReLU networks for functions on low dimensional manifolds. In *Advances in Neural Information Processing Systems*, volume 32, pages 8174–8184., 2019.

- [8] Minshuo Chen, Haoming Jiang, Wenjing Liao, and Tuo Zhao. Nonparametric regression on low-dimensional manifolds using deep ReLU networks: Function approximation and statistical recovery. *Inf. Inference*, 11(4):1203–1253, 2022.
- [9] Feng Dai and Yuan Xu. *Approximation Theory and Harmonic Analysis on Spheres and Balls*. Springer New York, New York, 2013.
- [10] Dinh Dũng and Van Kien Nguyen. Deep ReLU neural networks in high-dimensional approximation. *Neural Netw.*, 142:619–635, 2021.
- [11] Weinan E and Bing Yu. The deep Ritz method: A deep learning-based numerical algorithm for solving variational problems. *Commun. Math. Stat.*, 6(1):1–12, 2018.
- [12] Zhiwei Fang and Justin Zhan. A physics-informed neural network framework for PDEs on 3D surfaces: Time independent problems. *IEEE Access*, 8:26328–26335, 2020.
- [13] Zhiying Fang, Han Feng, Shuo Huang, and Ding-Xuan Zhou. Theory of deep convolutional neural networks II: Spherical analysis. *Neural Netw.*, 131:154–162, 2020.
- [14] Han Feng, Shuo Huang, and Ding-Xuan Zhou. Generalization analysis of CNNs for classification on spheres. *IEEE Trans. Neural Netw. Learn. Syst.*, 34(9):6200–6213, 2023.
- [15] Thomas Hamm and Ingo Steinwart. Adaptive learning rates for support vector machines working on data with low intrinsic dimension. *Ann. Statist.*, 49(6):3153–3180, 2021.
- [16] Nick Harvey, Christopher Liaw, and Abbas Mehrabian. Nearly-tight VC-dimension bounds for piecewise linear neural networks. In *Proceedings of Machine Learning Research*, volume 65, pages 1064–1068., 2017.
- [17] Dan Hendrycks and Kevin Gimpel. Gaussian error linear units (GELUs). *arXiv preprint*, 2016.
- [18] Yuling Jiao, Yanming Lai, Dingwei Li, Xiliang Lu, Fengru Wang, Yang Wang, and Jerry Zhijian Yang. A rate of convergence of physics informed neural networks for the linear second order elliptic PDEs. *Commun. Comput. Phys.*, 31(4):1272–1295, 2022.
- [19] Yuling Jiao, Guohao Shen, Yuanyuan Lin, and Jian Huang. Deep nonparametric regression on approximate manifolds: Nonasymptotic error bounds with polynomial prefactors. *Ann. Statist.*, 51(2):691–716, 2023.
- [20] Iain M. Johnstone. Oracle inequalities and nonparametric function estimation. *Doc. Math.*, III:267–278, 1998.
- [21] George Em Karniadakis, Ioannis G. Kevrekidis, Lu Lu, Paris Perdikaris, Sifan Wang, and Liu Yang. Physics-informed machine learning. *Nat. Rev. Phys.*, 3(6):422–440, 2021.
- [22] Diederik P. Kingma and Jimmy Ba. Adam: A method for stochastic optimization. In *International Conference on Learning Representations.*, 2015.
- [23] Serkan Kiranyaz, Onur Avci, Osama Abdeljaber, Turker Ince, Moncef Gabbouj, and Daniel J. Inman. 1D convolutional neural networks and applications: A survey. *Mech. Syst. Signal Process.*, 151:107398, 2021.

- [24] V. Koltchinskii and D. Panchenko. Empirical margin distributions and bounding the generalization error of combined classifiers. *Ann. Statist.*, 30(1):1–50, 2002.
- [25] Vladimir Koltchinskii. Local Rademacher complexities and oracle inequalities in risk minimization. *Ann. Statist.*, 34(6):2593–2656, 2006.
- [26] Vladimir Koltchinskii. *Oracle Inequalities in Empirical Risk Minimization and Sparse Recovery Problems*, volume 2033. Springer, Berlin, Heidelberg, 2011.
- [27] Vladimir Koltchinskii and Dmitriy Panchenko. Rademacher processes and bounding the risk of function learning. In *High Dimensional Probability II*, pages 443–457., 2000.
- [28] Nikola Kovachki, Zongyi Li, Burigede Liu, Kamyar Azizzadenesheli, Kaushik Bhattacharya, Andrew Stuart, and Anima Anandkumar. Neural Operator: Learning maps between function spaces with applications to PDEs. *J. Mach. Learn. Res.*, 24(89):1–97., 2023.
- [29] H. Blaine Lawson and Marie-Louise Michelsohn. *Spin Geometry (PMS-38)*, volume 38. Princeton University Press, Princeton, 1990.
- [30] Michel Ledoux and Michel Talagrand. *Probability in Banach Spaces*. Springer, Berlin, Heidelberg, 1991.
- [31] Guanhang Lei and Lei Shi. Pairwise ranking with Gaussian kernel. *Adv. Comput. Math.*, 50:1–56, 2024.
- [32] Zongyi Li, Nikola Kovachki, Kamyar Azizzadenesheli, Burigede Liu, Kaushik Bhattacharya, Andrew Stuart, and Anima Anandkumar. Neural Operator: Graph kernel network for partial differential equations. In *ICLR 2020 Workshop on Integration of Deep Neural Models and Differential Equations*, 2020.
- [33] Zongyi Li, Nikola Borislavov Kovachki, Kamyar Azizzadenesheli, Burigede Liu, Kaushik Bhattacharya, Andrew Stuart, and Anima Anandkumar. Fourier neural operator for parametric partial differential equations. In *International Conference on Learning Representations.*, 2021.
- [34] Hao Liu, Minshuo Chen, Tuo Zhao, and Wenjing Liao. Besov function approximation and binary classification on low-dimensional manifolds using convolutional residual networks. In *Proceedings of Machine Learning Research*, volume 139, pages 6770–6780., 2021.
- [35] Lu Lu, Pengzhan Jin, Guofei Pang, Zhongqiang Zhang, and George Em Karniadakis. Learning nonlinear operators via DeepONet based on the universal approximation theorem of operators. *Nat. Mach. Intell.*, 3(3):218–229, 2021.
- [36] Yiping Lu, Haoxuan Chen, Jianfeng Lu, Lexing Ying, and Jose Blanchet. Machine learning for elliptic PDEs: Fast rate generalization bound, neural scaling law and minimax optimality. In *International Conference on Learning Representations.*, 2022.
- [37] Yunqian Ma and Yun Fu. *Manifold Learning Theory and Applications (1st ed.)*. CRC Press, Boca Raton., 2011.
- [38] Tong Mao, Zhongjie Shi, and Ding-Xuan Zhou. Theory of deep convolutional neural networks III: Approximating radial functions. *Neural Netw.*, 144:778–790, 2021.

- [39] Tong Mao and Ding-Xuan Zhou. Approximation of functions from Korobov spaces by deep convolutional neural networks. *Adv. Comput. Math.*, 48(6):1–26, 2022.
- [40] Shahar Mendelson. A few notes on statistical learning theory. In *Advanced Lectures on Machine Learning: Machine Learning Summer School 2002 Canberra, Australia, February 11–22, 2002 Revised Lectures*, pages 1–40. Springer, 2003.
- [41] Hadrien Montanelli. Deep ReLU networks overcome the curse of dimensionality for generalized bandlimited functions. *J. Comput. Math.*, 39(6):801–815, 2021.
- [42] Hadrien Montanelli and Qiang Du. New error bounds for deep ReLU networks using sparse grids. *SIAM J. Math. Data Sci.*, 1(1):78–92, 2019.
- [43] M. Raissi, P. Perdikaris, and G. E. Karniadakis. Physics-informed neural networks: A deep learning framework for solving forward and inverse problems involving nonlinear partial differential equations. *J. Comput. Phys.*, 378:686–707, 2019.
- [44] Francisco Sahli Costabal, Simone Pezzuto, and Paris Perdikaris. Δ -PINNs: Physics-informed neural networks on complex geometries. *Eng. Appl. Artif. Intell.*, 127:107324, 2024.
- [45] Johannes Schmidt-Hieber. Deep ReLU network approximation of functions on a manifold. *arXiv preprint*, 2019.
- [46] Larry Schumaker. *Spline Functions: Basic Theory*. Cambridge University Press, Cambridge, 3rd edition, 2007.
- [47] Justin Sirignano and Konstantinos Spiliopoulos. DGM: A deep learning algorithm for solving partial differential equations. *J. Comput. Phys.*, 375:1339–1364, 2018.
- [48] Taiji Suzuki. Adaptivity of deep ReLU network for learning in Besov and mixed smooth Besov spaces: Optimal rate and curse of dimensionality. In *International Conference on Learning Representations.*, 2018.
- [49] Taiji Suzuki and Atsushi Nitanda. Deep learning is adaptive to intrinsic dimensionality of model smoothness in anisotropic Besov space. In *Advances in Neural Information Processing Systems*, volume 34, pages 3609–3621., 2021.
- [50] Zhuochao Tang and Zhuojia Fu. Physics-informed neural networks for elliptic partial differential equations on 3D manifolds. *arXiv preprint*, 2021.
- [51] Michael E. Taylor. *Partial Differential Equations*. Springer, New York, 2nd edition, 2011.
- [52] Frank W. Warner. *Foundations of Differentiable Manifolds and Lie Groups*, volume 94. Springer New York, New York, 1983.
- [53] Yun Yang and David B. Dunson. Bayesian manifold regression. *Ann. Statist.*, 44(2):876–905, 2016.
- [54] Yunfei Yang and Ding-Xuan Zhou. Nonparametric regression using over-parameterized shallow ReLU neural networks. *J. Mach. Learn. Res.*, 25:1–35, 2024.
- [55] Yunfei Yang and Ding-Xuan Zhou. Optimal rates of approximation by shallow ReLU^k neural networks and applications to nonparametric regression. *Constr. Approx.*, 2024.

- [56] Gui-Bo Ye and Ding-Xuan Zhou. Learning and approximation by Gaussians on Riemannian manifolds. *Adv. Comput. Math.*, 29(3):291–310, 2008.
- [57] Gui-Bo Ye and Ding-Xuan Zhou. SVM learning and L_p approximation by Gaussians on Riemannian manifolds. *Anal. Appl.*, 07(03):309–339, 2009.
- [58] Yuval Zelig and Shai Dekel. Numerical methods for PDEs over manifolds using spectral physics informed neural networks. *arXiv preprint*, 2023.
- [59] Ding-Xuan Zhou. Theory of deep convolutional neural networks: Downsampling. *Neural Netw.*, 124:319–327, 2020.
- [60] Ding-Xuan Zhou. Universality of deep convolutional neural networks. *Appl. Comput. Harmon. Anal.*, 48(2):787–794, 2020.
- [61] Tian-Yi Zhou and Xiaoming Huo. Learning ability of interpolating deep convolutional neural networks. *Appl. Comput. Harmon. Anal.*, 68:101582, 2024.